Community composition, migration and trophic positions of micronekton in two biogeochemical provinces of the South West Indian Ocean.

By Pavanee Annasawmy

Supervisors: **Dr. Frédéric Ménard (IRD)**
Dr. Jean-François Ternon (IRD)
Dr. Michel Potier (IRD)
Associate Professor Coleen Moloney (UCT)

Department of Biological Sciences
University of Cape Town
Rondebosch, Cape Town
South Africa 7701

April 2015

Minor dissertation submitted in partial fulfilment of the requirements for the degree of Masters of Science in Applied Marine Science

Contents

Abstract

Micronekton fauna was investigated as part of a multi-disciplinary research project carried out in two different bioregions of the South West Indian Ocean: the East African Coastal Province (EAFR) and the Indian South Subtropical Gyre (ISSG). Food web structure was addressed using stable isotopes. Since particulate organic matter had high $\delta^{15}N$ values in the ISSG province, copepods were chosen as baseline in trophic level estimations. Feeding regime and size were shown to influence the trophic position of micronekon. In the ISSG, carnivores (fishes and squids) and omnivores (crustaceans) had higher $\delta^{15}N$ values and trophic positions than filter feeders (gelatinous organisms such as salps and pyrosomes) and detritivores (leptocephali larvae. Fishes and squids encompassed a wide range of overlapping isotopic niches suggesting that organisms across different trophic levels feed on the same resources. Estimated trophic levels ranged from 1.67 to 4.73, showing that micronekton in the ISSG can be tertiary consumers. An average enrichment value of 6.7 ‰ was recorded between the sampled micronekton specimens and swordfish *Xiphias gladius* in the ISSG. Trawls, being selective in nature, were shown to sample smaller-sized micronekton with a lower trophic position than the micronekton being eaten by swordfish. In the EAFR, mean $\delta^{15}N$ values of micronekton were higher than in the ISSG, exhibiting slightly higher trophic levels. Mesoscale dynamics in the EAFR provide mechanisms that enrich surface layers in nutrients and chlorophyll-a, therefore contributing to a higher abundance and micronekton species richness. In the ISSG, the large-scale wind-driven anticyclonic gyre pushes the nitracline, thermocline and deep chlorophyll maximum deeper in the water column, influencing the diel migration patterns of micronekton, with a significant proportion of micronekton staying in deep layers or slightly above the thermocline at dusk. Regardless of the differences in the ISSG and EAFR in $\delta^{15}N$ values and trophic positions of micronekton, larger-sized swordfish sampled from these two provinces had similar mean $\delta^{15}N$ values since swordfish are highly migratory and forage in different parts of the Indian Ocean. However, smaller-sized swordfish specimens had lower mean $\delta^{15}N$ values. With a combination of trawl surveys, stable isotope estimates, stomach content and acoustic analyses, this study shed new light on trophic interactions in the oligotrophic ISSG province.

Plagiarism Declaration

I know the meaning of plagiarism and declare that all of the work in this dissertation, save for that which is properly acknowledged, is my own.

Acknowledgements

I would like to acknowledge all the work carried out by the scientific/ non-scientific staff on board the R/V *ANTEA* and R/V *Dr Fridtjof Nansen*, the staff members who analysed the samples collected at sea and all those people who played a key role in the data processing procedures after the cruises in the ISSG and in the EAFR. I would also like to acknowledge the work of all those who created "clean" Microsoft Excel spreadsheets with the complete data sets for me to work on.

I would like to thank my supervisors Frédéric Ménard, Jean-François Ternon and Michel Potier for their guidance all throughout this project and for their time, effort, patience, helpful comments and numerous corrections of the draft versions of this report. I am thankful to them and to Dr. Philippe Curry for hosting me in Sète and taking the time to impart some of their valuable knowledge and skills on me. Special thanks to Jean-François, who never let me down, who made me feel very welcome in Sète, who always took the time and effort to reply to my numerous scientific questions and who provided quick feedbacks and precious suggestions and advice on how to improve this report. Special thanks to Francis Marsac who chose me to carry out this project in France. I would also like to thank all the interns, PhD students, people on CDDs, CDIs and all the researchers at the UMR, Marbec, Sète, for their advice and support with R, for their friendship and for all the good times and laughter.

I am also thankful to Coleen Moloney for the high quality of her "Numerical Skills" lectures that she gave us as part of the AMS course at UCT. The statistical skills I gained in South Africa proved to be invaluable during this Master's project here in France. I am also grateful to Coleen for promptly replying to all my emails and for taking the time and effort to read and correct this report, despite the fact that I sent it to her very late.

Last but not least, my sincere thanks to my family, without whom, I would not be here today. Thanks to them for always supporting me, for helping me realise all of my dreams and for believing in me even when I have stopped believing in myself.

Financial support to carry out this Master's project in France was provided by the International Centre for Education, Marine and Atmospheric Sciences over Africa (ICEMASA), the Western Indian Ocean Marine Science Association (WIOMSA) and the University of Cape Town's Marine Research Institute (Ma-Re).

I. Introduction

In open-sea ecosystems, tunas, sharks, toothed cetaceans and swordfish occupy the highest trophic level in the food web. They form large biomasses of top predators and are widely distributed in the world's oceans. Being targeted by industrial fisheries, they are important sources of revenue to many island states in the Indian Ocean, with the past 20 years seeing a rise in the total catch of tuna and swordfish (FAO, 2006; Ménard *et al*., 2007). Fisheries remove an important biomass of top predators every year, subsequently having an impact on the food web as a whole (Essington *et al*., 2002; Schindler *et al*., 2002). For an ecosystem approach to fisheries, it is important to investigate every link in the food web from lower to higher trophic levels (FAO, 2003; Young *et al*., 2015). Previous studies have demonstrated the opportunistic feeding behaviour of top predators (e.g. Ménard *et al*., 2006) in which micronekton organisms are the main prey item (Potier *et al*., 2007; Allain *et al*., 2012). Micronekton are actively swimming organisms, forming an intermediate trophic link between top predators and lower trophic levels in what is thought to be a rather simple food chain in the tropical ocean (Potier *et al*., 2007) of:

Phytoplankton → *Zooplankton* → *Micronekton* → *Top predators*

Knowledge of the biological processes and environmental mechanisms that affect the distribution of micronekton had been of great value in investigating the distribution and yield of large oceanic fish stocks which are affected by the patterning of food supply (Drazen *et al*., 2011). In the central Indian Ocean, limited data are available on the environmental forcing and mesopelagic organisms that form a key link in the transfer of energy across the food web (Sabarros *et al*., 2009). Longhurst (2007) partitioned the world's oceans into a set of provinces based on various biological, chemical and physical properties. These provinces are also important in the study of the spatial heterogeneity of tuna and swordfish catches, with some habitats being more favourable to tuna and swordfish (Longhurst, 2007; Fonteneau, 1997; Reygondeau *et al*., 2012). The availability of prey (i.e. micronekton) could explain some of the different ecological niches. Two such provinces are found in

the Indian Ocean, the ISSG (Indian South Subtropical Gyre) and the EAFR (East African Coastal Province) both having distinct environmental properties that are of particular interest in this study.

The MICROTON cruise was conducted in 2010 on board the Research Vessel *ANTEA* from IRD (Institut de Recherche pour le Développement) in the ISSG province, where fishing pressure is low. The main focus of my Master's project was to investigate some of the environmental and biological variables influencing the trophic position of micronekton in the food web of the so-called oligotrophic ISSG province, using not yet analysed data from the MICROTON cruise. The different food web components (particulate organic matter, phytoplankton, zooplankton and swordfish) along with the factors likely to influence the trophic position of micronekton (notably, the vertical movements, distribution, diel cycles, abundance, composition, diversity, feeding regime and size of micronekton) are investigated in detail.

This Master's project also aims to compare the ISSG province with the EAFR province, two contrasting biogeochemical provinces. Both the ISSG and EAFR have distinct environmental properties that can affect the distribution and concentration of phytoplankton, zooplankton and micronekton. In turn, this may affect the distribution of large pelagic such as swordfish and tuna. The Mozambique Channel (MZC) in the EAFR, bounded by the Mozambican coast and the western coast of Madagascar, is influenced by numerous mesoscale eddies. This region is also under intense and seasonal fishing pressure. In contrast, the ISSG province, which is dominated by a large basin-wide anticyclonic gyre south of the equator (Stramma and Lutjeharms, 1997; Lutjeharms, 2006) does not experience the same ecosystem dynamics as the EAFR province and is said to be oligotrophic. Data (acoustic, trawl, stomach content of *Xiphias gladius* and stable isotope signatures) from cruises carried out in the MZC (MESOP cruises) and in the ISSG (MICROTON cruise) were made available by the IRD to be analysed statistically in the light of the environmental variables governing these two provinces.

II. Literature Review

II. 1 Physical environment

Longhurst (2007) identified various biogeochemical provinces that cover the earth's oceans, with each province having particular environmental characteristics in terms of bathymetry, surface currents, hydrology, distribution of chlorophyll pigments, nutrient concentrations and stratification indices. The physical and biological environment of the ISSG (focus of the 2010 MICROTON cruise) is studied in more detail in this Master's report. A comparison is made with the EAFR, which has been the focus of the MESOP cruises, the results of which were recently published in a special issue of Deep Sea Research II (Ternon *et al*., 2014).

II.1.1 The Indian South Subtropical Gyre Province (ISSG)

Located between ~10°S and 40°S (Longhurst, 2007), the ISSG (Figure 1), has a total surface area of ~6.48 million km^2, with mean surface chlorophyll-a values of $\leq$ 0.07 mg m^{-3} (Jena *et al*., 2012). This region, being characterised by low levels of nutrients and phytoplankton populations, is said to be oligotrophic in nature (Jena *et al*., 2012). Approximately 40% of the surface of the earth is covered by oligotrophic gyres, mostly in the tropical and subtropical areas, forming the largest ecosystems in each of the major ocean basins (McClain *et al*., 2004).

The main circulation feature in the ISSG is the South Equatorial Current (SEC), forming the northern boundary of a large wind-driven anticyclonic gyre (Stramma and Lutjeharms, 1997; Pous *et al*., 2014). At about 60°E, when the SEC reaches the Mascarene plateau, the inflow splits into two cores with the northern core passing between 10°S and 14°S and the southern core passing near Mauritius between 17°S and 20°S (Pous *et al*., 2014). This prevailing large-scale anticyclonic circulation pattern of the ISSG leads to physical downwelling, thereby limiting the supply of nutrients and chlorophyll-a pigments to the surface layers (Jena *et al*., 2013). The oligotrophic conditions extend 50-60 m deep in the water column (Jena *et al*., 2012).

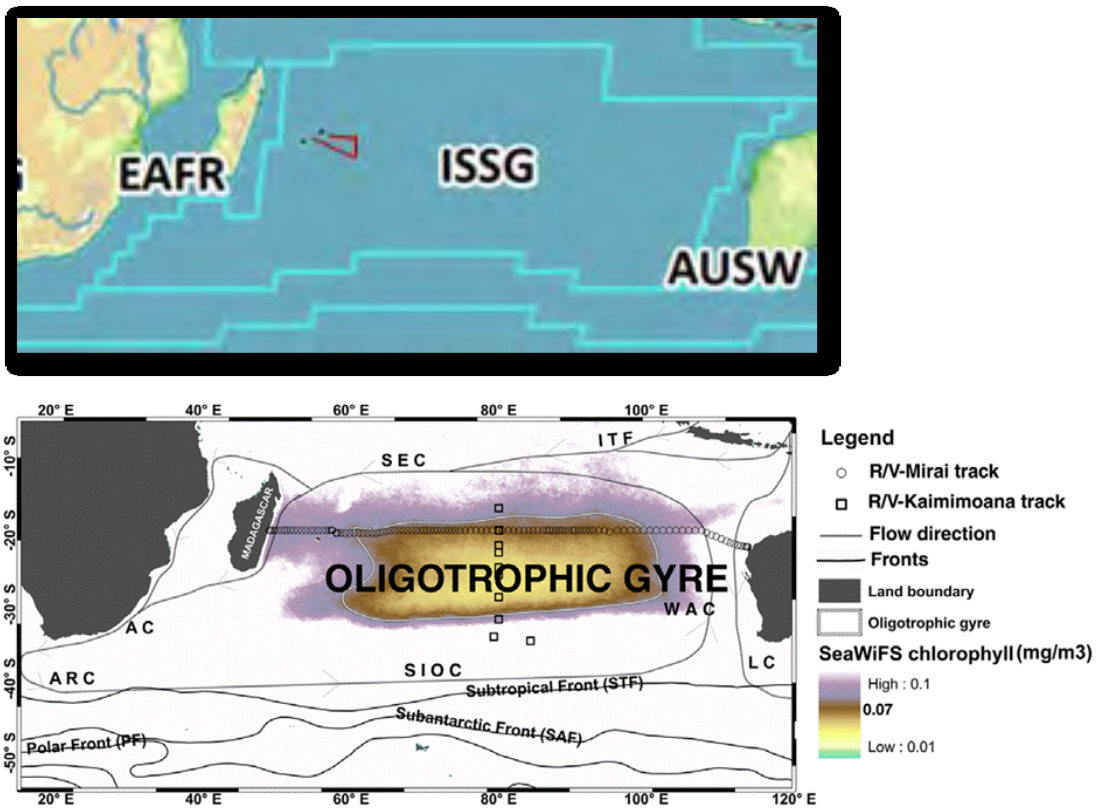

Figure 1 The upper panel shows the biogeochemical provinces as identified by Longhurst (2007), with the approximate cruise track of MICROTON 2010 labelled by red lines. The AUSW (Australia-Indonesia Coastal Province), EAFR and ISSG provinces, are delimited by pale blue lines. The lower panel shows the location of the oligotrophic gyre in the ISSG delimited by the 0.07 mg m^{-3} line from satellite sea surface chlorophyll data (Jena *et al*., 2013). The Agulhas Current (AC), Agulhas Return Current (ARC), South Equatorial Current (SEC) and hydrographic fronts (Subtropical Front, Subantarctic front and Polar front) are also represented.

II.1.2 The East African Coastal province (EAFR)

The EAFR province extends from 5°S to Cape Agulhas (Longhurst, 2007) (Figure 1). Madagascar has an effect on the SEC, causing the spin-off of eddies from the northern and southern tip of the island into the MZC (Schouten *et al*., 2003; Quartly and Srokosz, 2004). Mesoscale cyclonic and anticyclonic eddies cross the MZC and feed the Agulhas Current (AC) to the south (Schott and McCreary, 2001). In cyclonic eddies, Coriolis forces create surface divergence of water masses, causing a rise in the cold, nutrient-rich waters of the thermocline, favourable to enhanced primary production in the centre of the eddy. Conversely, anticyclonic eddies generate a surface convergence of water masses towards the centre of the eddy, leading to a fall in the thermocline and a positive sea level anomaly (detected by satellite altimetry) (Bakun, 2006).

Eddies are thought to play an important role in deep-sea ecosystems by structuring and concentrating biomass in areas of low productivity (McGillicuddy *et al*., 1998; Oschlies and Garçon, 1998; Tew-Kai and Marsac, 2009). Tropical surface waters away from coastal zones are relatively poor in nutrients and do not have seasonal phytoplankton blooms related to vertical mixing as in temperate regions. Mesoscale eddies therefore play a key role in the biological productivity in these areas, particularly in the MZC, where eddy activity is remarkably intense (Tew-Kai and Marsac, 2009). The western side of the MZC typically exhibits enhanced levels of chlorophyll-a coinciding with the southwestward trajectory of eddies offshore from the Mozambique coast (Tew Kai and Marsac, 2009). Currents at the edge of mesoscale eddies export primary productivity away from the Mozambique coast towards the open ocean.

Eddies have also been shown to influence the distribution and aggregation patterns of micronekton (Sabarros *et al*., 2009, Ménard *et al*., 2014) by concentrating organisms at the periphery, where strong local horizontal gradients of sea level anomalies are found. This impacts the distribution, behaviour and feeding strategies of upper trophic levels (swordfish, tuna and frigate birds) that prey on micronekton (Weimerskirch *et al*., 2004; Potier *et al*., 2014; Jaquemet *et al*., 2014).

II.2 Biological environment

Diatoms, dinoflagellates, prochlorophytes and *Synechococcus* (prokaryotic cyanobacteria) are all primary producers that shape the succession of different organisms along a trophic gradient in pelagic food webs (Parsons and Lalli, 2002). Phytoplankton cells have various pigment compositions specific to their particular taxon. These pigments, such as chlorophyll- a (Chl-a), chlorophyll-b (Chl-b), chlorophyll-c (Chl-c) and carotenoids can have a photosynthetic or a photoprotective role (Jeffrey *et al*., 1997). Chlorophyll pigment composition analyses can provide taxonomic information regarding the structure of phytoplankton communities in the ocean (Jeffrey and Vesk, 1997), since these organisms are adapted to the biogeochemical characteristics of the waters where they live and to the level of light available. Phytoplankton having high photoprotective pigment contents and small cell

sizes, such as *Prochlorococcus*, are dominant in surface oligotrophic layers (Alvain *et al*., 2008) whereas diatoms are found in nutrient-rich waters (Sarthou *et al*., 2005).

In contrast to autotrophic phytoplankton, zooplankton are heterotrophic, i.e. they obtain their energy through organic matter (Lalli and Parsons, 1997), such as phytoplankton. Zooplankton are free-swimming animals that can vary in size from a fraction of a millimetre to several metres long (as some jellyfish and pyrosomes) (Miller, 2007). Knowledge of zooplankton composition is scarce in both the EAFR and ISSG. Most of the observations available were collected during the International Indian Ocean Expedition (IIOE) 50 years ago (1959- 1965), where zooplankton biovolume was found to be higher in the northern monsoon-driven part of the Indian Ocean compared to the southwest region (Rao, 1973) (Figure 2).

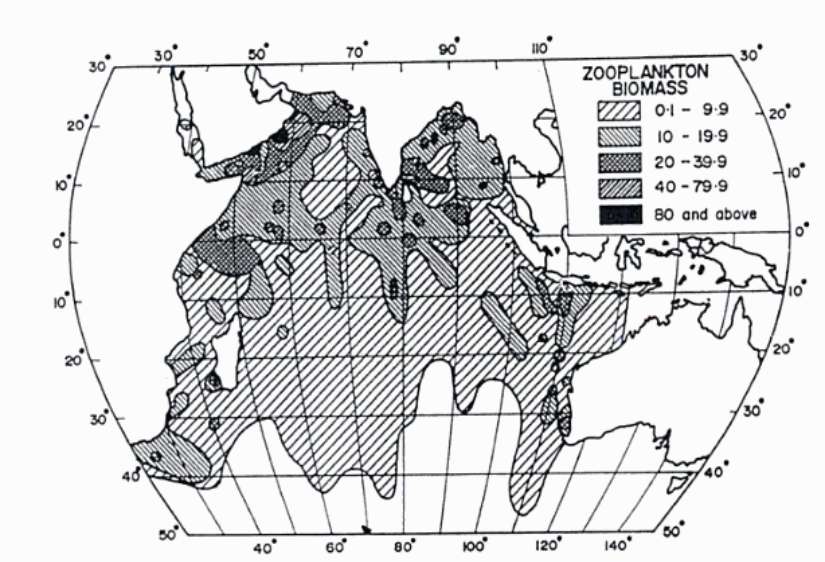

Figure 2 Zooplankton biovolume (mL 100 $^{-3}$) in the Indian Ocean, from vertical hauls (200 m depth to the surface) made during IIOE (Gupta and Desa, 2001).

In the MZC, mean zooplankton biovolumes ranged from 0.2 mL m^{-3} (associated with relatively warm waters (> 23°C) at 100 m and positive sea level anomalies, characteristic of anticyclonic eddies), to a maximum of approximately 0.7 mL m^{-3} (associated with relatively cool water (<20°C) at 100 m and negative sea level anomalies, characteristic of cyclonic eddies) (Huggett, 2014).

Micronekton, which are thought to form a key trophic link between zooplankton and top predators (Potier *et al*., 2007), are a taxonomically diverse group of organisms, consisting of fish species, squids, crustaceans and gelatinous organisms. Micronekton are known to undergo vertical migration

towards the euphotic zone at night and towards deeper layers during the day during the process of diel vertical migration (DVM) (Lebourges-Dhaussy *et al*., 2000; Brodeur *et al*., 2005). Diel Vertical Migration is a widespread behaviour in marine plankton and fish species, possibly triggered by a change in illumination intensity at crepuscular periods. This behaviour, which is common in fish communities, is explained by predator avoidance, feeding opportunity, bioenergetic efficiency or a combination of all of these factors (Lebourges-Dhaussy *et al*., 2000; Mehner, 2012).

Mesopelagic fish are typically the dominant group of micronekton inhabiting the world's tropical oceans (Clarke, 1980**;** Gjøsaeter and Kawaguchi, 1980). Approximately 30 families of mesopelagic fishes were reported to inhabit the mesopelagic zone (Gjøsaeter and Kawaguchi, 1980). These fishes have shown adaptations to their environment by having various mouth morphologies (zooplankton eaters with small jaws) or (large-jawed fish-eating predators), in response to a wide range of prey that are found in the water column (Steele, 2009).

Squids, namely *Sthenoteuthis oualaniensis* or species of the Enoploteuthidae family*,* also inhabit the mesopelagic zone and are important components of marine food webs (Coll *et al*., 2013). Just like the mesopelagic fishes, squids can be both predators on other micronekton and zooplankton (Cherel and Hobson, 2005), and prey for a wide range of top predators such as sharks, marine mammals and other fishes (Bello, 1991; Young *et al*., 2015). Recent studies in the western North Pacific, have shown that squids occupy trophic positions at tertiary to quaternary trophic levels (Watanabe *et al*., 2006), reflecting the versatility in their feeding behaviour and dietary habits (Coll *et al*., 2013; Navarro *et al*., 2013).

Crustaceans also represent a significant proportion of the micronekton biomass and are important zooplankton-eaters (Foxton and Roe, 1974; Hopkins *et al*., 1994). Some organisms (of the *Funchalia* genus, for example) typically feed on chaetognaths, euphausiids, olive-green debris containing phytoplankton and protists, and even nematocysts (Hopkins *et al*., 1994; Schram *et al*., 2010). Some species of crustaceans can be food for squids, midwater fishes and commercially important epipelagic fishes such as albacore tuna, therefore also supporting upper trophic levels (Hopkins *et al*., 1994).

Gelatinous organisms usually have transparent, barrel-shaped bodies and are composed of various groups, including salps and pyrosomes. Both salps and pyrosomes have morphological adaptations for non-selective filter feeding (von Harbou, 2009). Since salps are filter feeders, they are often chosen as the basal organism in trophic level estimations (Cherel *et al*., 2010; Ménard *et al*., 2014).

At the top of the pelagic food web are predatory fishes like swordfish (*Xiphias gladius*) and yellowfin tuna (*Thunnus albacares*), which feed on micronekton. *Xiphias gladius* is highly migratory but with its main location between 45°N and 45°S (Palko *et al*., 1981; Abascal *et al*., 2010). The past 20 years have seen a rise in the catch of tunas and billfishes in the western Indian Ocean (FAO, 2006; Ménard *et al*., 2007). Environmental factors and differences in low-trophic level species between the EAFR and ISSG can affect the abundance and spatial dynamics of top predators, which depend on food availability (Reygondeau *et al*., 2012). This can have a subsequent impact on the capture of tuna and swordfish by industrial fisheries in the ISSG and EAFR.

II.3 Ways of studying micronekton

Micronekton distribution and diversity is studied through a combination of complementary tools: acoustic recordings and pelagic trawls at different depths, and stomach contents of large fish predators such as swordfish and tuna. Improved information on the large scale distribution, DVM patterns, aggregation behaviour (Handegard *et al*., 2013) and relative biomass of micronekton are possible with acoustic surveys (Young *et al*., 2015). Abundance, biodiversity, species richness estimates and taxonomic composition can be investigated with trawl surveys (Potier *et al*., 2014). Stomach content analyses are also an important part of food web understanding for they allow descriptions of diet composition with high taxonomic resolution (sometimes to species level) (Young *et al*., 2015). In this study, stomach content analyses were used to identify and compare the diet composition of swordfish, an important top predator in the EAFR and ISSG. Yet, stomach content analyses also have some major drawbacks. For example, they provide only snap-shot data on recently digested food (Bamstedt *et al*., 2000) and under-represent soft-bodied animals that undergo rapid digestion in the predators'

stomachs (Schmidt *et al*., 2003). *In vitro* incubation is another technique used to get insights into feeding rates (Boyd *et al*., 1984), but can suffer from artefacts. Indeed, organisms can behave unnaturally in an artificial setting (Boyd *et al*., 1984) and the natural food assemblage is not easily simulated in experiments (Schmidt *et al*., 2003).

Biomarkers, which integrate the diet over a longer period of time than stomach contents, are used as an alternative tool to study food web interactions. Stable isotopes of carbon and nitrogen were used to assess the trophic position of micronekton with respect to swordfish and plankton. Some limitations exist with this technique. Ecosystems can have multiple organic inputs and consumers can have more than two food sources, which cannot always be distinguished by using one or two isotope tracers (Schmidt *et al*., 2003). Season, geographical region, species composition and metabolic pathway of photosynthesis can further impact isotope ratios, even for phytoplankton organisms (Michener and Schell, 1994). This spatial or temporal variability in the baseline of the food web hinders comparisons between local and migrating consumers as well as those differing in turnover and growth rate (Fry *et al*., 1983; Simenstad and Wissmar 1985).

Despite these limitations, stable isotope analysis provides a useful approach to estimate the trophic position of an organism. With increasing trophic level, $\delta^{15}N$ values increase, reflecting the trophic position of the organism (Vanderklift and Ponsard, 2003). An enrichment of 3-4‰ is seen in $\delta^{15}N$ values at each trophic level (Michener and Lajtha, 2007). In contrast, little variation occurs in $\delta^{13}C$ values along the food chain. Differences in $\delta^{13}C$ values thus help indicate the various sources of primary production, such as inshore versus offshore, or pelagic versus benthic contributions to food intake (Hobson *et al*., 1994; Rubenstein and Hobson, 2004).

II.4 Specific aims and objectives

Using data collected during a scientific cruise carried out in 2010, the main objectives of this project are:

1) Investigate the trophic position and diel vertical migration patterns of micronekton in an oligotrophic environment.

2) Describe the food web structure in the ISSG, from phytoplankton to swordfish.

3) Compare stomach contents of swordfish sampled in the prospected area with species composition of micronekton collected by trawling

4) Compare food web structure in ISSG and EAFR (MZC) using data from previous cruises conducted in the MZC.

Based on prior understanding of oceanographic conditions and primary productivity of the ISSG, it was hypothesized that the ISSG province was an oligotrophic region dominated by a large-scale anticyclonic gyre, hence impacting the community composition, diel vertical migration and trophic position of micronekton.

III. Materials and Methods

III.1 Satellite monitoring of the oceanic environment

Satellite altimetry can be used to monitor sea surface topography. In this study, sea surface level anomaly (SLA) was used, which corresponds to the difference between measured sea surface height and the mean height calculated at the same location from a 10-year (1992-2013) reference time series. At the mesoscale (~100 km), variations in sea level anomalies describe the sea level rise (positive SLA) and fall (negative SLA) respectively corresponding to anticyclonic and cyclonic eddies. Maps of sea level anomalies (MSLAs) are produced by Ssalto/Duacs and distributed by AVISO and CNES (http://www.aviso.oceanobs.com). Delayed time (DT) MSLAs with a daily and 1/3°resolution were used. Geostrophic sea surface current anomalies (cm s^{-1}), calculated using SLA, are distributed by AVISO at the same spatial and temporal resolution. The eddy kinetic energy (EKE) was calculated from altimetry geostrophic currents using the classical equation:

$$EKE\ (cm^2 s^{-2}) = ½\ (u^2 + v^2)$$

where u and v represent the zonal and meridional components of the surface geostrophic current anomaly (cm s^{-1}).

Values of the sea level anomaly (cm) and geostrophic velocity anomaly (cm s^{-1}) corresponding to each CTD or trawl station were interpolated from the altimetric products at the dates and locations of the stations.

The MODIS satellite, with a daily and 4 km resolution, produces sea surface color (SSC) images (http://oceanocolor.gsfc.nasa.gov/). Since they are sensitive to cloud coverage, SSC was averaged over an 8-day period to get limited cloud coverage maps. SSC is used as a proxy to assess surface oceanic primary production. In addition, sea surface chlorophyll concentrations corresponding to each CTD or trawl station were interpolated from the SSC maps on the dates of the cruises.

The MODIS Sea Surface Temperature (SST) was used to provide the SST at the time that the cruises took place (http://oceancolor.gsfc.nasa.gov/). The same spatial and temporal resolutions and the same averaging procedures were used as those for the ocean colour product.

III.2 The MICROTON Cruise

The MICROTON cruise was carried out on board the R/V *ANTEA* from 19 March to 5 April 2010 in the ISSG province (Figure 3). Data from samples collected at sea allowed investigation of physical (hydrology, currents, temperature and salinity vertical distribution), biogeochemical (oxygen, nutrients, particulate organic matter, chlorophyll-a concentrations, phytoplankton pigments) and biological properties of the water column.

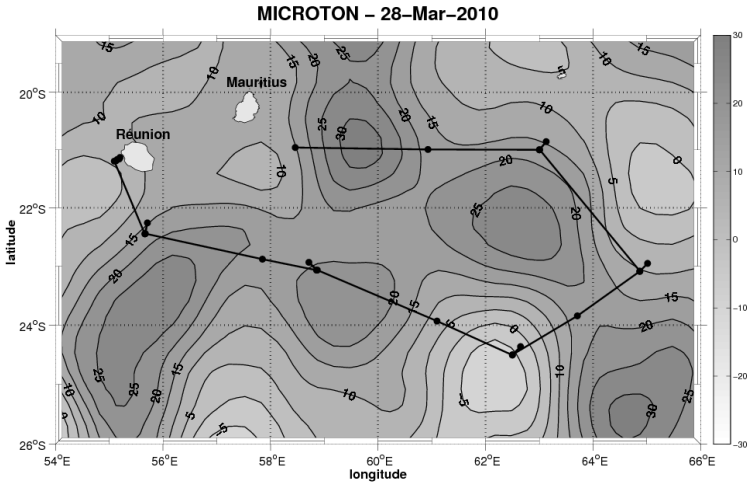

Figure 3 Cruise track of MICROTON in the ISSG province between 21°S and 24°30S and from 55°E to 64°50E (Jean-François Ternon, IRD, Sète France). Contours represent the sea level anomaly (in cm) measured by altimetry in the middle of the cruise (28 March 2010) and the dots along the cruise track represent CTD stations. The grey color bar represents the sea level anomaly (in cm).

Nineteen pelagic trawls were carried out in order to sample micronekton. Data from stomach contents of swordfish collected during previous cruises (Ménard and Potier, unpubl. data) were sorted and added to the diet study.

Details about the collection methods of particulate organic matter, nutrients, zooplankton, micronekton, and pre-processing procedures of acoustic responses can be found in APPENDIX A.

III.2.1 Hydrology and Acoustic Doppler Current Profiler (ADCP)

On board the R/V *ANTEA*, CTD casts were conducted vertically, profiling the temperature, salinity, dissolved oxygen and fluorescence of the water column up to a depth of 1000 m (Lamont *et al*., 2014). During MICROTON, 18 vertical CTD profiles were recorded and data from 11 stations were used for further analyses.

The thermocline is a layer within a body of water where there is a rapid change of temperature with depth. Since the vertical resolution of observations is usually insufficient to resolve the maximum temperature gradient (Yang and Wang, 2009), the 20°C isotherm depth is used as a proxy of the thermocline depth for tropical ocean studies (Durand and Delcroix, 2000; Meinen and McPhaden, 2000). The average (± S.D.) depths of the thermocline were calculated across all stations using temperature values recorded from CTD casts.

Vertical current profiles (L-ADCP- current profiler attached to the CTD frame) were also measured during the MICROTON cruise. L-ADCP data were used to investigate the vertical structure of the current field.

III.2.2 Particulate organic matter, nutrients and chlorophyll pigments

Particulate organic matter (POM) was collected at 5 m (referred to as POM-Surf) and at the depth of the deep chlorophyll maximum (DCM) (referred to as POM-Fmax) using precombusted 25 or 47 mm glass-fiber filters (0.7 µm mesh size) that filtered 4 to 8 L (depending on the load of each sample) of seawater. The stable isotope signatures of the POM samples were determined at a laboratory ashore (see below).

Seawater was also sampled for nitrate, nitrite, phosphate and silicate at different depths (between the surface and 1000 m). The nitrate and nitrite concentrations were used to determine the depth (m) of

the nitracline. Lamont *et al*. (2014) defined the upper limit of the nitracline as the depth (m) at which the change in nitrogen (nitrate and nitrite) concentrations is greater than or equal to 0.2 µM over a 10 m depth interval, as linearly interpolated between discrete sampling depths. This criterion was used to assess the nitracline depth at each sampling station.

Water samples were collected at 5 m and at the DCM before filtration for chlorophyll-a and other pigment measurements. Up to 500 mL of seawater was filtered on 25mm (0.7 µM mesh size) filters for each measurement (chlorophyll-a and pigments). Chlorophyll-a was used for the calibration of the fluorometric sensor of the CTD. The following pigments were recorded:

- The chlorophylls : Chl-a, Chl-b, Chl-c_2, Chl-c_3, Divinyl chlorophyll-a (DVChla), Mono-Chla
- The photosynthetic carotenoids (PSC) and photoprotective carotenoids (PPC)

The chlorophylls were grouped into TChla (total chlorophyll-a), TChlb (total chlorophyll-b) and TChlc (total chlorophyll-c). The photo-pigment indices, TChla, TChlb and TChlc, were derived to investigate the changing contribution of chlorophylls and carotenoids to the total pigment pool (Barlow *et al*., 2007). The total concentration of pigments (TP) was calculated by taking the total concentrations of TChla, TChlb, TChlc, PPC and PSC (APPENDIX B). The pigments were further classified according to the organisms in which they were found i.e. either diatoms, flagellates or prokaryotes (Barlow *et al*., 2007) (details on the methodology is in APPENDIX B).

III.2.3 Zooplankton sampling

A Bongo net with a 200 µm mesh size sampler for zooplankton was used for oblique profiles (0-600 m depth). The Hydrobios Multinet type Midi with a 200 µm mesh and 0.25 m^2 mouth area was used to sample zooplankton from a depth of 200 m to the sea surface in five depth layers (Huggett, 2014). The samples were frozen on board at -20°C before being processed further for stable isotope analyses. In the laboratory, samples were sorted into two main groups, copepods and mysids. Other taxa, being less than 300 µm in size, were discarded.

III.2.4 Acoustic data collection and processing

Acoustic data were continuously collected (day and night) using four frequencies (38, 70, 120 and 200 kHz). In this and previous studies, only the 38 kHz data were used for further statistical analyses because they had the greatest vertical range among the frequencies common to all the surveys conducted in the ISSG and the EAFR (Béhagle *et al*., 2014).

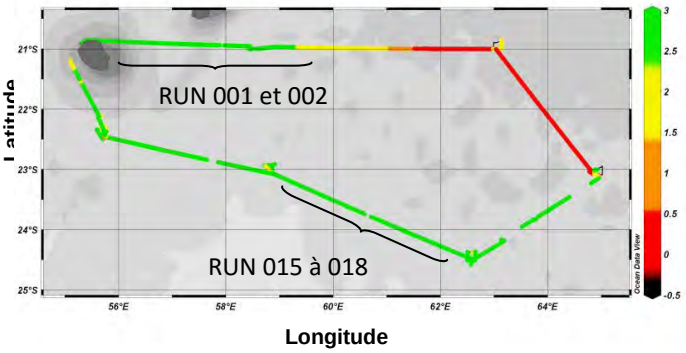

Figure 4 Map of the MICROTON cruise track, with the transects where an acoustic signal was recorded and the quality of such signal (ranging from 0 to 3), as seen by the color bar (Daroux, 2011).

As part of a previous study (Daroux, 2011), the runs 001 and 002, and 015 and 018 of the MICROTON cruise (Figure 4) were analysed by echo-integrating the water column within each of 37 layers of 20 m depth, between the surface and 740 m. The micronekton acoustic density was determined by the Nautical Area Scattering Coefficient (NASC, s_A, m^2mi^{-2}), which can be used as a proxy of relative biomass of micronekton (e.g. Béhagle *et al*., 2014). The s_A was calculated for each acoustic profile with a 20 m vertical resolution. The along track sampling unit in this study was 1 nautical mile. The water column was separated into three depth categories: 10- 200 m (surface layer), 200- 400 m (intermediate layer) and 400- 740 m (deep layer) (Béhagle *et al*., 2014).

In this study, indicators were used to characterize the acoustic vertical profiles. The depths at which 50% and 75% of the total s_A value were found in the water column were computed for each sampling unit during day and night. This indicator gives an indication of the vertical migration of the deep scattering layer.

III.2.5 Pelagic trawls

Trawls were carried out on micronekton aggregations detected by acoustics during day time, whereas during the night they were conducted on sound scattering layers, i.e. 0- 200 m (Ménard *et al*., 2014).

Micronekton were sampled with a 40-m long International Young Gadoid Pelagic Trawl, which has a cod-end lined with 5 mm knotless nylon delta mesh netting. The trawls were towed at a speed of 3-4 knots for 30 minutes (Ménard *et al*., 2014). Micronektonic organisms were sorted onboard and identified to the lowest possible taxon. The soft tissues of some individuals, selected according to their occurrence and abundance, were collected for isotope analyses (details of the procedure are given in APPENDIX C). These tissues included dorsal muscles for fishes, the abdomen for crustaceans, mantles for squids, body walls for siphonophorans, and tissues of pelagic gastropod molluscs, leptocephali larvae and salps (Ménard *et al*., 2014).

III.2.6 Stomach content data of swordfish

The swordfish *Xiphias gladius* was used as a biological sampler of micronekton by providing information on the diversity of the micronekton fauna occurring within predator foraging ranges. Relationships between sizes of the different hard part structures (cephalopod beaks and otoliths, parasphenoids and dentary length of mesopelagic fishes) (Potier *et al*., 2007) and the weights of individuals were used to estimate the reconstituted weight of every prey item (M. Potier, IRD Montpellier, pers. comm.). The diet data used in this study comes from a larger data set that is currently being used for a broad investigation on the feeding ecology of swordfish in the Indian Ocean (F. Ménard and M. Potier, IRD Marseille and Montpellier, pers. comm.).

III.2.7 Stable isotope analyses

Stable isotope analyses were performed on samples of POM (from the surface and at the DCM), soft tissues of zooplankton (copepods and mysids) and on micronekton. Stable isotope values of the muscle tissue of swordfish were also made available by IRD. All samples had already been processed before the start of this MSc project, using the procedures described in Appendix C.

Using the $\delta^{15}N$ stable isotope values of micronekton and swordfish, the trophic level of each specimen was calculated using the equation proposed by Minagawa and Wada (1984):

$$\text{Trophic level} = 2.0 + \frac{\delta^{15}N_i - \delta^{15}N_{primary\ consumer}}{3.2}$$

The copepod group (which has an average ± S.D. δ^{15}N value of 4.72 ± 0.93 ‰ in this study) was chosen as the primary consumer species for estimating trophic levels from the ISSG province.

III.3 Cruises in the Mozambique Channel

Data from the MZC were collected during previous cruises on board the R/V *Dr Fridtjof Nansen* (IMR, Norway) between 13-23°S and 35-43°E from 28 November to 17 December 2008 (MC08A) and the R/V *ANTEA* in the EAFR from 27 October to 23 November 2009 between 23-26°S and 35-39°E (MESOP 2009, MC09B) and from 12 April to 6 May 2010 between 14-23°S and 39-43°E (MESOP 2010: MC10A). Further details (cruise tracks, times and dates) of the MZC cruises can be found in the Deep Sea Research II special issue that has been recently published (Ternon *et al*., 2014)

The environmental data from leg 1 of MESOP 2010 (which had global spatial coverage of the central MZC) were compared with those from MICROTON. Stable isotope data from MESOP cruises were also used in the statistical analyses. Diet data came from stomach contents of swordfish collected with longline sets during extra cruises in the ISSG province (Ménard and Potier, pers. comm.) and during ECOTEM cruises carried out in the MZC in 2002 and 2004.

III.4 Data visualisation and analysis

Visual interpretation of the environmental data from leg 1 from MESOP 2010 and MICROTON was carried out using the free software package Ocean Data View (ODV) (Schlitzer, 2013). Vertical distributions along a cruise transect of the environmental descriptors (nitrate, chlorophyll-a concentrations and temperature) were mapped onto ODV using the SECTION mode, which also allowed the station points to be plotted. Interpolations of data gaps between sampling stations were made using the DIVA (Data-Interpolating Variational Analysis) gridding option in ODV. Vertical

distributions of the variables are all presented along the ship's track (x axis= distance from the first hydrographic station, in km).

Additionally, Matlab routines were used to extract altimetry information for the date and location of each station sampled and to plot the distribution of sea level anomalies. The Interactive Data Language (IDL)-based satellite data visualisation software was used to extract and plot SSC for the date and location of each station.

Classical statistical methods were employed with the statistical package R (Table 1). The null hypothesis, H_0 of no significant effect and an alternative hypothesis, H_1, were set at the beginning of each test, with the null hypothesis being rejected if the p-value was less than the chosen threshold level of 0.05. In these cases, there is a significant result, with the sampled data offering enough evidence to support the alternative hypothesis.

Table 1 Statistical tests carried out on acoustic, trawl, stomach content and stable isotope data from the ISSG and EAFR.

Variables	Investigations	Corresponding statistical analyses
A.Environmental	Difference in mean eddy kinetic energy, chlorophyll-a concentrations, SST, thermocline, nitracline and DCM depths between the EAFR and ISSG	Wilcoxon rank sum test
B. Acoustic	1) Difference in acoustic density estimates (s_A) between day and night in the ISSG across all the depth categories	Wilcoxon rank sum test
	2) Difference in acoustic density estimates (s_A) between all thirty-seven depth layers (L_{10-20}, L_{20-40}, L_{40-60}….$L_{720-740}$) for day and night in the ISSG	Kruskal-Wallis (Non-parametric test)
	3) Test to investigate the DVM of micronekton across the water column with indicators at 75% for day and night acoustic density estimates.	Wilcoxon rank sum test
C. Trawls	Difference in trawl composition across four broad categories (gelatinous organisms, crustaceans, fishes and squids) between EAFR and ISSG	• MANOVA • Pairwise Wilcoxon rank sum test
D. Stomach content	1) Difference in the proportion of gelatinous organisms, fishes, crustaceans and squids caught by trawls and swordfish	Wilcoxon rank sum test
E. Biodiversity Indices	Differences between the EAFR and ISSG in the Shannon diversity index and species richness resulting from trawl and stomach content data	Wilcoxon rank sum test
F. Isotopes	1) Difference in $\delta^{15}N$ and $\delta^{13}C$ among the categories (Particulate Organic Matter-Surface, Particulate Organic Matter-Fmax, Zooplankton Mysids, Zooplankton Copepods, Gelatinous, Crustaceans, Fishes, Squids and Swordfish): (a) in the ISSG (b) in the EAFR (for all categories except zooplankton)	• MANOVA • Kruskal-Wallis • Pairwise Wilcoxon test
	2) Difference in nitrogen and carbon stable isotope signatures between organisms having different feeding regimes	• ANOVA • Tukey Post-hoc test

	(carnivorous, omnivorous, filter-feeding, detritivorous) in the ISSG.	
	3) Relationship between the sizes (mm) of the carnivores of the micronekton specimens collected in trawls in the ISSG and their nitrogen isotope signatures.	• Spearman correlation coefficient • Linear regression
	4) Relationship between the sizes (mm) of the swordfish specimens and their $\delta^{15}N$ values in the EAFR and ISSG.	• Spearman correlation coefficient • Linear model
	5) Differences in $\delta^{15}N$ and $\delta^{13}C$ isotope signatures among the different broad classes (POM, micronekton and swordfish) between the EAFR and ISSG.	• MANOVA • Kruskal-Wallis • Pairwise Wilcoxon test

To check for normality, the residuals (difference between observed and expected values) were plotted on histograms and qq-plots in R, and visually checked (Quinn and Keough, 2002).Shapiro-Wilks test of Normality were also carried out in the statistical package R. To check for homoscedasticity, a scatterplot of the standardized residuals against the fitted values was drawn and checked visually (Quinn and Keough, 2002). The residuals should roughly form a "horizontal band" around the "0" line.

Accumulation curves were plotted in Microsoft Excel to investigate the sampling efforts of trawls and swordfish between the EAFR and ISSG. The species richness values, obtained from diversity tests using the statistical package Vegan in R, were plotted against the trawl or stomach number.

Isotopic niches were determined using the Stable Isotope Bayesian Ellipses in R (SIBER) package for R version 3.1.3. The trophic niche width (standard ellipse corrected area, SEAc calculated using Bayesian inference) of each broad class (POM, zooplankton, micronekton and swordfish) was described in terms of the area the group occupies on a $\delta^{13}C$-$\delta^{15}N$ biplot based on all the individuals within the group. Comparisons of the isotopic niche width of each broad category were made between the standard ellipses (which might reflect the feeding strategy) of each category and between the EAFR and ISSG.

Data on the feeding habits of micronekton species were obtained from the literature. .Mesopelagic fishes are thought to prey on a wide variety of prey but mainly on copepods, amphipods, euphausiids and ostracods (Young *et al*., 2015). They were thus classified as carnivores, i.e. organisms feeding on secondary consumers (zooplankton) and tertiary consumers (other fish species). Squids were also

classified as carnivores since they are known to prey on copepods, amphipods, euphausiids, larvae and fries of carnivorous fish (Arkhipkin *et al*., 1998), and also on lanternfishes (for larger-sized squid specimens) (Young *et al*., 2015). Crustaceans were classified as omnivores since they feed on zooplankton, euphausiids and copepods, and they are also known for occasional herbivory (Tanaka *et al*., 2007). Gelatinous organisms on the other hand, were classified as filter feeders. Leptocephali larvae, being reported to feed on detrital materials (Otake *et al*., 1990), were classified as detritivores. These micronekton organisms were segregated in terms of their nitrogen and carbon stable isotope ratios using statistical tests such as ANOVA (Analysis of Variances) in R to determine the influence of diet on carbon and nitrogen stable isotope ratios in the tissues.

For meaningful comparisons and since isotope analyses were not conducted on copepods during MESOP, the trophic levels of fishes, crustaceans, squids and swordfish from the EAFR, were calculated using *Salpa maxima* (which has an average $\delta^{15}N$ value of 5.1 in the EAFR) as the primary consumer species.

IV. Results

IV.1 Environmental characteristics of the ISSG province

At the time of the cruise, mesoscale anticyclonic eddies of moderate amplitude were recorded in the ISSG province (at stations 1, 3, 13-18) as shown by the positive SLA in Figure 5A. A cyclonic eddy was recorded at station 10 on 28 March 2010, characterized by a negative sea level anomaly (Figure 5B).

(A) **(B)**

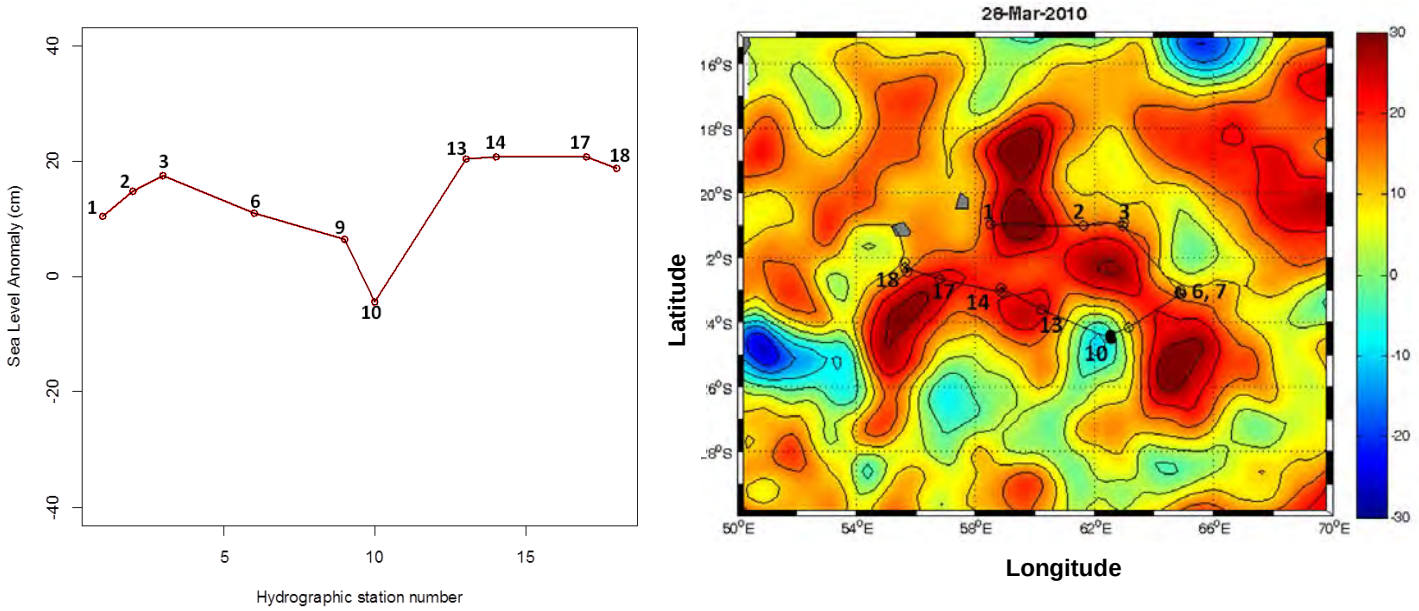

Figure 5 (A) Sea level anomaly (cm) at the hydrographic stations of the cruise MICROTON plotted against the station number. The stations at which SLA was recorded are labelled on the line graph. (B) SLA map showing the MICROTON cruise transect on the 28 March 2010. Stations 1, 2, 3, 6, 7 and 13-18, found at the edge of anticyclonic eddies (red), had positive SLA whereas station 10, found at the edge of a cyclonic eddy (blue), had negative SLA. The color bar indicates sea level anomalies (cm).

Surface currents were stronger at the edge of mesoscale eddies and decreased in strength towards the centre of cyclones (clockwise rotation) and anticyclones (anticlockwise rotation) (Figure 6A). The mean (± S.D.) current velocity was faster in the top 400 m below the sea surface (0.19 ± 0.11 ms^{-1}) and slowed with depth (Figure 6B). The mean (± S.D.) eddy kinetic energy calculated at the sampling stations was relatively low at 188.4 ± 109.8 cm^2s^{-2}.

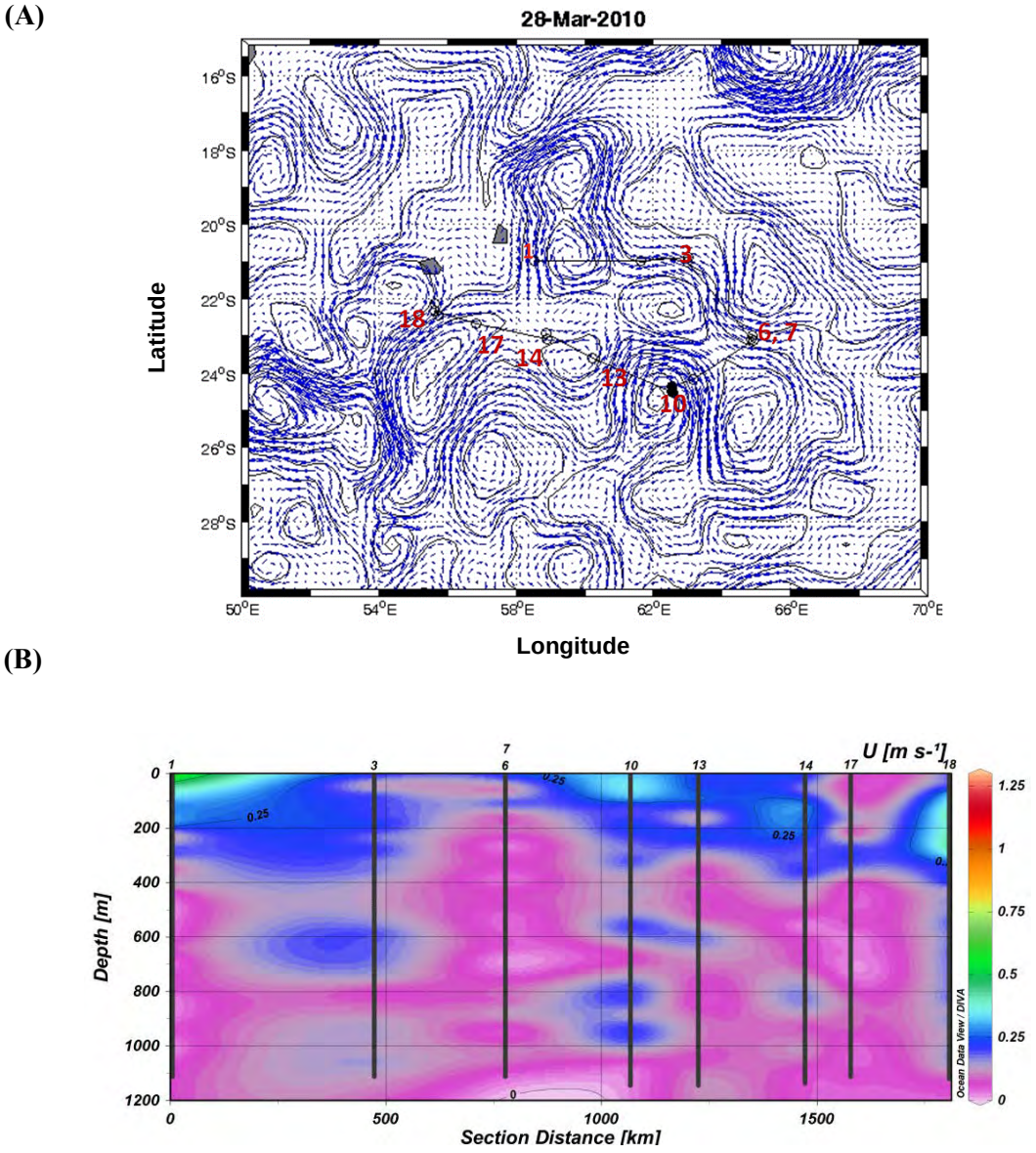

Figure 6 (A) Quiver plot showing the surface currents (calculated from sea surface topography) in the ISSG province during MICROTON on 28 March 2010 (relative scale). (B) Vertical section plot of L-ADCP currents (in m s^{-1}) during MICROTON cruise for stations 1 to 18. Vertical lines correspond to the stations with L-ADCP profiles. Color bar represents the current velocity (m s^{-1}).

Nitrate concentrations were below the minimum level of detection in the first 200 to 400 m below the sea surface and increased gradually with depth till 1000 m where 30 µmol L^{-1} was recorded (Figure 7A). The highest concentrations of chlorophyll-a were recorded between 100 to 200 m depth (at the DCM) at stations 1 and 3 (mean value ± S.D. of 0.11 ± 0.07 µg L^{-1}) and low concentrations were recorded between stations 6 to 18, with mean (± S.D.) of 0.06 ± 0.04 µg L^{-1} (Figure 7B). The surface water during MICROTON had an average (± S.D.) temperature of 27.3 ± 0.6°C (Figure 7C).

A.

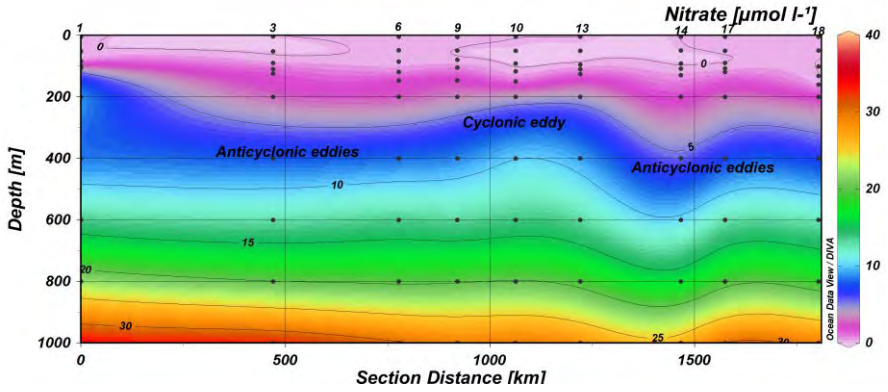

B.

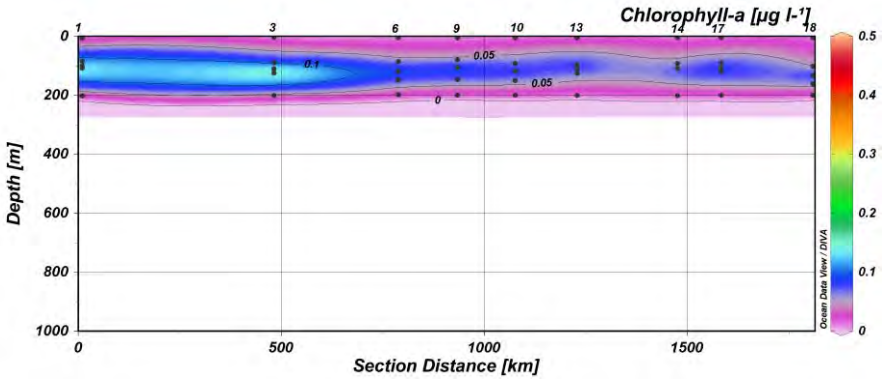

C.

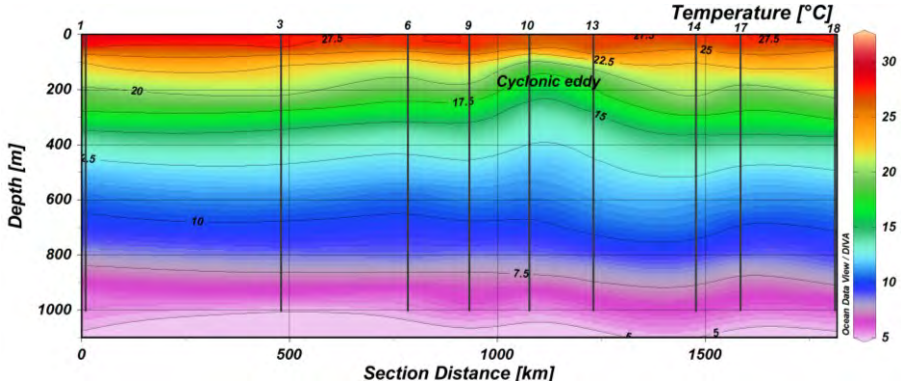

Figure 7 Vertical distributions in MICROTON of (A) nitrate concentrations (µmol L^{-1}), (B) chlorophyll-a concentrations (µg L^{-1}), (C) temperature (°C) for stations 1 to 18. Vertical lines and dots correspond to the stations with CTD profiles.

The average (± S.D.) nitracline and DCM depths were calculated as 98.3 ± 27.8 m and 116.4 ± 11.8 m respectively. The average (± S.D.) thermocline depth was 179.6 ± 49.8 m and was similar across all the stations (except at station 10 where the thermocline was calculated as 97 m below the sea surface).Troughs in the nitracline corresponded to stations where anticyclones were present and a

crest at station 10 (caused by a cyclonic eddy) showed the upwelling of cold, nutrient-rich waters from deep to surface layers (Figure 7A).

The mean concentrations of TChla (total chlorophyll-a), PPC (photoprotective carotenoids) and PSC (photosynthetic carotenoids) found at the surface (0 m and 5 m) and at the DCM in the ISSG are shown in Table 2. The ratios of the total amount of chlorophyll-a to total pigments ($TChla/_{TP}$), of the total amount of PPC to total pigments ($PPC/_{TP}$) and of the total amount of PSC to total pigments ($PSC/_{TP}$) were calculated. The relative mean percentages of diatoms, flagellates and prokaryotes are also given in Table 2 (see APPENDIX B for all calculations).

Table 2 Phytoplankton pigment concentrations recorded during MICROTON in the ISSG, their concentrations relative to the total and relative contributions by different taxonomic groups.

MICROTON N=9	Mean ± S.D.	
	Surface (5 m)	DCM
TChla (mg m^{-3})	0.07 ± 0.01	0.24 ± 0.03
PPC (mg m^{-3})	0.10 ± 0.01	0.12 ± 0.01
PSC (mg m^{-3})	0.03 ± 0.00	0.15 ± 0.02
TP (mg m^{-3})	0.22 ± 0.02	0.61 ± 0.06
$TChla/_{TP}$	0.32 ± 0.02	0.39 ± 0.03
$PPC/_{TP}$	0.46 ± 0.02	0.19 ± 0.01
$PSC/_{TP}$	0.15 ± 0.01	0.25 ± 0.03
Diatoms (%)	9.35 ± 1.12	5.16 ± 0.96
Flagellates (%)	34.94 ± 2.06	76.75 ± 1.29
Prokaryotes (%)	55.30 ± 2.97	17.30 ± 1.93

A higher mean (± S.D.) concentration of total pigments (0.61 ± 0.06 mg m^{-3}) was observed at the DCM compared to the surface (0.22 ± 0.02 mg m^{-3}) at 5 m. There was a relatively higher percentage of the total biomass of prokaryotes at the surface (55.30 ± 2.97% at 5 m) than at the DCM where the mean (± S.D.) relative percentages was 17.30 ± 1.93%. Flagellates showed the opposite pattern, with a greater percentage of the relative biomass at the DCM (76.75± 1.29%), and reduced percentages near the surface (34.94 ± 2.06%). Diatoms were equally distributed between surface waters and the DCM and occurred in relatively low biomass.

IV.2 Comparison of environmental characteristics from the EAFR and ISSG

Variations in sea level anomalies in the EAFR (ranging from -40 cm to 40 cm) at the sampled stations were much higher than the variations in SLA observed in the ISSG (ranging from -8 cm to 20 cm). Mesoscale features were observed during MESOP 2010 as shown by the positive SLA (anticyclones) at stations 2, 8-11, 14 and 15 whereas a sharp decrease in SLA (corresponding to cyclones) was observed at stations 4-6 and 16-19 (Figure 8A).

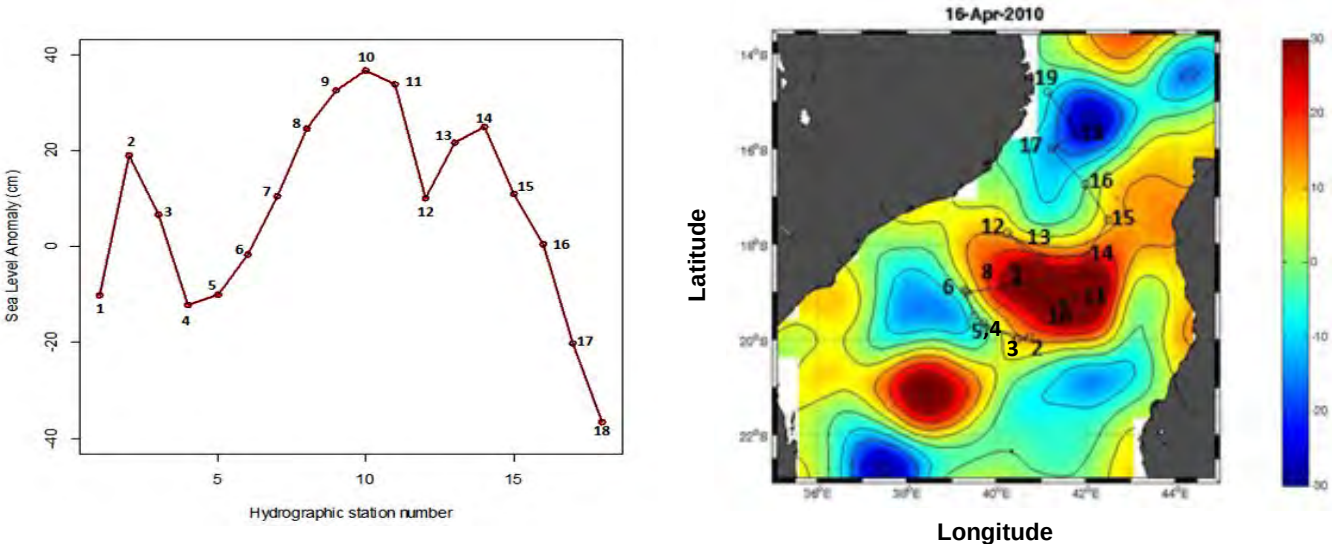

Figure 8 (A) Sea level anomaly at the hydrographic station of the first leg of MESOP 2010, plotted against the station number. (B) SLA map showing the cruise transect on 16 April 2010. Stations 2, 8, 12 and 14 found at the edge of anticyclonic eddies (red), and stations 9-11, found in the centre of anticyclones, had positive SLA whereas stations 4-6 and 16-19, found at the edge or in the centre of cyclonic eddies (blue), had negative SLA. Color bar indicates sea level anomalies (cm).

Similar to results in the ISSG province, surface currents were strong at the edge of mesoscale eddies and decreased in strength towards the centre of mesoscale features in the EAFR, with the fastest currents recorded at stations 2, 3, 13 and 19 (Figure 9A, B). Surface currents in the MZC were stronger than surface currents in the ISSG, ranging from 0.25 to 1.25 m s^{-1} (Figure 9B). Mean (± S.D.) eddy kinetic energy calculated for the stations during MESOP 2010 in the EAFR was 1141.8 ± 812.48 cm^2s^{-2}, which is six times greater than the mean eddy kinetic energy recorded in the ISSG province ($W= 331$, $P < 0.05$).

(A)

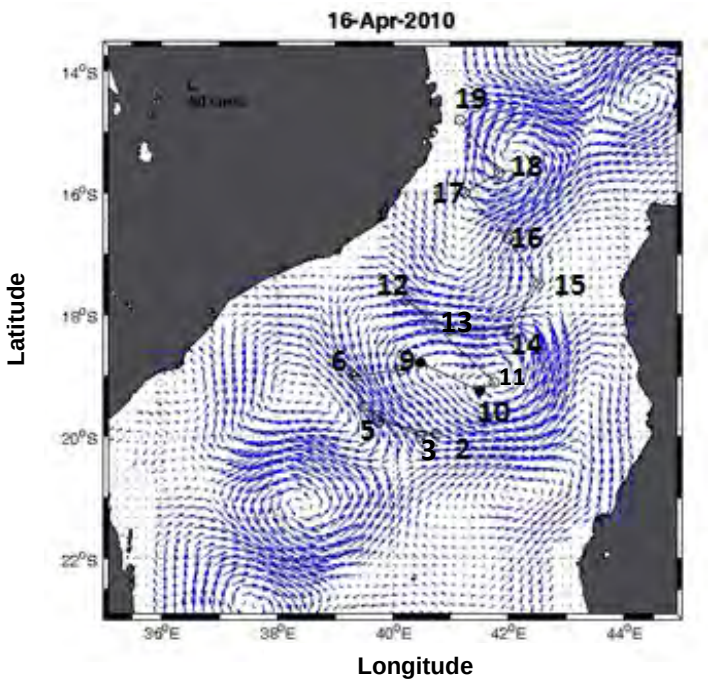

(B)

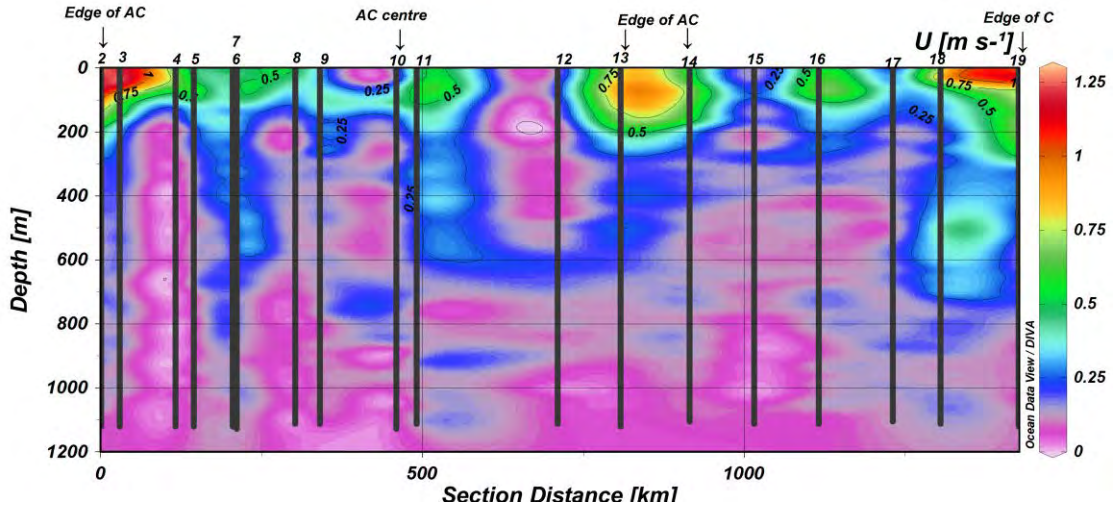

Figure 9 (A) Quiver plot showing the surface currents (calculated from sea surface topography) in the EAFR during MESOP on 16 April 2010. (B) Vertical section plot of L-ADCP currents (in m s^{-1}) during MESOP 2010 for stations 1 to 19. Vertical lines indicate stations with L-ADCP profiles and the color bar indicates the current velocity (in m s^{-1}).

The sea surface color image (Figure 10A), averaged over an 8-day period, shows the ISSG province in the blue spectrum, characterised by low levels of nutrients and low chlorophyll concentrations. The vertical distribution of nitrates in the EAFR were similar to the distribution observed in the ISSG province, with nitrate concentrations increasing from the surface to deeper layers (Figure 10B). The

EAFR province had enhanced levels of chlorophyll-a and other pigments, with a mean (± S.D.) chlorophyll-a value of 0.29 ± 0.13 µg L^{-1}, measured across all stations during the MESOP 2010 cruise. Surface chlorophyll-a concentrations recorded during MICROTON were much lower (mean ± S.D. of 0.03 ± 0.01 µg l^{-1}) (Figure 10C) across all stations (W= 342, P < 0.05). Warmer temperature (29.8 ± 0.3°C on average) was recorded in the surface layer during MESOP 2010 (Figure 10D) compared to MICROTON (W= 361, P < 0.05).

(A)

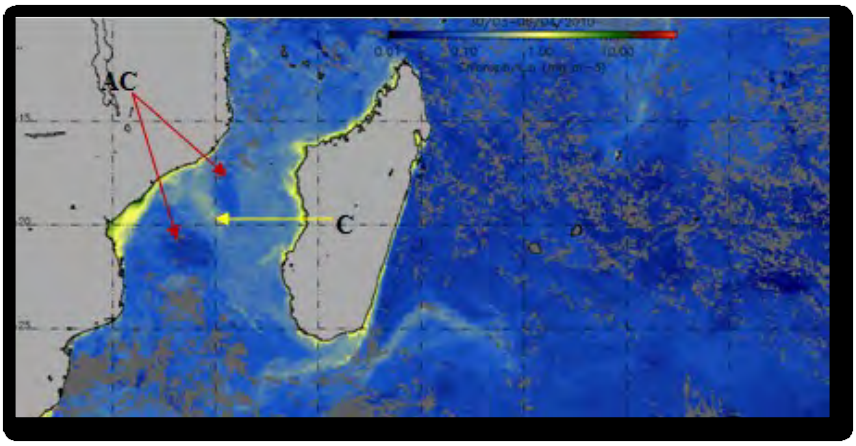

(B)

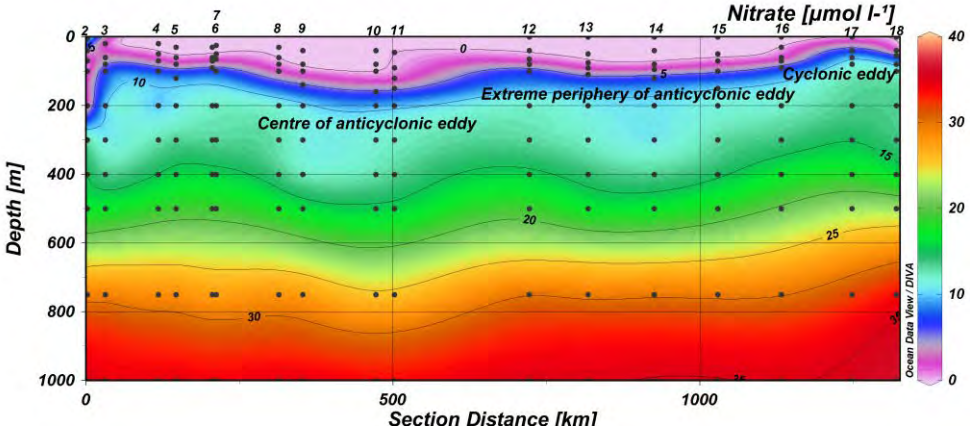

(C)

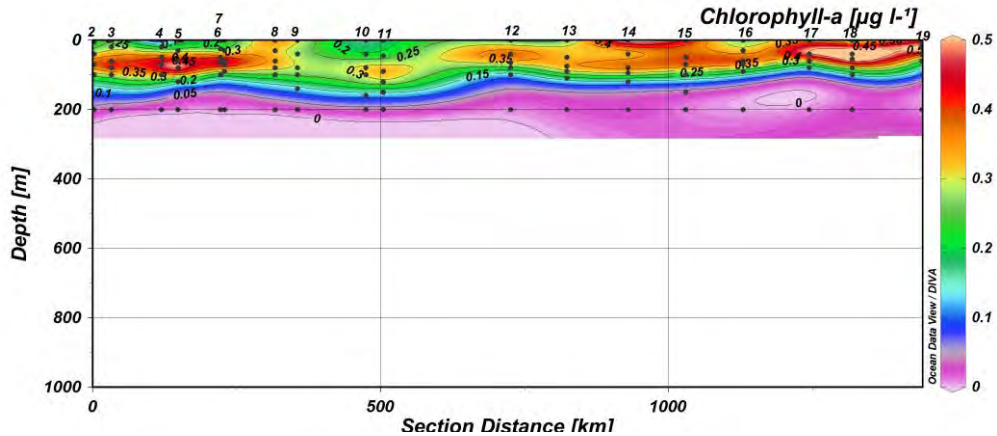

(D)

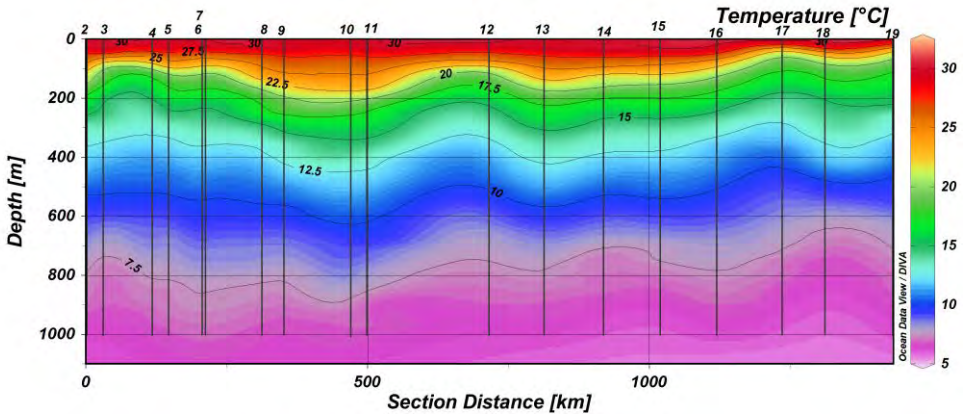

Figure 10 (A) Satellite image of chlorophyll-a distribution in the EAFR and ISSG, integrated over an 8-day period, from 30 March to 6 April 2010 (MODIS, 03/30 to 04/06/2010). The red arrows show the presence of anticyclonic eddies (AC) and the yellow arrow shows a cyclonic eddy (C) in the MZC. Vertical distributions during MESOP 2010 of (B) nitrate concentrations (µmol L^{-1}) for stations 1 to 18, (C) chlorophyll-a concentrations (µg L^{-1}) and (D) temperature (°C) for stations 1 to 19. Vertical lines and dots correspond to the stations with CTD profiles.

Mesoscale eddies (a cyclone and two anticyclones) are shown in Figure 10A close to the Mozambique coast which has high SSC values. Surface chlorophyll filaments are shown to extend from the coast into the MZC. On average, the nitracline and mean DCM depths were much shallower during MESOP 2010 than during MICROTON and were found at mean (± S.D.) depths of 70.4 ± 24.2 m and 76.3 ± 16.7m respectively (DCM: W=8, $P < 0.05$, nitracline: W= 37.5, $P < 0.05$). There was also an expansion in the vertical distribution of nitrates from surface to deeper layers during MICROTON, corresponding to the general deepening of the vertical structures in the (anticyclonic) subtropical gyre. Compared to the EAFR, the surface layer was relatively poor in nutrients in the ISSG, resulting in lower levels of primary production. The average (± S.D.) thermocline depth (179.6 ± 49.8 m) recorded during MICROTON was deeper than the mean (± S.D.) thermocline depth (138.5 ± 46.7 m) during MESOP 2010 (W= 98, $P < 0.05$).

Troughs in the nitracline, DCM and thermocline can be observed at stations in the centre or at the periphery of anticyclonic eddies (8-11 and 13-15), whereas stations found in the centre or at the periphery of cyclonic eddies showed a rise in the average depths of the nitracline, DCM and thermocline (Figure 10). The thermocline rose to a depth of 60 m in the presence of a cyclonic eddy

(station 17) during MESOP 2010 and fell to a minimum depth of 209 m in the anticyclone (station 10). Similar patterns were observed for the nitracline and DCM with a rise up to 5 m in the nitracline depth at station 19 and a rise up to 40 m in the DCM depth at station 18 (cyclonic eddy). In the presence of an anticyclonic eddy, the nitracline was recorded at a minimum depth of 105 m (station 11) and the DCM was at a minimum depth of 108 m (station 9).

Total pigments in the EAFR exhibited a similar pattern as in the ISSG province, with higher mean (± S.D.) concentrations at the DCM (0.91 ± 0.35 mg m^{-3}) compared to the first 5 m below the sea surface, where a mean (± S.D.) concentration of 0.34 ± 0.07 mg m^{-3} was observed (Table 3). The total pigment concentration was 20% higher in the EAFR than the ISSG province. Similar to the ISSG, a greater relative percentage of the biomass of prokaryotes (63.84 ± 8.12%) was calculated at 5 m in the EAFR, compared to the DCM, where only 13.27 ± 3.10% was present. The percentage of flagellates was greater at the DCM (79.57 ± 4.26%) compared to 5 m depth (31.72 ± 7.06%).

Table 3 Phytoplankton pigment concentrations recorded during MESOP 2010 in the EAFR, their concentrations relative to the total and relative contributions by different taxonomic groups

MESOP 2010 N=22	Mean ± S.D.	
	Surface (5 m)	DCM
TChla (mg m^{-3})	0.15 ± 0.04	0.37 ± 0.13
PPC (mg m^{-3})	0.12 ± 0.02	0.10 ± 0.05
PSC (mg m^{-3})	0.05 ± 0.02	0.27 ± 0.11
TP (mg m^{-3})	0.34 ± 0.07	0.91 ± 0.35
$TChla/_{TP}$	0.44 ± 0.04	0.41 ± 0.03
$0PPC/_{TP}$	0.35 ± 0.06	0.11 ± 0.01
$PSC/_{TP}$	0.14 ± 0.02	0.30 ± 0.02
Diatoms (%)	4.45 ± 1.53	6.09 ± 2.62
Flagellates (%)	31.72 ± 706	79.57 ± 4.26
Prokaryotes (%)	63.84 ± 8.12	13.27 ± 3.10

At 5 m depth, the percentage of the total biomass of diatoms in the ISSG (9.35 ± 1.12%) was twice that for the EAFR (4.45 ± 1.53%), whereas the percentage of prokaryotes was greater in the EAFR (63.84 ± 8.12%) than the ISSG (55.30 ± 2.97%).

In summary, the ISSG province is a region with low mean eddy kinetic energy, weak surface currents and low mesoscale activity compared to the EAFR. The DCM, nitracline and thermocline depths are also deeper in the water column compared to the EAFR due to the anticyclonic subtropical gyre, with

occasional shoaling in the DCM, nitracline and thermocline in the presence of cyclonic eddies (which are relatively scarce in the ISSG). The chlorophyll-a and total pigment concentrations recorded during MICROTON were higher at the DCM than at 5 m and both chlorophyll-a and total pigment concentrations were higher in the EAFR than ISSG. A greater biomass of flagellates was found at the DCM whereas prokaryotes were mainly concentrated at the surface in both the ISSG and EAFR.

For the sake of clarity, results from acoustic and trawl surveys and stomach content analyses are presented in both the ISSG and EAFR in the following sections.

IV.3 Results of acoustic surveys in the ISSG and EAFR

Acoustic densities recorded between 0 and 740 m in the ISSG province were 50% greater during the night than during the day with different distributions across the three depth categories (Figure 11) (W= 28984, n=1895, $P < 0.05$). During night time, approximately 75% of the total acoustic densities were found in the surface layer (between 10-200 m) whereas only 20% were found in the deep layer (between 400-740 m) in the ISSG. During day time, 60% of acoustic densities were found in the deep layer whereas 30% were found in the surface layer. During MICROTON, the intermediate layer gathered approximately 5% of the acoustic densities during the night and 10% during the day.

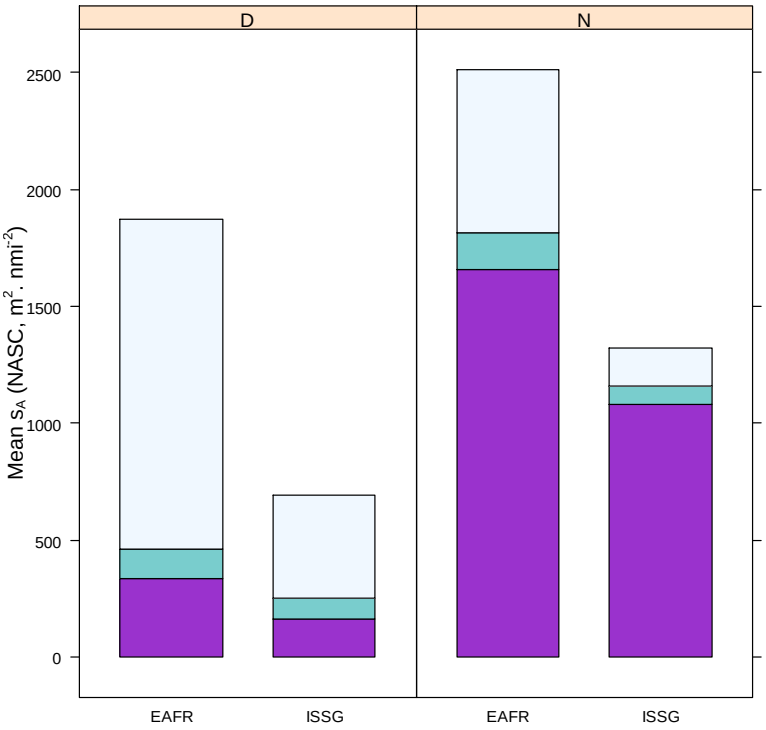

Figure 11 Mean s_A in EAFR and ISSG for day (D) and night (N) data. Purple portion of the bar chart represents the s_A in the surface layer (10-200 m), middle blue portion represents the s_A in the intermediate layer (200-400 m) whereas the pale blue portion represents the s_A in the deep layer (400-740 m).

Significant differences in the acoustic densities were found in all thirty-seven 20 m-depth layers (L_{10-20}, L_{20-40}, L_{40-60}….$L_{720-740}$) between day and night (Kruskal-Wallis test, n= 1895, $P < 0.05$).

In the EAFR province, approximately 65% of acoustic densities were recorded in the surface layer (10- 200 m) during the night, whereas only 28% were found in the deep layer (400-740 m) (Figure 11). The surface layer gathered 17% of acoustic densities during the day whereas 76% were recorded in the deep layer. The intermediate layer in the EAFR had a greater percentage of acoustic densities than the ISSG during the day (approximately 6%) and a lower percentage during the night (12%).

Mean vertical profiles (Figure 12) show the depths at which 50% and 75% of the acoustic responses (calculated from the sea surface) were found in the water column.

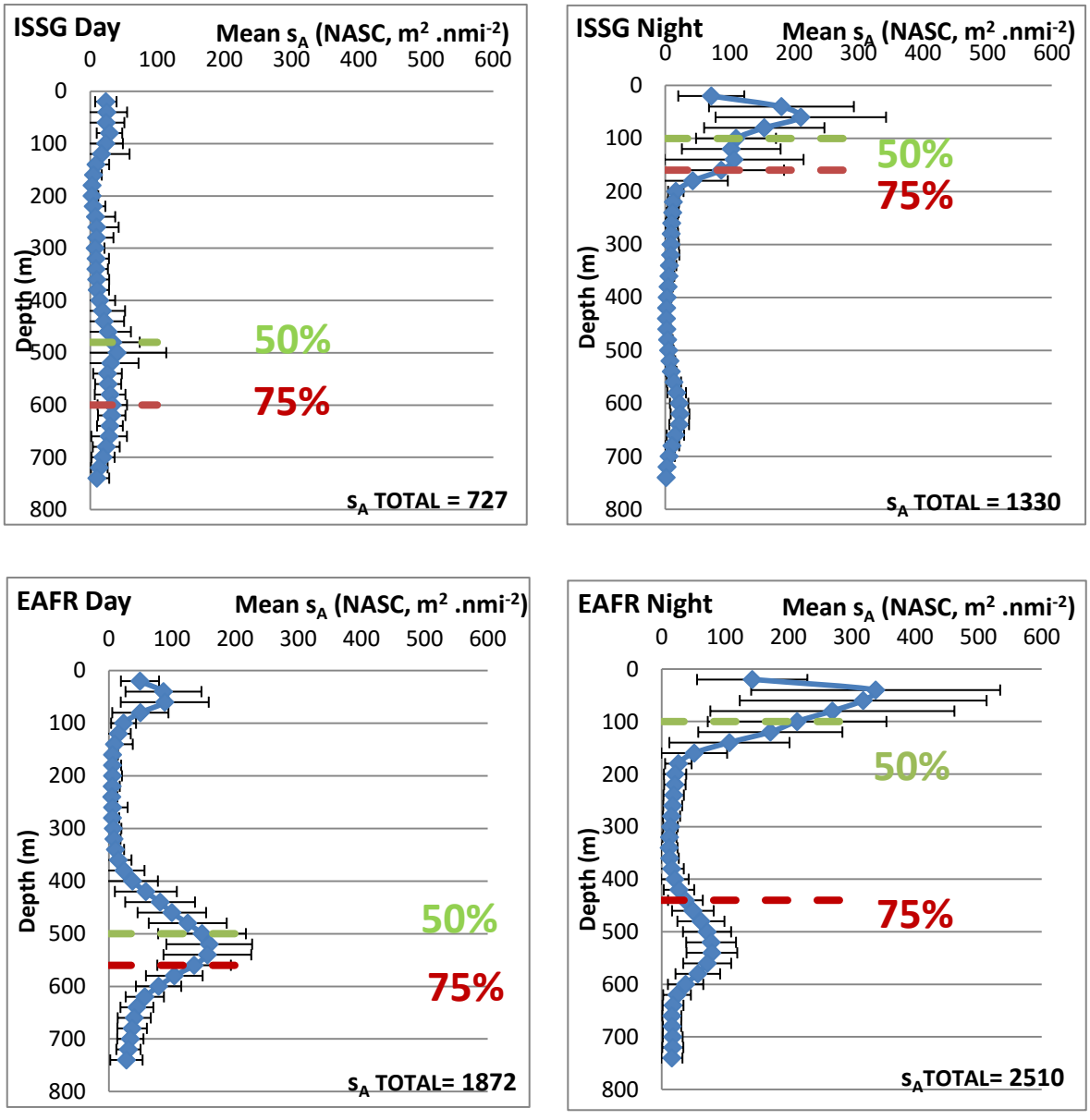

Figure 12 Mean ± (S.D.) vertical profiles during the day and night in the EAFR and ISSG. The total acoustic densities, recorded in the EAFR and ISSG during the day and night, is given. The indicators 50% (green) and 75% (red) show the maximum depths reached by 50% and 75% of these acoustic responses from the sea surface.

The day time mean vertical profile in the ISSG is flatter than the day time vertical profile in the EAFR, with a low total acoustic response of 727 m^2 nmi^{-2} recorded in the ISSG (Figure 12). During the day, 50% and 75% of the micronekton acoustic densities were found between the sea surface and maximum depths of 480 and 600 m respectively in the ISSG province. During the night, most of the micronekton acoustic estimates were found between the surface and maximum depths of 100 and 160 m in the ISSG province. During the night in the ISSG, 25% of the acoustic densities were recorded between 100 and 160 m and 25% were recorded below 160m.

In the EAFR, the 50% indicator showed the night time acoustic estimates to be distributed in the shallow layer (between the surface and a maximum depth of 100 m) whereas the 75% indicator showed that 75% of the acoustic responses were distributed from the surface to a maximum depth of 440 m. Therefore, more than 25% of the acoustic responses were distributed in the deep layer (between 400 and 740 m) during the night in the EAFR. A pronounced bi-modal distribution was observed during the day and night in the EAFR province. Acoustic data from the EAFR showed significant differences between day and night in the depths at which 50% ($W= 380813$, $n= 1252$, $P < 0.05$) and 75% ($W= 365494$, $n= 1252$, $P < 0.05$) of the total s_A were reached.

There were also differences in the EAFR and ISSG in the depths at which 75% of the total s_A were reached during the day ($W= 115800$, $n= 1895$, $P < 0.05$) and night ($W= 166967$, $n= 1895$, $P < 0.05$).

IV.4 Micronekton assemblage in the ISSG and EAFR

A total of 346 micronekton organisms from 35 taxa were identified in trawls in the ISSG province. Micronekton taxa were broadly divided into four categories: gelatinous organisms (for example, *Salpa maxima* and *Pyrosommatida* spp.), crustaceans (e.g. *Funchalia taaningi*), fishes (e.g. *Diaphus* spp.) and squids (e.g. *Sthenoteuthis oualaniensis*). Fishes dominated the total catch (61% by number) representing 19 genera and 27 species. Gelatinous organisms and squids represented 16% (by number) of the total catch whereas crustaceans represented 7% (Figure 13).

The proportion of fishes in the catch decreased by 20% from day time to night time. Proportions of the three other categories of micronekton increased from day time to night time (by 9% for gelatinous organisms and 10% for crustaceans whereas a small 1% increase was observed for squids from day to night (Figure 13).

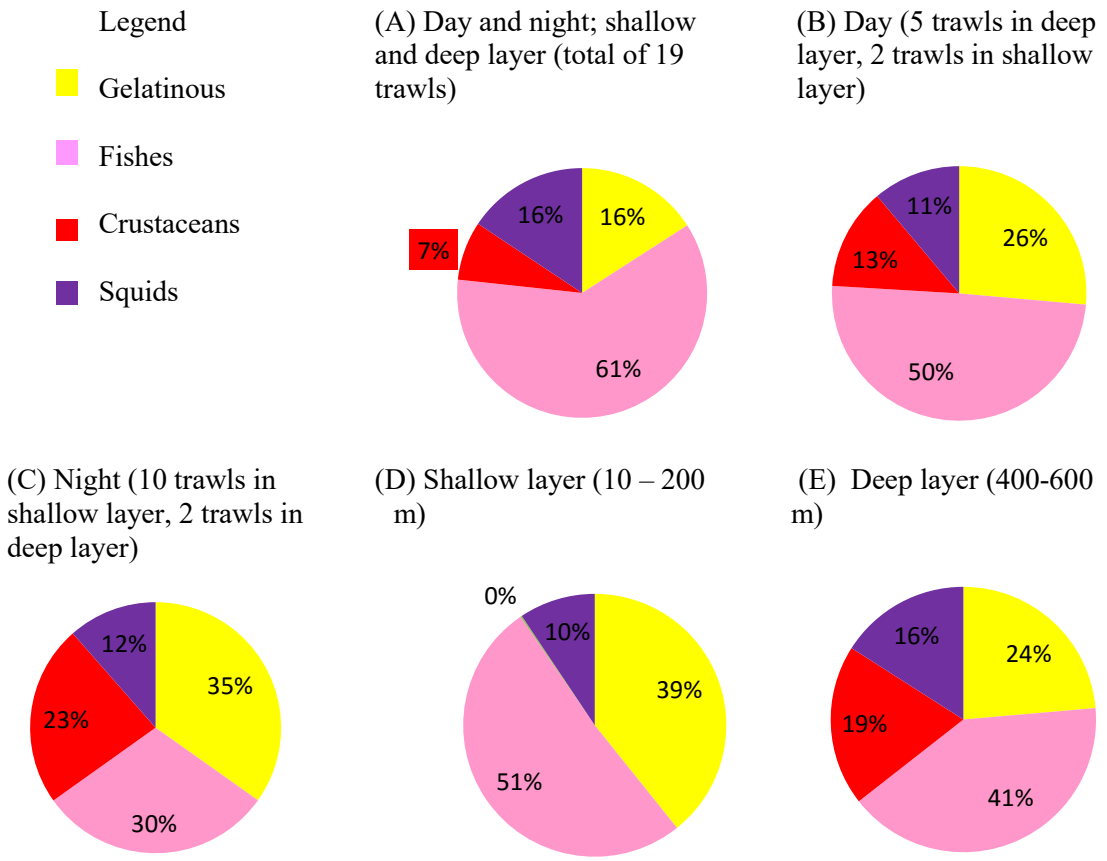

Figure 13 Pie charts of the percentage of micronekton caught in trawls during (A) day and night across all depth categroies; (B) day and (C) night across all depth categories; (D) shallow layer (0-200 m) and (E) deep layer (400-600 m) during the day and night in the ISSG province.

The distributions by depth layer were different for the different groups in the ISSG province. Among the micronekton, fishes dominated the total catch in deep and surface layers with a decrease of 10% from the surface to the deep layers. Gelatinous organisms had a similar pattern, with a 15% decrease from the surface to deep layers. The proportion of squids increased from the surface to the deep trawls whereas crustaceans, which were absent from surface trawls, represented 19% of the catch observed in deep trawls (Figures 13).

Within the micronekton, fishes from the Myctophidae family (*Ceratoscopelus*, *Benthosema* and *Diaphus*) were the most widely caught in the ISSG (Figure 14). The fishes, *Diaphus* and *Ceratoscopelus*, and the crustacean, *Thysanopoda*, were dominant in trawl surveys in the EAFR province. Among the 11 most abundant micronekton samples, the only squid specimen present was *Abraliopsis* in both the ISSG and EAFR.

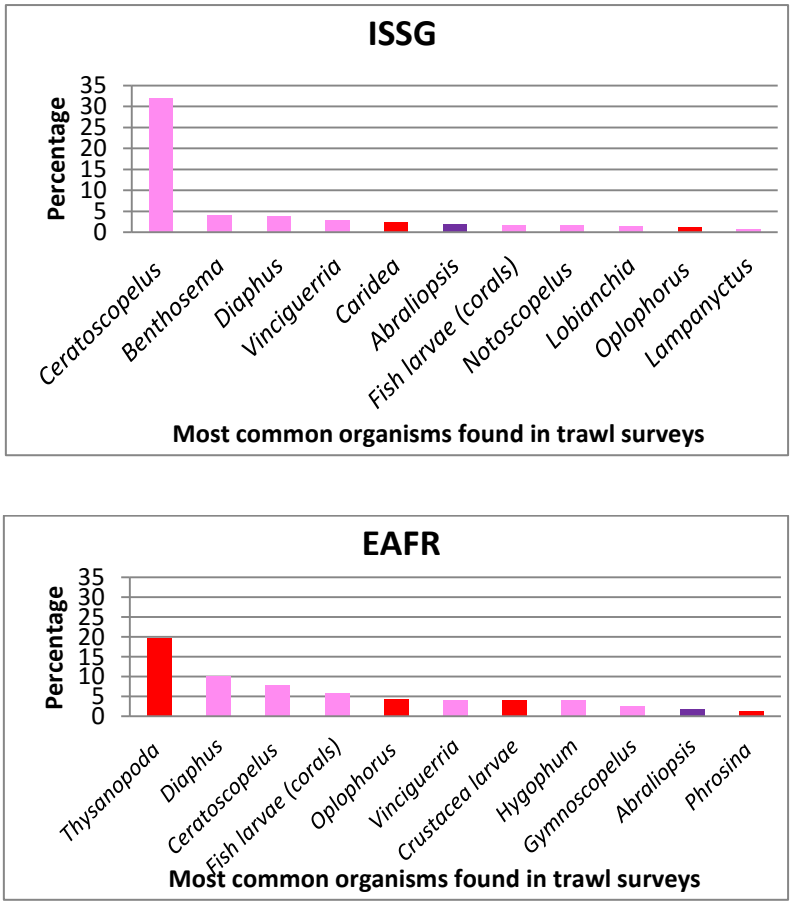

Figure 14 Percentage (by number) of the 11 most abundant organisms caught by trawls in the ISSG and EAFR. Red bars represent crustaceans, pink bars represent mesopelagic fishes and purple bars represent squids.

Overall, a greater cumulative percentage of fishes dominated the trawls in both the ISSG and EAFR (Figure 15).

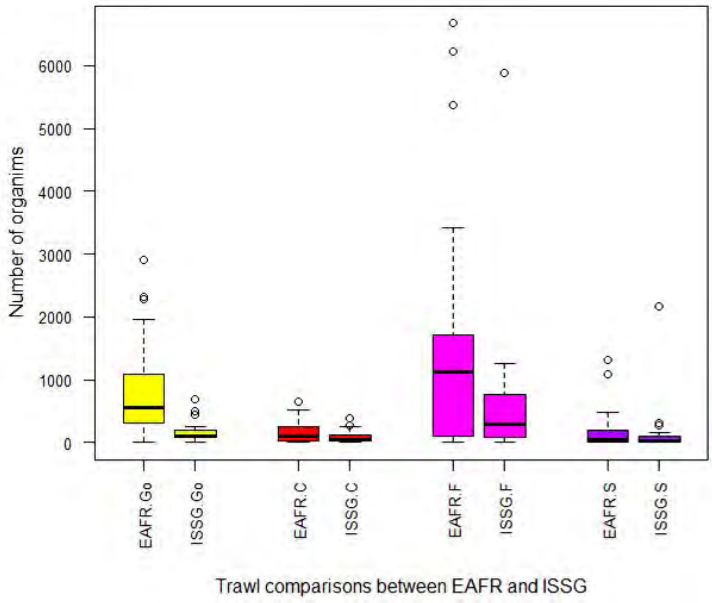

Figure 15 Comparisons between trawls in the EAFR and ISSG (day and night included) of the numbers of gelatinous organisms (Go), crustaceans (C), fishes (F) and squids (S) represented by yellow, red, pink and purple bars respectively.

All broad categories of micronekton were systematically found in greater numbers in trawls from the MZC compared to trawls in the ISSG province both during the day and night (MANOVA, Wilk's $Lambda_{1,\ 2,\ 3}$= 0.72, 0.71, 0.91, df_1=57, P < 0.05 for region; P < 0.05 for day/night; P = 0.29 for interaction between region and day/night). There was a significant difference between the EAFR and ISSG in the numbers of gelatinous organisms and fishes caught in trawls but no significant differences were found for crustaceans and squids, with these organisms being caught least frequently in both provinces (Pairwise Wilcoxon tests, Gelatinous: W= 644.5, df_1= 38, df_2= 18, P < 0.05; Crustaceans: W= 471.5, df_1= 38, df_2= 18, P = 0.10; Fishes: W= 497.0, df_1= 38, df_2= 18, P < 0.05; Squids: W= 390.5, df_1= 38, df_2= 18, P =0.75).

Compared to trawl surveys, swordfish sampled a greater proportion of squids, especially of the genus *Ommastrephes,* in the ISSG. The fishes *Scopelarchus* and *Myctophum* were the most abundant genera recovered in the stomach contents of swordfish in the EAFR province (Figure 16). The micronekton organisms, *Ommastrephes*, *Diaphus*, *Diretmichthys*, *Onykia, Sthenoteuthis,* and *Cubiceps* were caught

by this top predator in both provinces whereas gelatinous organisms were the rarest items found in stomach samples (absent in Figure 16).

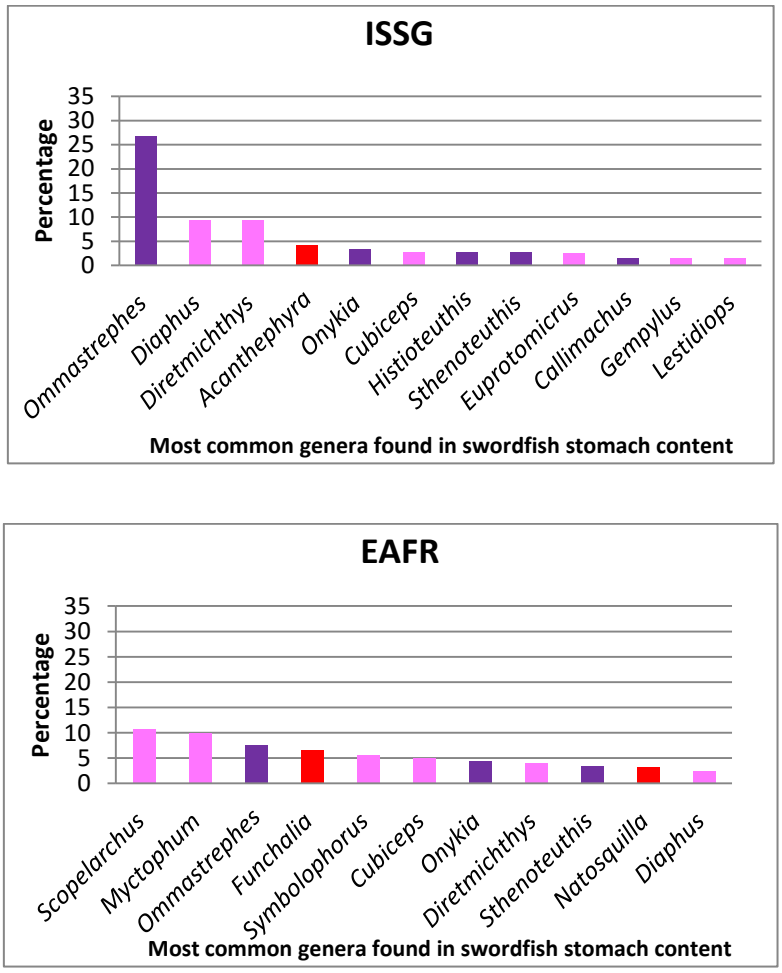

Figure 16 Percentage (by number) of the 11 most abundant organisms found in the stomachs of *Xiphias gladius* in the ISSG and EAFR. Red bars represent crustaceans, pink bars represent the fishes and purple bars represent squids.

There was a significant difference in the occurrence of crustaceans (W= 253, n= 38, $P < 0.05$), fishes (W= 3912.5, n= 131, $P < 0.05$) and squids (W= 664, n= 56, $P < 0.05$) in trawls and swordfish stomachs, with a greater percentage of squids found in the stomach content of *Xiphias gladius* (Figure 16). No significant differences were found in the occurrence of gelatinous organisms in trawls or swordfish stomach content (W= 8, n= 9, $P = 0.14$).

A significant difference was found between the ISSG and EAFR provinces in the abundance and richness of species in trawl data (Shannon diversity index, W=507, n= 58, $P < 0.05$; Species richness,

W= 420.5, n= 58, P < 0.05). Stomach contents of *Xiphias gladius*, caught in the EAFR and ISSG, also showed significant differences in the species richness and abundance of micronekton (Shannon diversity index: W=11171, n= 261, P < 0.05; Species richness: W= 11375.5, n= 261, P < 0.05) with a greater abundance of species in swordfish stomach content from the EAFR province (Figure 17A).

The species accumulation curves for trawl and stomach content data do not have a well-defined plateau. The trawl species richness in the ISSG province was greater than in the EAFR, although fewer trawls were carried out in the ISSG (19 trawls in total). Extrapolation of the fitted trawl logarithmic curve for the ISSG (dashed red line in Figure 17B) shows that if the same constant effort was applied, a greater number of new species might have been identified during MICROTON than during the MESOP cruise.

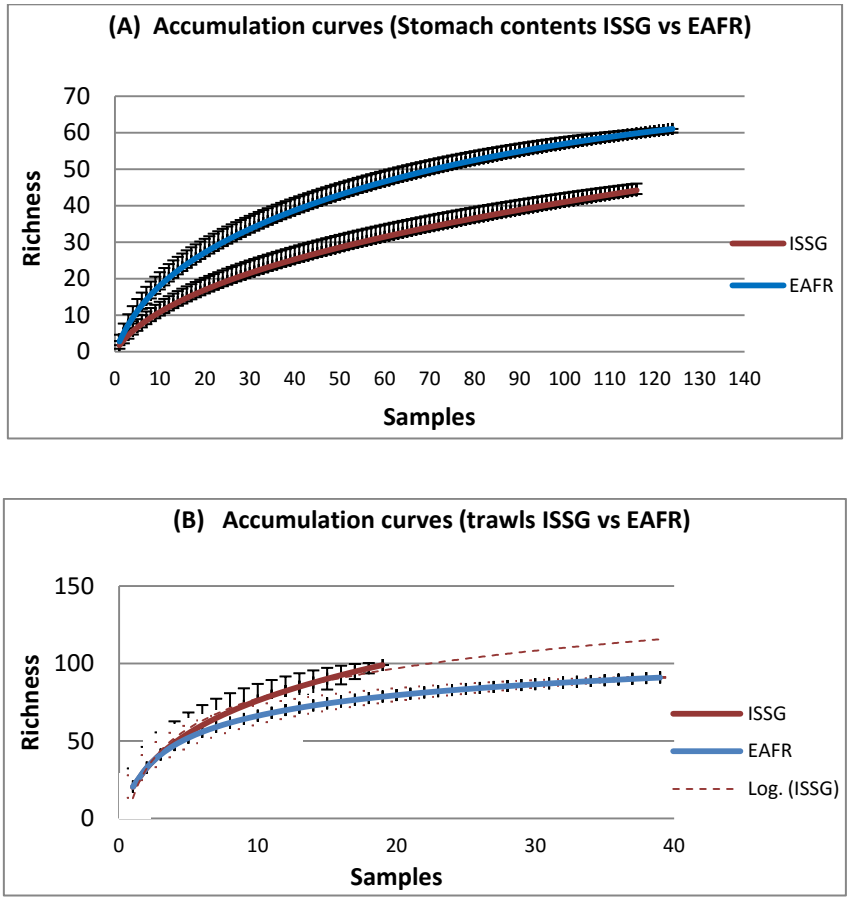

Figure 17 Species accumulation curves for the EAFR and ISSG from (A) swordfish stomach contents and (B) trawl data. Error bars are the corresponding standard deviations shown in black. Extrapolation of the data series for ISSG is shown by the red broken line.

IV.5 Stable isotope analysis (the ISSG province)

The nine broad categories (listed in Table 4) were segregated by their isotope signatures of both nitrogen (Kruskal-Wallis chi-squared = 452.1, df = 8, $P < 0.05$) and carbon (Kruskal-Wallis chi-squared = 485.2, df = 8, $P < 0.05$).

POM-Fmax (5.6 ± 0.9‰), zooplankton (5.1 ± 0.9‰) and gelatinous organisms (5.3 ± 1.9‰) had approximately similar mean (± S.D.) values of $\delta^{15}N$ (Pairwise Wilcoxon tests, $P > 0.05$), but they were distinguished by their $\delta^{13}C$ values. Gelatinous organisms differed significantly in their $\delta^{15}N$ values from crustaceans, squids and swordfish (Pairwise Wilcoxon tests, $P < 0.05$).The mean (± S.D.) nitrogen isotope values of fishes (8.7 ± 1.5‰) and squids (8.9 ± 1.4‰) were more similar than the mean (± S.D.) nitrogen isotope values of crustaceans (7.8 ± 1.9‰) (Table 4).

Table 4 Mean and standard deviation of $\delta^{15}N$ and $\delta^{13}C$ stable isotope values for the micronekton broad categories in the ISSG.

Broad category	$\delta^{15}N$ isotope values (in ‰)	$\delta^{13}C$ isotope values (in ‰)
	Mean ± S.D.	
Swordfish	15.1 ± 0.4	-16.7 ± 0.3
Squids	8.9 ± 1.4	-17.6 ± 0.7
Fishes	8.7 ± 1.5	-18.4 ± 0.5
Crustaceans	7.8 ± 1.9	-18.0 ± 0.3
Gelatinous	5.3 ± 1.9	-20.3 ± 1.1
Mysids	5.4 ± 0.8	-20.6 ± 0.3
Copepods	4.7 ± 0.9	-20.9 ± 0.4
POM-Surf	6.3 ± 0.8	-24.0 ± 0.3
POM-Fmax	5.6 ± 0.9	-24.7 ± 0.6

The $\delta^{15}N$ stable isotope values of POM ranged from 3.9 to 7.3‰. Zooplankton $\delta^{15}N$ isotope signatures ranged from 2.6 to 6.7‰. Micronekton (crustaceans, fishes and squids) had the largest range in $\delta^{15}N$ (3.0 to 13.5‰) with a mean (± S.D.) of 8.4 ± 1.7‰. Swordfish specimens in the ISSG exhibited the highest $\delta^{15}N$ isotope values, ranging from 13.8 to 16.2‰, with a mean (± S.D.) of 15.1 ± 0.4‰.

Biplots of $\delta^{15}N$ and $\delta^{13}C$ (Figure 18) showed a clear segregation between POM, zooplankton, micronekton (crustaceans, fishes and squids) and swordfish (MANOVA, Wilk's lambda, $df_1 = 8$, $df_2 = 581$, $F_{1176}=522.5$, $P < 0.05$).

The standard ellipses of POM-Surf and POM-Fmax partially overlapped (Figure 18) and no significant differences were found in the $\delta^{15}N$ stable isotope values of POM-Surf and POM-Fmax (Pairwise Wilcoxon test, $P = 0.18$). The standard ellipse area (SEA) of gelatinous organisms encompassed those of the two zooplankton types, with gelatinous organisms displaying a wider isotopic niche width ($SEA_c = 6.36$) than copepods ($SEA_c = 1.31$) and mysids ($SEA_c = 0.68$). Crustaceans, fishes and squids also had overlapping standard ellipses, with mesopelagic fishes and squids having more similar niche widths ($SEA_c = 2.39$ and 2.83 respectively) than crustaceans ($SEA_c = 1.56$). However, crustaceans, fishes and squids could not be differentiated by their $\delta^{15}N$ isotope signatures (Pairwise Wilcoxon tests, $P > 0.05$).

Pairwise comparisons showed that the carbon stable isotope values of gelatinous organisms and zooplankton were not significantly different ($P = 1.00$). All other means differed significantly in their $\delta^{13}C$ values ($P < 0.05$).

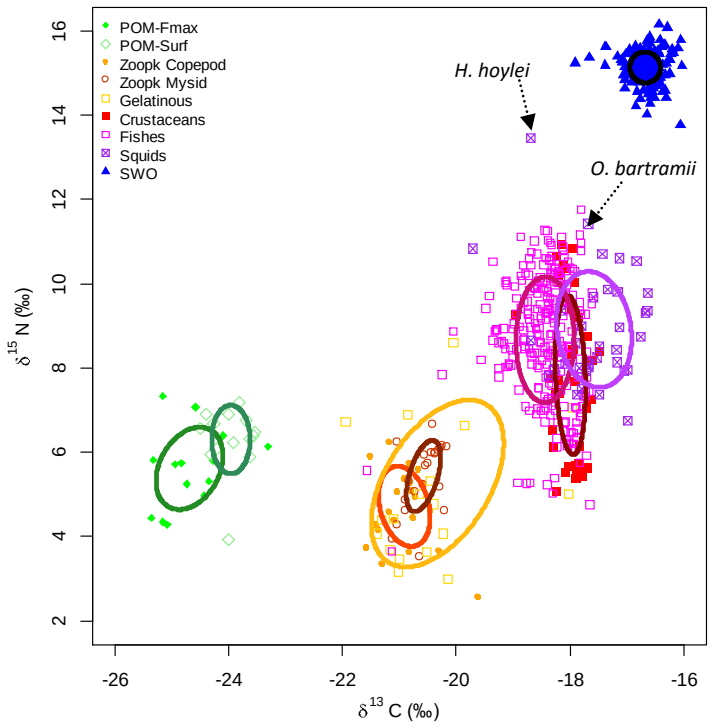

18 Bivariate plot of $\delta^{15}N$ and $\delta^{13}C$ values (‰) for POM (found at the DCM and at the surface), copepods, mysids, gelatinous organisms, crustaceans, mesopelagic fishes, squids and swordfish in the ISSG province. Standard ellipse areas (coloured solid lines) provide estimates of the isotopic niche area of each of these categories, calculated using SIBER. The squid species, *Histioteuthis hoylei* and *Ommastrephes bartramii* are shown by the broken arrows.

Ascending the food web from zooplankton via micronekton to swordfish, $\delta^{15}N$ and $\delta^{13}C$ stable isotope values of consumers generally increased. With the copepod group chosen as primary consumer species (estimated trophic level of 2.0); the estimated trophic levels of the three broad classes (crustaceans, fishes and squids) were 2.98, 3.24 and 3.32 respectively. These micronekton taxa were therefore found at higher trophic levels than POM, gelatinous organisms and zooplankton.

Additionally, within the squids sampled, estimated trophic levels ranged from 3.09 (*Abraliopsis* spp.with mean (±S.D.) $\delta^{15}N$ value of 8.23 ± 0.71‰), to 4.10 (for one *Ommastrephes bartramii* specimen with $\delta^{15}N$ value of 11.42‰) and 4.73 (for one *Histioteuthis hoylei* specimen with $\delta^{15}N$ value of 13.45‰). Some of the crustaceans and fishes were found at a lower trophic level than squids, having estimated trophic level values of 2.34 (crustacean *Funchalia taaningi* with mean (±S.D.) $\delta^{15}N$ value of 6.05 ± 0.83‰) and 2.33 (mesopelagic fish *Lestrolepsis intermedia* with mean (±S.D.) $\delta^{15}N$ value of 5.78 ± 0.58‰). Swordfish specimens had higher trophic level values (5.26) than the other categories. Organisms with different feeding regimes had significantly different $\delta^{15}N$ (ANOVA, $F_{3,341}$= 38.0, $P < 0.05$) and $\delta^{13}C$ (ANOVA, $F_{3,341}$=74.5, $P < 0.05$) values. The range of $\delta^{15}N$ and $\delta^{13}C$ values for carnivores (mostly mesopelagic fishes and squids) and omnivores (mainly crustaceans) partially overlapped (Figure 19). For $\delta^{13}C$ values, two groups can be observed: detritivores- filter feeders and carnivores-omnivores.

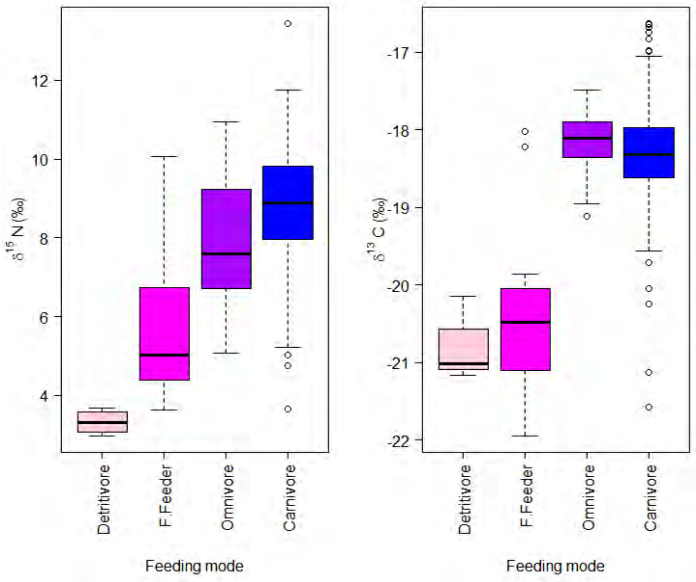

Figure 19 Box and Whisker diagrams showing the medians (thick black line in box plots), the interquartile ranges, (Q_1 to Q_3), and the spread of $\delta^{15}N$ and $\delta^{13}C$ values (‰) across four different feeding modes of micronekton – carnivores (represented by blue boxes), omnivores (purple boxes), filter feeders (magenta boxes) and detritivores (pale pink boxes).

Pairwise comparisons showed the $\delta^{15}N$ values of filter feeders, detritivores, omnivores and carnivores to be different ($P < 0.05$). Organisms from the two groups (omnivores and carnivores, filter feeders and detritivores) rely on different food sources (Pairwise Wilcoxon tests, $P = 0.27$ for $\delta^{13}C$ isotope signatures of carnivores-omnivores and $P = 0.51$ for $\delta^{13}C$ isotope signatures of filter feeders-detritivores).

Figure 20 shows the progression in trophic levels of the micronekton, from detritivores (found at the lowest trophic level), to carnivores (mostly mesopelagic fishes and squids) found at the highest trophic level.

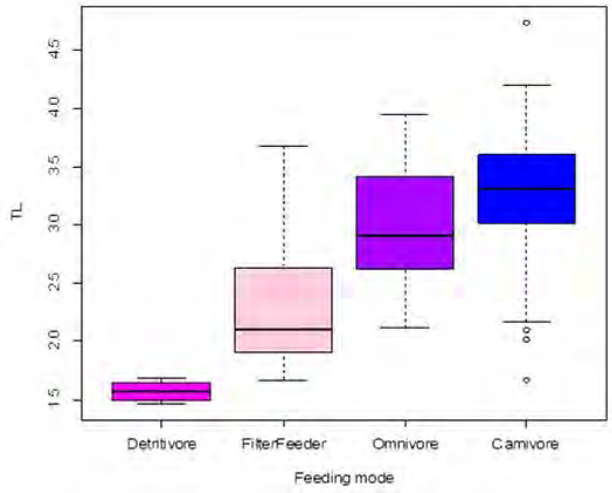

Figure 20 Box and Whisker diagram showing the medians (thick black line in box plots), the interquartile ranges, (Q_1 to Q_3), and the spread of trophic level values across four different feeding modes (carnivores, omnivores, detritivores and filter feeders) of micronekton in the ISSG.

No clear relationship was found between $\delta^{15}N$ stable isotope values and the size (in mm) of the carnivorous micronekton species (Figure 21) collected in trawls in the ISSG province ($r=0.04$, $F= 0.66$, $n=270$, $P = 0.4$).

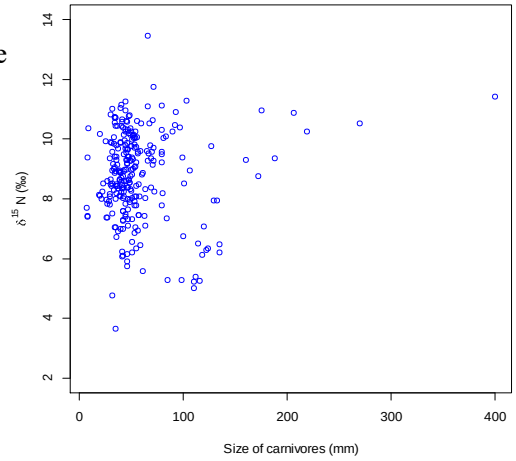

Figure 21 Scatter plot showing the relationship between $\delta^{15}N$ isotope values (‰) and the size of the carnivores of micronekton (mm).

The relationships between the $\delta^{15}N$ isotope values of two squid specimens (*S. oualaniensis* and *Abraliopsis* spp.) and three fish taxa (*C. warmingii*, *L. intermedia* and *S. evermanni*) and size (mm) were not straightforward (Figure 22). However, there is a clear distinction in the sizes of organisms between the ISSG and EAFR. For the same body length, organisms from the EAFR tended to have higher $\delta^{15}N$ stable isotope values compared to organisms from the ISSG.

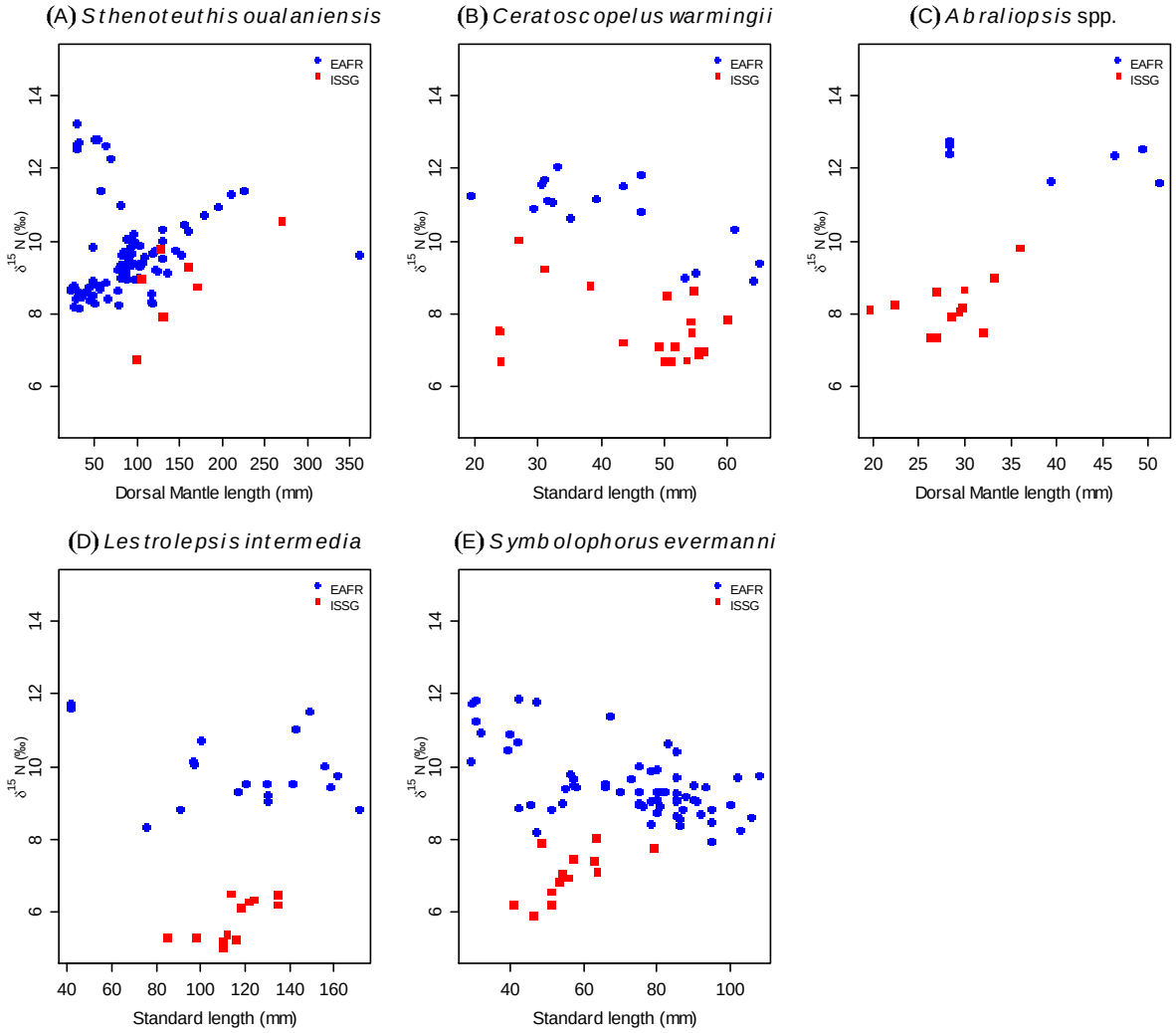

Figure 22 $\delta^{15}N$ values (‰) plotted against body lengths (mm) for (A) *Sthenoteuthis oualaniensis*, (B) *Ceratoscopelus warmingii*, (C) *Abraliopsis* spp., (D) *Lestrolepsis intermedia* and (E) *Symbolophorus evermanni*. Body lengths included dorsal mantle lengths (mm) for (A) and (C); standard lengths (mm) for (B), (D) and (E) in the EAFR (blue) and ISSG (red).

A positive relationship was found between $\delta^{15}N$ values of swordfish tissues and sizes (mm) of swordfish in both the EAFR and ISSG.

The $\delta^{15}N$ values of swordfish also differed significantly as a function of size and region (Linear model, $F_{2, 349}= 345$, $P < 0.05$) (Figure 23). In the EAFR, the lower $\delta^{15}N$ values of swordfish were, mean (± S.D.) 11.1 ± 0.64‰, for smaller-sized individuals having mean (± S.D.) body lengths of 864 ± 156 mm. Individuals having body lengths of 1593 ± 323 mm had higher mean (± S.D.) $\delta^{15}N$ values (14.4 ± 0.37‰) in the EAFR. Larger-sized (body length > 1000m) swordfish specimens in the ISSG had mean (± S.D.) $\delta^{15}N$ values of 15.1 ± 0.36‰.

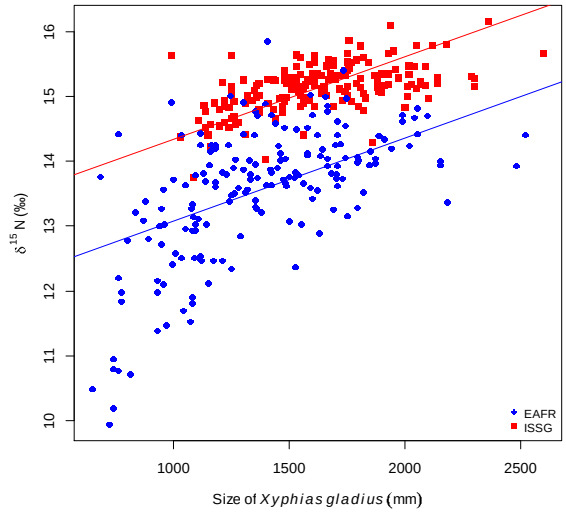

Figure 23 Scatter plot showing the relationship between $\delta^{15}N$ values (‰) and the size of *Xiphias gladius* (mm) in the ISSG (red) and EAFR (blue). Simple linear regressions for $\delta^{15}N$ values vs. body length (mm) are shown by red and blue lines.

Fitting a linear regression to $\delta^{15}N$ values of swordfish against size and extrapolating the line of best fit shows that, overall, there is no continuity in nitrogen isotopes between the size of the predators and the size of the micronekton sampled in the ISSG whereas there is a continuity in the nitrogen isotopes between the size of micronekton and that of swordfish sampled in the EAFR (Figure 24).

(A) ISSG **(B) EAFR**

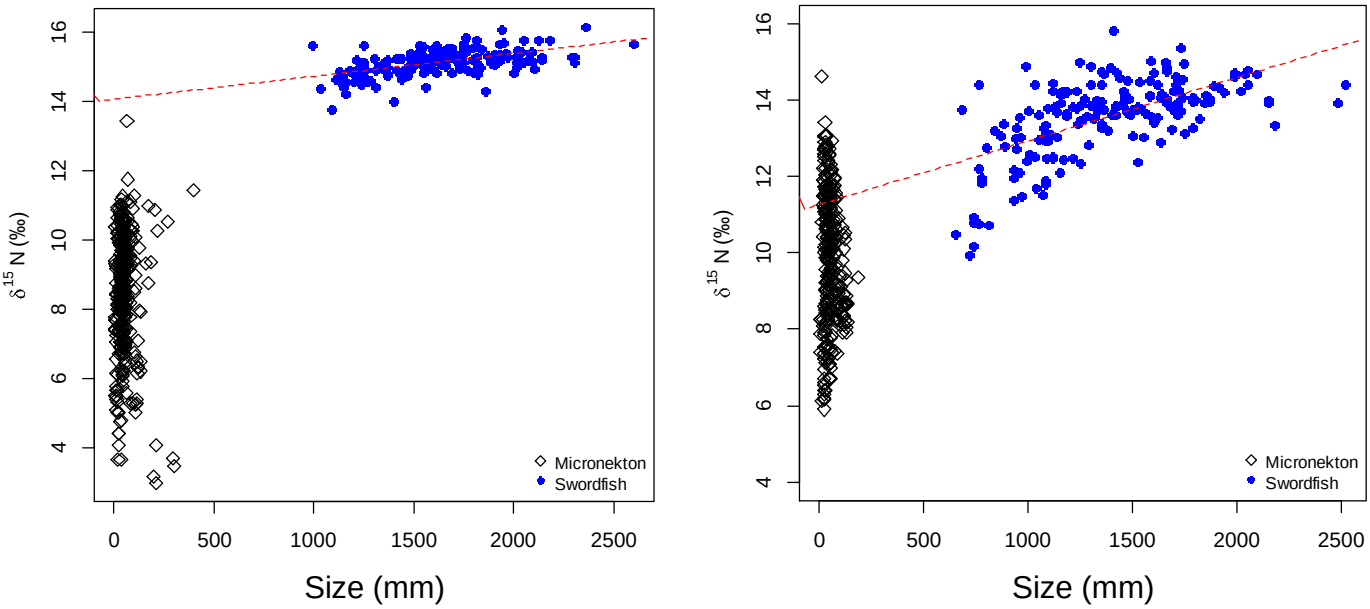

Figure 24 Scatterplot showing the relationship between $\delta^{15}N$ isotopic values (‰) and the size (mm) of swordfish (blue) and micronekton (black) in (A) the ISSG and (B) the EAFR, with the lines of best fit to the swordfish data in red.

IV.6 Comparison of stable isotope analyses from the ISSG and EAFR

Biplots of $\delta^{15}N$ and $\delta^{13}C$ (Figure 25) showed a clear segregation between POM, micronekton and swordfish in the EAFR in both $\delta^{15}N$ (Kruskal-Wallis chi-squared = 371, df = 6, $P < 0.05$) and $\delta^{13}C$ values (Kruskal-Wallis chi-squared = 424, df = 6, $P < 0.05$). Stable isotope analysis was not carried out on zooplankton samples collected on the MESOP 2010 cruise.

The standard ellipse areas of POM-Surf and POM-Fmax did not overlap and each of these groups seemed to occupy a unique isotopic niche space. POM-Surf and POM-Fmax were segregated by their $\delta^{15}N$ values (Pairwise Wilcoxon test, $P < 0.05$) but not by their $\delta^{13}C$ values (Pairwise Wilcoxon test, $P = 0.05$) in the EAFR. Pairwise comparisons also showed that $\delta^{15}N$ values of gelatinous organisms and POM- Surf did not differ significantly ($P = 0.30$) in the EAFR whereas the carbon isotope signatures of gelatinous organisms differed significantly from that of POM (Pairwise Wilcoxon tests, $P < 0.05$). Based on the standard ellipse areas, crustaceans, fishes and squids seemed to occupy the same trophic position (Figure 25). Compared to the ISSG, where there was a clear segregation between micronekon and swordfish, some of the micronekton organisms in the EAFR (notably the squids and mesopelagic fishes) and the swordfish specimens shared the same $\delta^{15}N$ and $\delta^{13}C$ values.

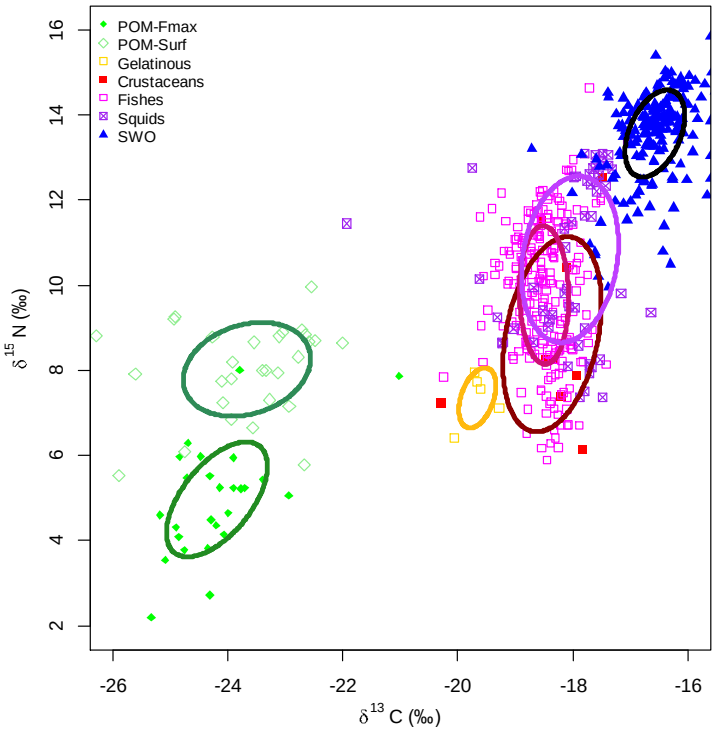

Figure 25 Bivariate plot of $\delta^{15}N$ and $\delta^{13}C$ values (‰) for POM (found at the DCM and at the surface), gelatinous organisms, crustaceans, fishes, squids and swordfish in the EAFR province. Standard ellipse areas (SEA, coloured solid lines) provide estimates of the niche area of each of these groups, calculated using SIBER.

Significant differences were found in $\delta^{15}N$ and $\delta^{13}C$ values among all the broad categories in both the ISSG and EAFR (MANOVA, Wilk's lambda, $df_1 = 1$, $df_2 = 8$, $df_3 = 6$, $df_4 = 1105$, $P < 0.05$ for region, broad class and for both the region and broad class).

POM-Surf in the EAFR had higher $\delta^{15}N$ stable isotope values (from approximately 6 to 10‰) than POM found at the DCM and POM-Surf found in the ISSG (Figure 26A).There is a clear distinction in $\delta^{13}C$ stable isotope values between POM, zooplankton, micronekton and swordfish, both in the ISSG and EAFR (Figure 26B).

The estimated mean trophic levels of the micronekton broad classes were 3.17, 3.46 and 3.72 respectively in the EAFR. The tissues of micronekton in the EAFR were more enriched in $\delta^{15}N$ than tissues of micronekton from the ISSG with crustaceans, fishes and squids in the ISSG having estimated mean trophic levels of 2.98, 3.24 and 3.32 respectively. Micronekton in the EAFR were found at a slightly higher trophic level than micronekton in the ISSG.

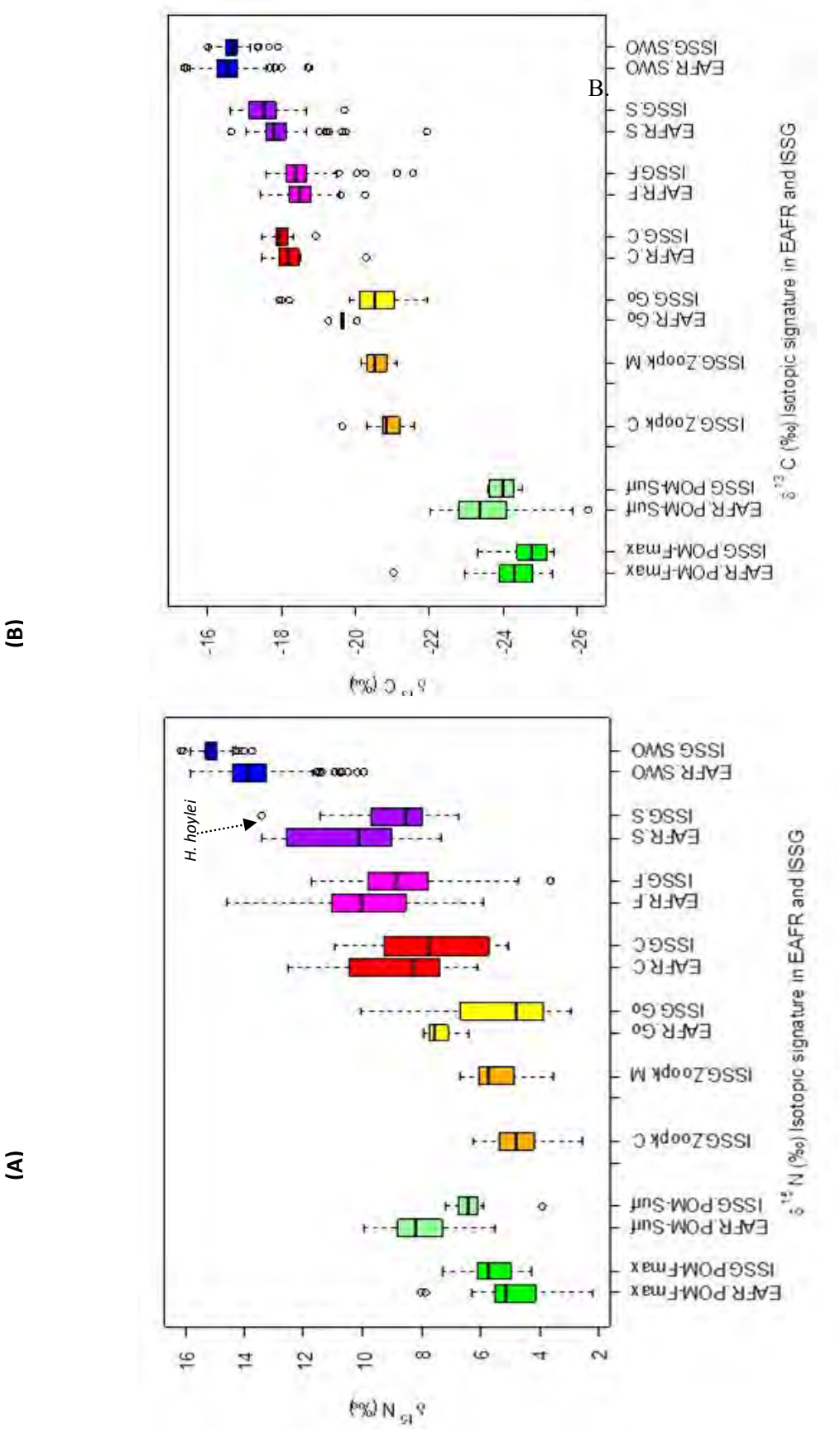

Figure 26 Box and Whisker diagrams comparing EAFR and ISSG values of the medians (thick black line in box plots), the interquartile ranges (Q_1 toQ_3), and the spread for (A) $\delta^{13}C$ (B) $\delta^{15}N$ values (‰) across nine broad categories labelled POM-Fmax, POM-Surf, Zoopk C (Zooplankton Copepods), Zoopk M (Zooplankton Mysids), G (Gelatinous organisms), C (Crustaceans), F (Fishes), S (Squids) and SWO (Swordfish). The squid species, *Histioteuthis hoylei*, is shown with the broken arrow.

V. Discussion

V.1 Open ocean systems: from low to high trophic levels

Although MICROTON covered only a small part of the ISSG province, results showed that the main environmental forcing in the region is the wide-scale Subtropical (anticyclonic) Gyre, which leads to a large physical downwelling, pushing nutrients (the nitracline) and chloroplyll (the DCM) deeper in the water column, therefore leading to an oligotrophic environment that impacts both low and high trophic levels.

The oceanic low trophic levels are dominated by different groups of phytoplankton, which have developed adaptation mechanisms to their habitat. Prokaryotes, which have a high proportion of the photo-pigment PPC (photoprotective role) (Barlow *et al*., 2014), proliferate in oligotrophic environments (Cavicchioli *et al*., 2003), especially in the high irradiance, low nutrient surface environment (Table 2). Flagellates, having higher concentrations of TChla and PSC in their cells, are better adapted to survive in the low-light, nutrient-replete conditions of the DCM. DVChla is a pigment contributing to TChla (found to be abundant at the DCM) and is indicative of the prokaryotic group *Prochlorococcus*.

With their small cell size, *Prochlorococcus* is capable of surviving at low resource concentrations (Ward *et al*., 2012) and in highly stratified oligotrophic waters, extending deeper in the water column (Christaki *et al*., 1999) than the second dominant prokaryotic group, *Synechococcus*. In the equatorial Pacific Ocean, *Prochlorococcus* have been measured down to a depth of 150 m (Vaulot *et al*., 1995), whereas in the subtropical North Pacific Ocean, low concentrations of *Procholorococcus* were still observed at 200 m (Campbell and Vaulot, 1993). *Prochlorococcus* and *Synechococcus,* which are at the base of marine food webs, are shown to be dominant phytoplankton species in Figure 27 in the ISSG province (Alvain *et al*., 2008).

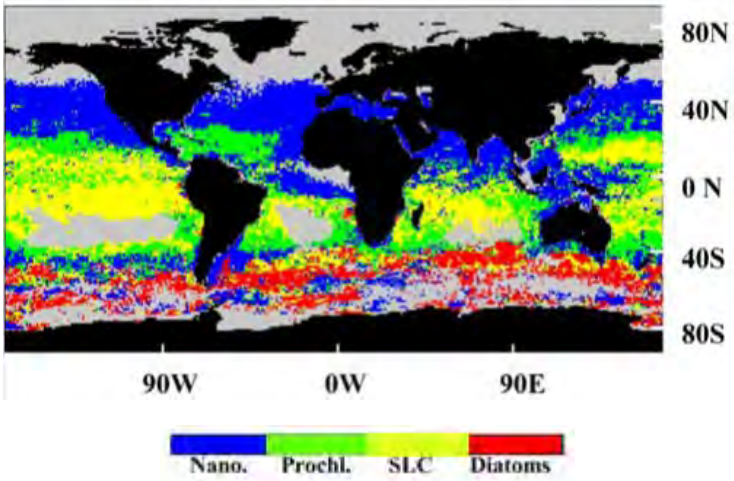

Figure 27 Map, (derived from satellite SSC), of the standard phytoplankton groups dominating the world's oceans. Distribution of nanoeukaryotes (deep blue), *Prochlorococcus* (green), *Synechococcus* (SLC, yellow) and diatoms (red) are shown (Alvain *et al*., 2008).

The distribution of major phytoplankton groups in Figure 27 is, however, subjected to seasonal cycles and interannual variability (Alvain *et al*., 2008). Field studies have identified different patterns in *Synechococcus* and *Prochlorococcus* abundance. In the central and subtropical North Pacific Ocean, close to Hawaii island, *Synechococcus* abundance was reduced compared to *Prochlorococcus* (Campbell and Vaulot, 1993), whereas the opposite pattern was observed in the northern Indian Ocean, where *Synechococcus* was more abundant (Veldhuis and Kraay, 1993; Campbell *et al*., 1994). These phytoplankton groups are prey to numerous microzooplankton (Landry, 2002) in all ocean basins.

Zooplankton is thought to act as a biological pump in marine ecosystems, connecting primary production and fish production (Fukuda *et al*., 2012). It is thought that the success and failure of the pelagic fishery is reliant, to a certain extent, on plankton availability (Gupta and Desa, 2001). Zooplankton production is generally low in open ocean systems compared to coastal waters, because waters bordering landmasses are more enriched with nutrients (Gupta and Desa, 2001). The zone between 20°S and 30°S in the Indian Ocean was reported to be poor in zooplankton (Gupta and Desa, 2001). The thermocline which acts as a density barrier in tropical latitudes, limits the passage of nutrients in surface euphotic layers, hence limiting primary productivity (Voituriez, 2003). Zooplankton biomasses have been shown to be correlated with areas of high chlorophyll

concentrations (Huggett, 2014). The ISSG, having relatively low chlorophyll values, can hence limit the proliferation of zooplankton communities. In contrast, mean zooplankton biomasses in the western, central and north Pacific Ocean were found to be several orders of magnitude higher with values of 45.1 mg m^{-3}, 25.4 mg m^{-3} and 21.5 mg m^{-3} during the winter months (Nagasawa, 2000), compared to the ISSG province.

Water-column dynamics, such as shoaling of the thermocline during cyclonic events (even in an oligotrophic and relatively homogenous environment like the ISSG), can further add to the complexity of DVM patterns of zooplankton. The deeper the thermocline (as is the case in the ISSG province), the more it can impact on the distribution of zooplankton in the water column. For some surface communities, the thermocline is the limit of descent at dawn, whereas some deep populations will migrate up to the thermocline at dusk (Tait, 1980), thereby influencing the distribution pattern and DVM of micronekton populations. Many mesopelagic fishes, including the myctophids, were reported to halt at the base of the thermocline (Tyler, 2003) where there is probably a greater concentration of available prey items (Rissik and Suthers, 2000).

The distribution of micronekton in the water column was investigated using hydroacoustic data. The majority of the acoustic responses detected during the survey can be attributed to migratory micronekton, usually distributed in the upper 200 m of the water column at night and migrating below 400 m during the day. Those daily ascents and descents of the micronekton during crepuscular periods (dusk and dawn respectively) corresponded to the well-known process of diel vertical migration (Lebourges-Dhaussy *et al*., 2000). The largest changes in micronekton distribution between day and night were observed with hydroacoustics in the shallow layer (10-200 m), with smaller changes in the deep layer (400- 740 m) and the intermediate layer (200- 400 m) exhibiting almost no changes (Figure 11). The shallow layer also showed a significant proportion of micronekon (25%) migrating slightly above the thermocline (between 100 and 160 m) at night. The mean vertical profile of acoustic densities was flatter during the day than night in the ISSG and the total acoustic response was greater during the night than the day, suggesting migration from layers deeper than 740 m, i.e. beyond the range of the 38 kHz transducer (Béhagle *et al*., 2014).

Trawl surveys provided information about the likely dynamics and vertical movements of each broad category of micronekton, with fishes and gelatinous organisms being more widely caught by nets across all depth categories, both during the day and night. The ten night trawls and two day trawls in the shallow layer (10- 200 m) caught a very low proportion of crustaceans and squids in the ISSG (Figure 13). However, net sampling is widely thought to undersample micronekton communities and hence underestimate their biomass (Kaartvedt *et al*., 2012, Young *et al*., 2015). Sampling gears do not capture mesopelagic fishes, crustaceans and squids quantitatively. This might be due to various influences such as extrusion through meshes (for smaller specimens) and net avoidance behaviour (for squids and fishes that are capable of rapid movement) (Brodeur *et al*., 2005; Kaartvedt *et al*., 2012). Soft-bodied gelatinous organisms can also undergo considerable damage in trawls, making identification impossible. Regardless of trawl type, acoustic abundance estimates always appear to be consistently higher by approximately one order of magnitude than net-based estimates (Kaartvedt *et al*., 2012). Furthermore, the question also arises of whether the 19 trawls sampled (as was the case during MICROTON) are representative of a whole ecosystem. However, despite such limitations, trawls are important for the sampling of biological samples for taxonomic identification, stable isotope analyses and hence investigation of the trophic position of organisms.

Fishes, crustaceans and squids are important components of pelagic food webs since they are fed on directly or indirectly by most pelagic predators (Young *et al*., 2015). Important predators of micronekton, such as swordfish, mimic the vertical migration pattern of micronekton. Top predators are adapted to undergo DVM, descending in deeper layers during the day and returning to the mixed layer after dusk to feed and to recover from the thermal and oxygen dept acquired by day (Abascal *et al*., 2010). Swordfish has been reported to forage near the surface to a maximum of 90m at night and as deep as 650 m by day, with a maximum depth recorded at 900 m (Carey and Robison, 1981; Chancollon *et al*., 2006). A small proportion of micronekton was found to remain in deep layers at night and surface layers during the day (further discussed in section V.3). Being able to reach very deep waters, swordfish species thus have access to a large size range of prey (Ménard *et al*., 2007), both during the day and night.

V.2 Trophic position of micronekton in the ISSG province

Stable isotope techniques provide a practical method of measuring the trophic relationships between food web components. The enrichment of $\delta^{15}N$ from one trophic level to the next provides a means to estimate the trophic level of individual taxa/size classes (Post, 2002). However for trophic level estimations, knowledge of the $\delta^{15}N$ reference baseline value is necessary. Particulate organic matter (POM) sampled by filtration of sea water is often used to determine the reference value for the food base (Lorrain *et al*., 2015).

Stable isotopes of carbon allow for discrimination of different sources of primary production, typically inshore vs offshore or pelagic vs benthic (Rubenstein and Hobson, 2004). The mean $\delta^{13}C$ stable isotope values of gelatinous organisms were similar to those of the two zooplankton types (approximately -20‰) (Table 4). The micronekton groups (crustaceans, fishes and squids) had intermediate $\delta^{13}C$ values (approximately -18‰) and swordfish had the lowest carbon isotope signatures (-16.7‰). Based on the $\delta^{13}C$ values, four distinct groups can be identified. A small enrichment of 0.5- 1.0‰ in $\delta^{13}C$ stable isotope values in animal tissues relative to their diets has been reported (DeNiro and Epstein, 1978; Michener and Kaufman, 2007). The predicted enrichment in ^{13}C can clearly be seen across the four groups (POM, zooplankton, micronekton and swordfish) in the ISSG province.

Within the micronekton, the $\delta^{13}C$ isotope signatures of crustaceans, fishes and squids were found to be significantly different. The "isotope routing" effect might be different for the different taxa, especially concerning the allocation of energy for reproduction and somatic growth. Isotopically different dietary components can be allocated or "routed" unequally among a consumer's tissues (Buchheister and Latour, 2011). This can account for differences in acquisition of the isotope signals of nitrogen and carbon.

The mean $\delta^{15}N$ values of POM collected at the surface (POM-Surf) and at the DCM were exceptionally high (6.0 ± 0.9‰ recorded). Filtration of sea water allows detritus, microbial heterotrophs and microzooplankton to be analysed in addition to POM (Lorrain *et al*., 2015), yielding

enhanced $\delta^{15}N$ values, as shown in this study conducted in an oligotrophic environment. For lack of a better baseline, copepods were used in trophic level estimations, despite potential seasonal and spatial variations in zooplankton isotope values. POM-Surf had higher $\delta^{15}N$ and lower $\delta^{13}C$ values than POM-Fmax. POM-Fmax is usually exposed to an enhanced level of phytodetritus and faecal pellets from the euphotic zone (Fanelli *et al*., 2011). This can be illustrated by the standard ellipse of POM-Fmax which was skewed to the right and was spread over a wider range of $\delta^{13}C$ values than the standard ellipse of POM-Surf (Figure 18). However, both share the same isotopic niches and, statistically, no significant differences were observed between surface POM and POM found at the DCM.

The zooplankton copepods and mysids had mean $\delta^{15}N$ values of 5.1 ± 0.9‰. Micronekton (crustaceans, fishes and squids) and swordfish had higher nitrogen isotope signatures than zooplankton (Table 4). An averaged ^{15}N enrichment of 3.3‰ was observed between zooplankton and micronekton as a whole, which agrees with the + 3.4 ± 1.1‰ enrichment in $\delta^{15}N$ per trophic level identified by Minagawa and Wada (1984). These two groups are therefore found at successive trophic levels (trophic level of 2 for zooplankton and averaged trophic level of 3.18 for micronekton).

Twice the average enrichment factor was found between *Xiphias gladius* and the micronekton specimens sampled during the trawl surveys (average enrichment value of 6.7‰). It seems that one trophic level is missing between the micronekton sampled by trawls (average trophic level of 3.18) and swordfish, which were found to have an average trophic level of 5.26. The trawl surveys therefore poorly sampled the micronekton organisms that are being directly preyed upon by swordfish. These top predators are known to feed on large organisms (such as *Histioteuthis hoylei* and the large "flying squid", *Ommastrephes bartramii*), capable of net avoidance behaviour. The two large squid species sampled (one 400-mm *O. bartramii* and one 66-mm *H. hoylei*) had estimated trophic levels of 4.10 and 4.73 respectively (also highlighted as outliers in Figures 18 and 26) and are found at an intermediate trophic step between swordfish and the other micronekton specimens caught by trawls.

Squids generally form shoals (Clarke, 1980) and have patchy and dispersed distributions (Rodhouse and Nigmatullin, 1996) in open ocean ecosystems. The distribution of adult squids is known to be scattered over extensive areas (Weimerskirch *et al*., 2005), with *Ommastrephid* squid species being divided into populations which spawn in different seasons and have different migratory behaviour (Okutani, 1977). These squid species are known to undergo large-scale migrations over the course of their lifespan, often spawning in the tropics or sub-tropics and migrating to high-latitude feeding grounds during major period of growth and maturation (O'Dor and Coelho, 1993). These might be reasons why large squids were not caught during the trawling and in the stomach content of *Xiphias gladius,* as swordfish are actively seeking out these larger-sized organisms that provide a lot of energy compared to smaller organisms with a diluted distribution, in this low-productivity ecosystem.

The feeding strategy of an organism can influence the carbon and nitrogen isotope signature of its tissues and hence its trophic position. Despite previous studies showing that the tissues of detritivores are enriched in ^{15}N (Ménard *et al*., 2014), leptocephali larvae, which were reported to feed mainly on detrital and dissolved organic matter (Otake *et al*., 1990; Ménard *et al*., 2014), had the lowest mean (± S.D.) nitrogen stable isotope values of 3.3 ± 0.31‰. The standard ellipse area was particularly wide among gelatinous filter feeders and spread over a wide range of $\delta^{13}C$ values (from -18.0‰ to -21.9‰) (Figure 18), emphasizing the generalized feeding behaviour of salps and pyrosomes which results in the different $\delta^{13}C$ stable isotope values of these organisms from the $\delta^{13}C$ stable isotope values of zooplankton and the other micronekton groups.

Statistical results and Figure 20 showed that detritivores and filter feeders can be pooled into one group and carnivores and omnivores into a second group. These two groups of organisms rely on two different food sources. The tissues of carnivores and omnivores were more enriched in $\delta^{13}C$ than the tissues of filter feeders and detritivores, which are similar to results of a previous study conducted in the oligotrophic NW Indian Ocean, where carnivores had higher $\delta^{13}C$ and $\delta^{15}N$ values than any other feeding modes (Fanelli *et al*., 2011).

The stable isotope ratios of crustaceans, fishes and squids displayed a continuum of values over the $\delta^{15}N$ range of 10 ‰, confirming a wide spectrum of feeding strategies. These micronekton organisms occupied similar isotopic niche space (Figure 18) and might even be competing for zooplankton, which is a main food source for mesopelagic fishes and crustaceans. The spread in the standard ellipses of crustaceans, fishes and squids along the $\delta^{15}N$ axis suggests that a wide range of species belonging to different trophic levels exploited a single food source. Furthermore, the similarity in the niche widths and standard ellipses of mesopelagic fishes and squids highlights the carnivorous feeding behaviour of these organisms, which had higher $\delta^{15}N$ values than organisms with other feeding modes. One hypothesis, which might account for the high $\delta^{15}N$ values, is that the food chain length of carnivores is greater than that of detritivores and filter feeders, thus allowing enrichment of tissues in ^{15}N at each intermediate trophic step. Furthermore, the range of $\delta^{15}N$ isotope values of omnivores and carnivores overlap, because omnivores mostly feed on the same organisms (zooplankton, euphausiids, copepods) as carnivores, but they are also known for occasional herbivory (Tanaka *et al*., 2007).

Of relevance is the fact that some organisms change feeding habit during growth. Squids, for example, are known to feed on microplankton at the larval stage and gradually start feeding on larger prey items (copepods, euphausiids, amphipods and peneids) as they grow in size and their tentacles become more developed (FAO, 2010). An important consideration, therefore, is the size of the organism sampled, because large organisms can catch larger prey as they grow and this can be reflected in $\delta^{15}N$ values of the predator (Ménard *et al*., 2014; Hunt *et al*., 2014). However, despite previous studies showing the influence of body length of micronekton on $\delta^{15}N$ (Parry, 2008), this study did not detect any significant relationships between size of some species of micronekton (three fish taxa and two squid species) and $\delta^{15}N$. The sample size of all the other micronekton specimens, because of the net sampling selectivity, was too small for significant comparisons.

Since carnivores typically exhibit higher nitrogen isotope values than organisms with other dietary habits, the potential relationship between micronekton size and a carnivorous feeding strategy was investigated and no significant relationship was identified. *Xiphias gladius* is a carnivore, feeding mainly on squids and other fish species (Stillwell and Kohler, 1985) during its entire lifetime, with a

preference for squids as it grows (Young *et al*., 2006). The standard ellipse width of swordfish sampled in the ISSG was very narrow (SEAc of 0.31). This might be due to the fact that all individuals of the population feed on a wide range of prey (being generalist predators), hence leading to a weak variability in the population and a narrow SEAc. The swordfish specimens sampled in the EAFR had mean (± S.D.) body lengths and $\delta^{15}N$ values of 1626 ± 300 mm and 15.1 ± 0.4‰. Larger-sized swordfish specimens were sampled in the ISSG. No continuity was observed in nitrogen isotopes between the size of swordfish and the size of the micronekton sampled in the ISSG (Figure 24). The gap observed might mean that the study mainly sampled the micronekton organisms in the ISSG that were being eaten by the prey of *Xiphias gladius*, hence missing one trophic level. The fact that no continuity existed between micronekton sampled and the swordfish specimens might also indicate predator-prey relationships between these two categories of organisms.

Statistically, the broad micronekton categories could not be differentiated by their nitrogen isotope signatures during MICROTON probably because of small sample sizes. The differences in the $\delta^{15}N$ values of mesopelagic fishes, crustaceans and squids did not exceed 0.9‰ and they had similar trophic level values of 2.98, 3.24 and 3.32 respectively. For individual species in the trawl surveys estimated trophic levels ranged from 2.28 (*F. taaningi*) to 4.73 *(*H. *hoylei*), showing that micronekton can be tertiary consumers in the ISSG. There is a likely bias in the stable isotope analysis for large-sized micronekton organisms, such as squids *O. bartramii* and *H. hoylei* (largely caught by *Xyphias gladius*), generally avoid nets and were thus poorly sampled and analysed.

V.3 Comparison with the EAFR province

The East African Coastal province is a more dynamic system than the ISSG, because of the presence of mesoscale features (cyclonic and anticyclonic eddies) in the Mozambique Channel (Schouten *et al*., 2003; Lutjeharms, 2006; Ternon *et al*., 2014). Significant variations in SLA were shown in this and previous studies (Ternon *et al*, 2014), with surface currents being very strong, coherent and directly connected to the eddy field compared to the ISSG province. Run-off from the Zambezi River enriches

the coastal waters of Eastern Africa with nutrients (Tew-Kai and Marsac, 2009). The total surface pigment concentration was found to be 20% higher in the prospected area in the EAFR than in the ISSG (Tables 2 and 3). Specific communities of phytoplankton such as *Prochlorococcus* were found to be dominant in surface waters while *Synechococcus* and picoeukaryotes were found to be less abundant (Zubkov and Quartly, 2003).

The enhanced kinetic activity within mesoscale eddies provides mechanisms that drive chlorophyll-enriched waters from the African coast into the MZC (Tew-Kai and Marsac, 2009; Huggett, 2014; Roberts *et al*., 2014) (Figure 10A). Satellite observations and statistical modelling by Tew-Kai and Marsac (2009) showed that cyclonic eddies are the main sources of primary productivity in the central MZC because cyclonic eddies create a vertical displacement of cold, nutrient-rich waters (McGillicuddy *et al*., 1998; Oschlies and Garçon, 1998; Bakun, 2006; Levy, 2008). Cyclonic eddies were also shown to result in higher zooplankton biovolumes in the MZC compared to anticyclonic eddies (Huggett, 2014; Lebourges-Dhaussy *et al*., 2014). Processes occurring at a sub-mesoscale level in the highly turbulent eddy boundaries also favour strong vertical movements, resulting in local enrichments (Levy, 2008). Tew-Kai and Marsac (2009) further suggested that eddies impacted the spatial distribution of upper trophic levels.

Similar to results in the ISSG province, the greatest changes in acoustic densities were detected in the shallow layer and smallest changes in the deep layer in the EAFR. A greater acoustic response was recorded in the EAFR compared to the ISSG (total s_A recorded in ISSG was almost half of the total s_A recorded in EAFR), confirming the oligotrophy of the ISSG province with low abundance of micronekton organisms. The indicators that were investigated further showed a bi-modal distribution of micronekton, which implies that some organisms stay in the shallow layer during the day and in the deep layer during the night. This resident strategy is further depicted in the "second mode" observed in the day and night vertical profiles for the EAFR, where there appears to be a "thinning out" of the acoustic responses between 400-600 m from day to night (Figure 12). This second mode is less pronounced in the ISSG province and is located between 550 and 650 m. It might be argued that a proportion of the micronekton organisms do not ascend at dusk, both in the EAFR and ISSG.

Interestingly, fishes from the Myctophidae family (most widely caught organisms in trawl surveys, Figure 14) were reported to exhibit a range of DVM behaviour, such as surface migration, midwater migration, passive migration and non-migration, where organisms stay in the deep layer during the night (Watanabe *et al*., 1999).

Within the micronekton, the number of gelatinous organisms caught in the EAFR was significantly different compared to the ISSG province (Figure 15), although gelatinous organisms were least common in trawl surveys from both regions. The damage incurred by soft-bodied organisms in trawls is not negligible. It may well be that the poor representation of gelatinous zooplankton in the net tows reflects their low abundances within the regions of investigation. However, information about the gelatinous zooplankton in the central Indian Ocean is scarce. Van Soest (1974b) reported that the micronekton organism, *Salpa maxima*, was a moderately abundant species distributed from 50°N to 45°S over all three oceans. However, most samples were collected in the northern and western Indian Ocean (along the MZC), with the ISSG province being poorly represented in the study. Additionally, salps have been reported to have a patchy distribution in much of the open ocean (Madin *et al*., 1996). *Leptocephali* larvae were reported to be abundantly distributed in the eastern Indian Ocean (Miller *et al*., 2011), along 110°E. During a trawl survey conducted by Legand (1969), 9.9% of the micronekton species collected were leptocephali and gelatinous cephalopods, the second most abundant micronekton organisms collected after fishes along the 110°E latitude. However, occurrence in hauls also depends on season and abundance (Castle, 1969). The gelatinous organisms *Carinaria lamarckii*, *Leptocephali* larvae, *Salpa maxima*, and *Siphonophora* were collected by Ménard *et al*. (2014) in the MZC, but they occurred in lesser numbers in the net tows compared to squids, crustaceans and fishes.

All micronekton broad categories were found in greater numbers in trawl surveys carried out in the EAFR than in the ISSG province, both during the day and night. However, from the accumulation curves, it seemed that a greater trawl effort was applied in the ISSG (greater species richness in the ISSG even though it is an oligotrophic environment). However, it should be noted that, during MICROTON, taxonomic identification of trawl samples might have been more accurate than during

MESOP cruises, allowing the identification of rarer specimens during MICROTON. Human bias is therefore not negligible when analysing trawl contents.

According to previous studies, a large number of pelagic predators (including swordfish), may opportunistically feed on gelatinous zooplankton (Avian and Rottini-Sandrini, 1988; Harbison, 1993; Cardona *et al*., 2012). However, gelatinous organisms were the rarest organisms found in the stomach contents of swordfish, because they could be undergoing rapid digestion/ disintegration. Stomach contents of swordfish in the ISSG province had a low abundance and species richness, which might account for the narrower standard ellipse area of swordfish in the ISSG compared to EAFR. The proportion of fishes and squids caught in trawls and by the swordfish specimens differed significantly which is related to the selectivity of these two "samplers" of micronekton. However, these results might be biased by the fact that stomach content data only show the status of an animal's stomach at the time the sample was taken (Polunin *et al*., 2001).

The carbon stable isotope values of the different micronekton groups observed in the ISSG were similar to $\delta^{13}C$ isotope values of crustaceans, fishes and squids recorded during the MESOP cruise in the MZC. However, the tissues of micronekton organisms in the EAFR were more enriched in ^{15}N than the tissues of micronekton in the ISSG (Figure 26). Differences in nitrogen and carbon isotope values between cruises might be due to different environmental variables governing these two regions or the difference in the size of micronekton sampled from these two regions.

POM-Surf was more enriched in ^{15}N than POM-Fmax in the EAFR, with the standard ellipse area spread over a wider range of $\delta^{13}C$ values (Figure 25), probably because POM-Surf in the MZC is subjected to local enrichments and exchange of organic molecules with the coast, (possibly due to riverine outflow) combined with the influence of mesoscale eddies. Based on the differences in nitrogen isotope signatures in a previous study by Ménard *et al*. (2014) in the MZC, organisms within the micronekton group were classified into different trophic levels, such as the leptocephali larvae, which have the lowest $\delta^{15}N$ values and consequently are found at a low trophic level. In other oligotrophic environments, such as the NW Mediterranean, Fanelli *et al*. (2011) also found that filter

feeders feeding on POM had depleted nitrogen and carbon isotopic signatures and were consequently found at a low trophic level, whereas carnivores of micronekton had high mean annual $\delta^{15}N$ values and were found at a higher trophic level.

Similar to results for the ISSG province, crustaceans, fishes and squids had higher trophic levels than gelatinous organisms in the EAFR. The standard ellipse area of gelatinous organisms (mainly *Carinaria lamarckii* specimens sampled in our study) was very narrow, suggesting the specialised feeding behaviour of this organism. Some species of mesopelagic fishes (e.g. *Cubiceps pauciradiatus* with an estimated trophic level of 4.98) and squids (e.g. *Onychoteuthis* spp. with an estimated trophic level of 4.60) shared the same isotopic niche space as swordfish in the EAFR (Figure 25). Large-sized squids are generally found at higher trophic levels than other micronekton organisms (Young *et al*., 2015). In the ISSG province, most of the specimens sampled were small in size and do not feed within the micronekton group, but rather feed on smaller-sized plankton species, accounting for the lack of a significant difference in $\delta^{15}N$ values between squids and mesopelagic fishes.

Ménard *et al*. (2014) found positive significant relationships between $\delta^{15}N$ and body length of only three fish taxa and one squid species (*S. oualaniensis*) sampled in the MZC. Despite the same sampling gear being used in both the EAFR and ISSG, micronekton sampling seemed to be even more conservative in the ISSG compared to the EAFR. Indeed, a more restricted size class seemed to have been sampled during MICROTON for each individual taxon (notably, *Abraliopsis* spp., *L. intermedia* and *S. evermanni* in Figure 22). Two plausible hypotheses might be that organisms are smaller in the ISSG or, conversely, fewer specimens were caught in the ISSG (small sample size), that are not representative of the whole population. Some species of micronekton in the EAFR also had higher $\delta^{15}N$ values compared to micronekton in the ISSG at any given size.

The 353 swordfish individuals sampled (181 in EAFR and 172 in ISSG), ranged in size from about 550 to 2500 mm and a positive linear relationship was observed between $\delta^{15}N$ of all swordfish specimens and size (Figure 23). In the EAFR ecosystem, some of the micronekton organisms and the swordfish specimens exhibit the same $\delta^{15}N$ stable isotope values while having different sizes. This

suggests that they occupy the same trophic level and do not have predator-prey relationships. In recent studies, the fixed $\delta^{15}N$ value of 3.4‰ used to estimate relative species trophic position has also been questioned. Stable nitrogen isotope values have been shown to vary among species and across taxa (Caut *et al*., 2009). Furthermore, the enrichment between trophic levels has been demonstrated to change along the food chain, becoming smaller in the upper parts of the food webs as shown in Figure 28 (Hussey *et al*., 2014). This might account for the overlap in $\delta^{15}N$ values observed between micronekton and swordfish in the EAFR province.

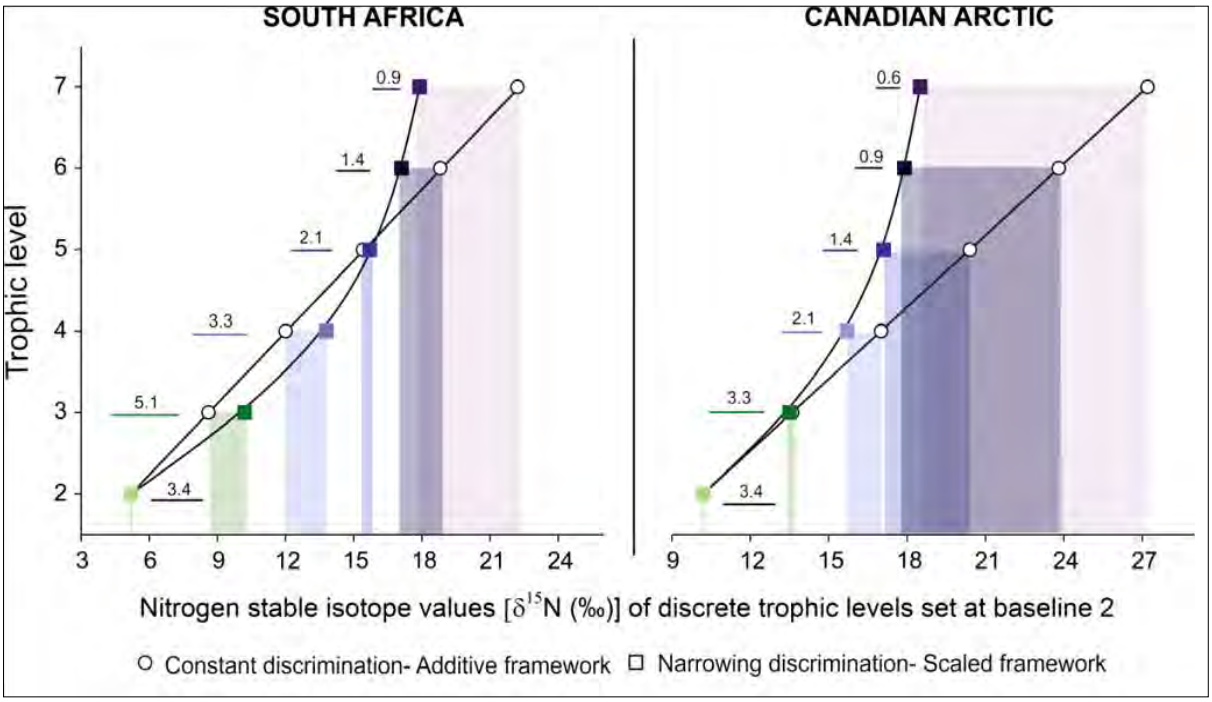

Figure 28 Relationship between trophic level (set as baseline 2) and $\delta^{15}N$ stable isotope values (‰) of zooplankton, teleost, elasmobranch species and shark (as apex predators) for South African and Canadian food webs. The shaded boxes represent the difference in $\delta^{15}N$ between methods, additive framework whereby an enrichment of 3.4‰ is observed between TL and scaled framework whereby the predicted enrichment between TL decreases with increasing trophic position. Numerical values represent the predicted enrichment across TL (Hussey *et al*., 2014).

Some of the smaller-sized swordfish specimens sampled in the EAFR had mean ± (S.D.) body lengths of 864 ± 156 mm and consequently lower mean (± S.D.) $\delta^{15}N$ values (11 .1 ± 0.6‰), compared to larger-sized swordfish having means (± S.D.) of 14.4 ± 0.4‰ in the EAFR. Larger-sized swordfish in the ISSG ranged in size from 1000 to 2500 mm and had $\delta^{15}N$ values ranging from 13.5 to16‰. Stomach content and stable isotope analyses of swordfish specimens off eastern Australia have also found significant overlap in the stable isotope values of top predators and those from lower trophic levels such as cephalopods (Young *et al*., 2006). The authors found that $\delta^{15}N$ values were associated

with increasing size of the swordfish, with smaller swordfish feeding on smaller fish such as myctophids, which was hence reflected in the low $\delta^{15}N$ values of the swordfish tissues. Other factors were deemed to be also important for there was significant variability in the $\delta^{15}N$ stable isotope values of mid-sized swordfish specimens (Young *et al*., 2006).

The standard ellipse area of swordfish was spread over a range of $\delta^{15}N$ values in the EAFR Previous studies have demonstrated that a population of generalist predators can actually be made of individual specialists that would forage on specific prey items (Bolnick *et al*., 2003; Woo *et al*., 2008; Matich *et al*., 2011). Since the biomass and diversity of micronekton are higher in the EAFR than the ISSG, individual swordfish organisms can have specialized diets, with each individual specialising on prey items different from other individuals of the population. Such specialisation would increase the individual feeding efficiency and would reduce the intra-specific competition. Recent studies on the foraging behaviour of the deep-dwelling swordfish specimens have shown specialization on prey sizes and species (Ménard *et al*., 2006; Ménard *et al*., 2007; Potier *et al*., 2007). Swordfish of different body length ranges could be preying upon different size classes of micronekton having different trophic positions in the EAFR. Size, therefore, is an important factor influencing the enrichment of tissues in $\delta^{15}N$ and hence the trophic position of large predatory pelagic fishes.

Ménard *et al*. (2014) already investigated the impact of mesoscale features on the $\delta^{15}N$ and $\delta^{13}C$ values of micronekton organisms in the MZC, with their results showing mesoscale eddies do not have a clear impact on the stable isotope signatures of micronekton, but cyclonic eddies were shown to occasionally influence the isotopic values of micronekton. In oligotrophic environments, eddies were shown to provide mechanisms by which the physical energy of the ocean system is converted to trophic energy in order to support biological processes (Barlow *et al*., 2014; Huggett, 2014). The resulting enhanced primary productivity due to mesoscale eddies and enhanced zooplankton biomass in the EAFR could favour the abundance of micronekton organisms in this zone compared to the ISSG province. However the direct links between these eddy fields and mesopelagic and large pelagic fishes are difficult to investigate (Potier *et al*., 2014).

VI. Conclusion

In conclusion, biogeochemical and biological responses are highly variable in different parts of the Indian Ocean and this is illustrated in the entire food web from low through to mid- and high trophic levels. Mid-trophic level micronekton organisms are key to the survival and health of top predators that are increasingly being fished in our oceans. Stable isotope methods, acoustic and trawl surveys allowed improved depiction of the trophic relationships and migration patterns of deep sea micronekton in two important biogeochemical provinces: one with high mesoscale activities, high nutrient and chlorophyll-a concentrations, high biodiversity of organisms (phytoplankton, zooplankton and micronekton) and high fishing pressure, and the other with low mesoscale activities, low nutrient and chlorophyll-a concentrations, low biodiversity of organisms and consequently low fishing pressure.

Despite human biases, possibly differing sampling efforts and net selectivity, our study showed that the food chain is more complex than initially thought, with various mechanisms and environmental factors (nitrate, pigment and chlorophyll-a concentrations, oxygen and temperature gradients, current shear and the large-scale anticyclonic pattern in the ISSG) impacting on the concentration, abundance, diversity, diel vertical migration patterns, size and dietary habits of micronekton organisms. Despite the lack of a correlation between the nitrogen isotopic signatures of micronekton and size, body length is known to play an important role in the trophic position of an organism, with smaller-sized micronekton being eaten by larger-sized micronekton which are, in turn, eaten by *Xiphias gladius*.

POM and micronekton tissues from the EAFR were more enriched in ^{15}N than POM and micronekton found in the ISSG, resulting in micronekton organisms having slightly higher trophic level positions in the EAFR compared to the ISSG. Further studies investigating the effect of seasonality, seamounts, and lunar patterns on micronekton biomass, distribution, migration and stable isotope values will add considerably to the knowledge of the trophic position of micronekton in the Indian Ocean and will be beneficial for an ecosystem approach to fisheries.

References

Abascal, F. J., Mejuto, J., Quintans, M., and Ramos-Cartelle, A. (2010). Horizontal and vertical movements of swordfish in the Southeast Pacific. *ICES Journal of Marine Science, 67*(3): 466-474.

Allain , V., Fernandez, E., Hoyle, S. D., Caillot, S., Jurado-Molina, J., Andréfouët, S., and Nicol, S. J. (2012). Interaction between Coastal and Oceanic Ecosystems of the Western and Central Pacific Ocean through Predator-Prey Relationship Studies. *PLOS One, 7*(5).

Alvain, S., Moulin, C., Dandonneau, Y., and Loisel, H. (2008). Seasonal distribution and succession of dominant phytoplankton groups in the global ocean: A satellite view. *Global Biogeochemical Cycles, 22*(3).

Arkhipkin, A. I., Laptikhovsky, V. V., Nigmatullin, Ch. M., Bespyatykh, A. V., and Murzov,S. A. (1998). Growth, reproduction and feeding of the tropical squid *Ornithoteuthis antillarum* (Cephalopoda, Ommastrephidae) from the central-east Atlantic. *Scientia Marina, 62*(3): 273-288.

Avian, M., and Rottini-Sandrini, L. (1988). Fishery and swimming of Pelagia noctiluca in the central and northern Adriatic Sea: middle term analysis. *Rapport de la Commission Intternationale pour la Mer Méditerrannée, 31(2)*: 231.

Bamstedt, U., Gifford, D. J., Irigoien, X., Atkinson, A., and Roman, M. (2000). Feeding, In *ICES zooplankton methodological manual*, Harris, R., Wiebe, P., Lenz, J., Skjodal, H. R., and Huntley, M. [eds.], Academic, p. 297- 399.

Bakun, A. (2006). Fronts and eddies as key structures in the habitat of marine fish larvae: opportunity, adaptive response and competitive advantage. *Scientia Marina, 70*: 105- 122.

Barlow, J., Gardner, T. A., Araujo, I. S., Avila-Pires, T. C., Bonaldo, A. B., Costa, J. E., Esposito, M. C., Ferreira, L. V., Hawes, J., Hernandez, M. I., Hoogmoed, M. S., Leite, R. N., Lo-Man-Hung, N. F., Malcolm, J. R., Martins, M. B., Mestre, L. A., Miranda-Santos, R., Nunes-Gutjahr, A. L., Overal, W. L., Parry, L., Peters, S. L., Ribeiro-Junior, M. A., da Silva, M. N. F., da Silva, M. C., and Peres, C. A. (2007). Quantifying the biodiversity value of tropical primary, secondary, and plantation forests. *Proceedings of the National Academy of Sciences of the United States of America. 104*(47): 18555- 60.

Barlow, R., Lamont, T., Morris, T., Sessions, H., and van den Berg, M. (2014). Adaptation of phytoplankton communities to mesoscale eddies in the Mozambique Channel. *Deep Sea Research Part II: Topical Studies in Oceanography, 100*: 106- 118.

Barlow, R., Marsac, F. Ternon, J. F., and Roberts, M. (2014). The Mozambique Channel: Mesoscale Dynamics and Ecosystem Responses. *Deep Sea Research Part II: Topical Studies in Oceanography, 100*: 1- 220.

Béhagle, N., du Buisson, L., Josse, E., Lebourges-Dhaussy, A., Roudaut, G., and Ménard, F. (2014). Mesoscale features and micronekton in the Mozambique Channel: An acoustic approach. *Deep Sea Research Part II: Topical Studies in Oceanography, 100*: 164- 173.

Bello, G. (1991). Role of cephalopods in the diet of the swordfish, *Xiphias gladius*, from the Eastern Mediterranean Sea. *Bulletin of Marine Science, 49*(1-2): 312- 324.

Bodin, N., Budzinski, H., Le Ménach, K., and Tapie, N. (2009). ASE extraction method for simultaneous carbon and nitrogen stable isotope analysis in soft tissues of aquatic organisms. *Analytica Chimica Acta, 643*(1–2): 54- 60.

Bolnick, D. I., Svanback, R., Fordyce, J. A., Yang, L. H., Davis, J. M., Hulsey, C. D., and Forister, M. L. (2003). The ecology of individuals: Incidence and implications of individual specialization. *The American Naturalist, 161*: 1- 28.

Boyd, C. M., Heyraud, M., and Boyd, C. N. (1984). Feeding of the Antarctic krill *Euphausia superba. Journal of Crustacean Biology, 4*: 123- 141.

Brodeur, R. D., Seki, M. P., Pakhomov, E. A., and Suntsov, A. V. (2005). Micronekton - What are they and why are they important? *PICES Annual Meeting,* 14-24 October 2004.

Buchheister, A., and Latour, R. J. (2011). Trophic Ecology of Summer Flounder in Lower Chesapeake Bay Inferred from Stomach Content and Stable Isotope Analyses. *Transactions of the American Fisheries Society, 140*: 1240- 1254.

Campbell, L., and Vaulot, D. (1993). Photosynthetic picoplankton community structure in the subtropical North Pacific Ocean near Hawaii (station ALOHA). *Deep-Sea Research I, 40(10)*: 2043- 2060.

Campbell, L., Nolla, H. A., and Vaulot, D. (1994). The importance of *Procholorococcus* to community structure in the Central North Pacific Ocean. *Limnology and Oceanography, 39(4)*: 954- 961.

Cardona, L., Alvarez de Quevedo, I., Borrell, A., and Aguilar, A. (2012). Massive consumption of gelatinous plankton by Mediterranean apex predators. *PLOS One, 7(3),* e31329.

Carey, F. G., and Robison, B. H. (1981). Daily patterns in the activities of swordfish, *Xiphias gladius*, observed by acoustic telemetry. *Fishery Bulletin, 79(2)*: 277- 292.

Castle, P. H. J. (1969). Species structure and seasonal distribution of Leptocephalie in the eastern Indian Ocean (110°E). *Cahiers Office de la Recherche Scientifique et Technique Outre-mer, série Océanographie, 7(2*): 53- 88.

Caut, S., Angulo, E., and Courchamp, F. (2009). Variation in discrimination factors ($\delta^{15}N$ and $\delta^{13}C$): the effect of diet isotopic values and applications for diet reconstruction. *Journal of Applied Ecology, 46*: 443- 453.

Cavicchioli, R., Ostrowski, M., Fegatella, F., Goodchild, A., and Guixa-Boixereu, N. (2003). Life under nutrient limitation in oligotrophic marine environments: an eco/physiological perspective of Sphingopyxis alaskensis (formerly *Sphingomonas alaskensis*). *Microbial Ecology, 45*(3): 203- 17.

Chancollon, O., Pusineri, C., and Ridoux, V. (2006). Food and feeding ecology of Northeast Atlantic swordfish (*Xiphias gladius*) off the Bay of Biscay. *ICES Journal of Marine Science, 63*: 1075- 1085.

Cherel, Y., and Hobson, K. A. (2005). Stable isotopes, beaks and predators: a new tool to study the trophic ecology of cephalopods, including giant and colossal squids. *Proceedings.of the Royal Society, 272*: 1601- 7.

Cherel, Y., Fontaine, C., Richard, P., and Labat, J. P. (2010). Isotopic niches and trophic levels of myctophid fishes and their predators in the Southern Ocean. *Limnology and Oceanography, 55*(1): 324- 332.

Christaki, U., Jacquet, S., Dolan, J. R., Vaulot, D., and Rassoulzadegan, F. (1999). Growth and grazing on *Prochlorococcus* and *Synechococcus* by two marine ciliates. *Limnology and Oceanography, 44*(1): 52- 61.

Clarke, T.A. (1980). Diets of fourteen species of vertically migrating Mesopelagic fishes in Hawaiian waters. *Fishery Bulletin, 78*(3).

Clarke, M. R. (1980). Cephalopods in the diet of sperm whales of the Southern Hemisphere and their bearing on sperm whale biology. *Discovery Report, 37*: 1- 324.

Coll, M., Navarro, J., Olson, R. J., and Christensen, V. (2013). Assessing the trophic position and ecological role of squids in marine ecosystems by means of food-web models. *Deep Sea Research Part II: Topical Studies in Oceanography, 95*: 21- 36.

Daroux, A. (2011). Etude de la structuration spatiale du micronekton par acoustique multifréquentielle dans l'Océan Indien. M-1. Institut Universitaire Européen de la Mer, Brest.

DeNiro, M. J., and Epstein, S. (1978). Influence of diet on the distribution of carbon isotopes in animals. *Geochimica Et Cosmochimica Acta, 42*(5): 495- 506.

Drazen, J. C., De Forest, L. G., and Domokos, R. (2011). Micronekton abundance and biomass in Hawaiian waters as influenced by seamounts, eddies, and the moon. *Deep-Sea Research Part 1, 58(5)*: 557- 566.

Durand, F., and Delcroix, T. (2000). On the variability of the tropical Pacific thermal structure during the 1979- 96 period, as deduced from XBT section. *Journal of Physical Oceanography, 30*: 3261- 3269.

Essington, T. E., Schindler, D. E., Olson, R. J., Kitchell, J. F., Boggs, C., and Hilborn, R.. (2002). Alternative fisheries and the predation rate of yellowfin tuna in the eastern Pacific Ocean. *Ecological Applications, 12*(3): 724-734.

Fanelli, E., Cartes, J. E. and Papiol, V. (2011). Food web structure of deep-sea macrozooplankton and micronekton off the Catalan slope: Insight from stable isotopes. *Journal of Marine Systems, 87*(1): 79- 89.

FAO, (2003). *Fisheries management 2. The ecosystem approach to fisheries.* FAO Technical guidelines for responsible fisheries, Rome: FAO, 4(2): 112.

FAO, (2006). *FAO Yearbook of Fishery Statistics Capture production,* 2004, Rome: FAO, pp. 98/1560.

FAO, (2010). *Cephalopods of the world. An annotated and illustrated catalogue of cephalopod species known to date*. Rome: FAO, 2(4).

Fonteneau, A. (1997). *Atlas of tropical tuna fisheries World catches and environment*. *Paris:* ORSTOM Editions, pp. 191.

Foxton, P. and Roe, H. S. J. (1974). Observations on the nocturnal feeding of some mesopelagic decapod Crustacea. *Marine Biology, 28*: 37- 49.

Fry, B., Scalan, R. S., and Parker, P. L. (1983). $^{13}C/^{12}C$ ratios in marine food webs of the Torres Strait, Queensland. *Australian Journal of Marine and Freshwater Research, 34*: 707- 716.

Fukuda, J., Yamaguchi, A., Matsuno, K., and Imai, I. (2012). Interannual and latitudinal changes in zooplankton abundance, biomass and size composition along a central North Pacific transect during summer: analyses with an Optical Plankton Counter. *Plankton and Benthos Research, 7(2)*: 64- 74.

Gjøsaeter, J., and Kawaguchi, K. (1980). A review of the world resources of Mesopelagic fish. Rome: *FAO*.

Gupta, R. S., and Desa, E. (2001). Zooplankton. In: *The Indian Ocean- A Perspective, vol. 2*: A.A.Balkema, India, pp. 434- 436.

Handegard, N. O., Huse, G., Macaulay, G., Godo, O. R., Buisson, L. D., Maury, O., Brehmer, P., Chalmers, S. J., De Robertis, A., Ressler, P. H., Kloser, R., and Stenseth, N. C. (2013). Towards an acoustic-based coupled observation and modelling system for monitoring and predicting ecosystem dynamics of the open ocean. *Fish and Fisheries, 14*(4): 605- 615.

Harbison, G. R. (1993). The potential of fishes for the control of gelatinous zooplankton. *International Council for the Exploration of the Sea, CM* 1999, ICES, pp. 10.

Hobson, K. A., Piatt, J. F., and Pitocchelli, J. (1994). Using stable isotopes to determine seabird trophic relationships. *Journal of Animal Ecology, 63*(4): 786.

Hopkins, T. L., Flock, M. E., Gartner, J. V., and Torres,J.J. (1994). Structure and trophic ecology of a low latitude midwater decapod and mysid assemblage. *Marine Ecology Progress Series, 109*: 143- 156.

Huggett, J. A. (2014). Mesoscale distribution and community composition of zooplankton in the Mozambique Channel. *Deep Sea Research Part II: Topical Studies in Oceanography, 100*: 119- 135.

Hunt, B. P. V., Allain, V., Menkes, C., Lorrain, A., Graham, B., Rodier, M., Pagano, M., and Carlotti, F. (2014). A coupled stable isotope-size spectrum approach to understanding pelagic food-web dynamics: A case study from the southwest sub-tropical Pacific. *Deep Sea Research Part II: Topical Studies in Oceanography, 113*: 208- 224.

Hussey, N. E., MacNeil, M. A., McMeans, B. C., Olin, J. A., Dudley, S. F. J., Cliff, J., Wintner, S. P., Fennessy, S. T., and Fisk, A. T. (2014). Rescaling the trophic structure of marine food webs. *Ecology Letters, 17*: 239- 250.

Jaquemet, S., Ternon, J. F., Kaehler, S., Thiebot, J. B., Dyer, B., Bemanaja, E., Marteau, C., and Le Corre, M. (2014). Contrasted structuring effects of mesoscale features on the seabird community in the Mozambique Channel. *Deep Sea Research Part II: Topical Studies in Oceanography, 100*: 200- 211.

Jeffrey, S. W. and Vesk, M. (1997). Introduction to marine phytoplankton and their pigment signatures. In *Phytoplankton pigments in oceanography: guidelines to modern methods,* S.W. - Jeffrey, R. F. C. Mantoura & S.W. Wright, (Eds.), Paris: UNESCO Publ., pp. 37- 84.

Jeffrey, S. W., Mantoura, R. F. C., and Wright, S. W. (1997). Development of pigment methods for oceanography: SCOR-supported Working Groups and objectives. In *Phytoplankton pigments in Oceanography,* France: UNESCO.

Jena, B., Sahu, S., Avinash, K., and Swain, D. (2013). Observation of oligotrophic gyre variability in the south Indian Ocean: Environmental forcing and biological response. *Deep-Sea Research Part I, 80*: 1- 10.

Jena, B., Swain, D., Avinash, K. (2012). Investigation of the biophysical processes over the oligotrophic waters of South Indian Ocean subtropical gyre, triggered by cyclone Edzani. *International Journal of Applied Earth Observations and Geoinformation, 18*: 49- 56.

Kaartvedt, S., Staby, A., and Aksnes, D.L. (2012). Efficient trawl avoidance by Mesopelagic fishes causes large underestimation of their biomass. *Marine.Ecology Progress Series, 456*: 1- 6.

Lalli, C. M. and Parsons, T. R. (1997). Zooplankton. In *Biological Oceanography: An Introduction,* (2nd ed.), UK: Elsevier Butterworth-Heinemann.

Lamont, T., Barlow, R. G., Morris, T. and van den Berg, M. A. (2014). Characterisation of mesoscale features and phytoplankton variability in the Mozambique Channel. *Deep Sea Research Part II: Topical Studies in Oceanography, 100*: 94- 105.

Landry, M. R., (2002). Integrating classical and microbial food web concepts: evolving views from the open-ocean tropical Pacific. *Hydrobiologia, 480*(1-3): 1- 3.

Lebourges-Dhaussy, A., Huggett, J., Ockhuis, S., Roudaut, G., Josse, E. and Verheye, H. (2014). Zooplankton size and distribution within mesoscale structures in the Mozambique Channel: A comparative approach using the TAPS acoustic profiler, a multiple net sampler and ZooScan image analysis. *Deep Sea Research Part II: Topical Studies in Oceanography, 100*: 136- 152.

Lebourges-Dhaussy, A., Marchal, É., Menkès, C., Champalbert, G. and Biessy, B. (2000). *Vinciguerria nimbaria* (micronekton), environment and tuna: their relationships in the Eastern Tropical Atlantic. *Oceanologica Acta, 23*(4): 515- 528.

Legand, M. (1969). Seasonal variations in the Indian Ocean along 110°E. VI. *Macroplankton and micronekton biomass. *Ibid, 20*: 77- 84.

Levy, M. (2008). The modulation of biological production by oceanic mesoscale turbulence. *Lecture Notes in Physics, 744*: 219- 261.

Longhurst, A. (2007). The Indian Ocean- Indian South Subtropical Gyre Province (ISSG). In *Ecological Geography of the Sea,* (2nd ed.), USA: Elsevie, pp. 285.

Lorrain, A., Graham, B. S., Popp, B. N., Allain, V., Olson, R. J., Hunt, B. P. V., Potier, M., Fry, B. Galvan-Magana, F., Menkes, C. E. R., Kaehler, S., and Ménard, F. (2015). Nitrogen isotopic baselines and implications for estimating foraging habitat and trophic position of yellowfin tuna in the Indian and Pacific Oceans. *Deep Sea Research Part II: Topical Studies in Oceanography,*113: 188- 198.

Lutjeharms, J. R. E. (2006). Flow through the Mozambique Channel. In *The Agulhas Current*, Berlin: Springer.

Madin, L. P., Kremer, P., and Hacker, S. (1996). Distribution and vertical migration of salps (Tunicata, Thaliacea) near Bermuda. *Journal of Plankton Research, 18(5)*: 747- 755.

Matich, P., Heithaus, M. R., and Layman, C. A. (2011). Contrasting patterns of individual specialization and trophic coupling in two marine apex predators. *Journal of Animal Ecology, 80*: 294- 305.

McClain, C. R., Signorini, S. R. and Christian, J. R. (2004). Subtropical gyre variability observed by ocean-color satellites. *Deep Sea Research Part II: Topical Studies in Oceanography, 51*(1–3): 281- 301.

McGillicuddy Jr, D. J., Robinson, A. R., Siegel, D. A., Jannasch, H. W., Johnson, R., Dickey, T. D., McNeil, J., Michaels, A. F., and Knap, A. H. (1998). Influence of mesoscale eddies on new production in the Sargasso Sea. *Nature, 394*: 263- 266.

Mehner, T. (2012). Diel vertical migration of freshwater fishes - proximate triggers, ultimate causes and research perspectives. *Freshwater Biology. 57*: 1342- 1359.

Meinen, C. S., and Mc Phaden, M. J. (2000). Observations of warm water volume change in the equatorial Pacific and their relationship to the El-nino and La-nina. *Journal of Climate, 13*: 3551- 3559.

Menard, F., Labrune, C., Shin, Y. J., Asine, A. S., and Bard, F. X. (2006). Opportunistic predation in tuna: a size-based approach. *Marine Ecology Progress Series, 323*: 223- 231.

Ménard, F., Lorrain, A., Potier, M., and Marsac, F. (2007). Isotopic evidence of distinct foraging ecology and movement pattern in two migratory predators (yellowfin tuna and swordfish) of the western Indian Ocean. *Marine Biology, 153*(2): 141- 152.

Ménard, F., Benivary, H. D., Bodin, N., Coffineau, N., Le Loch'h, F., Mison, T., Richard, P., and Potier, M. (2014). Stable isotope patterns in micronekton from the Mozambique Channel. *Deep Sea Research Part II: Topical Studies in Oceanography, 100*: 153- 163.

Michener, R., and Kaufman, L. (2007). Stable isotope ratios as tracers in marine food webs: and update. In *Stable Isotopes in Ecology and Environmental Science* R, (2nd ed.), USA: Blackwell, pp 238- 245.

Michener, R., and Lajtha, K. (2007). Stable Isotope Ratios as Tracers. In *Stable Isotopes in Ecology and Environmental Science,* (2nd ed.), USA: Blackwell, pp 255.

Michener, R. H., and Schell, D. M. (1994). Stable isotope ratios as tracers in marine aquatic food webs, In *Stable isotopes in ecology and environmental science*. Lajtha, K., and Michener, R. H. [eds.], USA: Blackwell, pp 138- 158.

Miller, C. B. (2007). The zoology of zooplankton. In *Biological Oceanography*, (5th ed.), UK: Blackwell, pp 111- 113.

Miller, M. J., Wouthuyzen, S., Ma, T., Aoyama, J., Suharti, S. R., Minegishi, Y., and Tsukamoto, K. (2011). Distribution, Diversity, and Abundance of Garden Eal Larvae off West Sumatra, Indonesia. *Zoological Studies, 50(2)*: 177- 191.

Minagawa, M., and Wada, E. (1984). Stepwise enrichment of ^{15}N along food chains: Further evidence and the relation between $\delta^{15}N$ and animal age. *Geochimica and Cosmochimica Acta, 48*: 1135- 1140.

Nagasawa, K. (2000). Winter zooplankton biomass in the subarctic North Pacific, with a discussion on the overwintering survival strategy of Pacific Salmon (*Oncorhynchus* spp.). *North Pacific Anadromous Fish Commission Bulletin, 2*: 21- 32.

Navarro, J., Coll, M., Somes, C. J., and Olson, R. J. (2013). Trophic niche of squids: Insights from isotopic data in marine systems worldwide. *Deep Sea Research Part II: Topical Studies in Oceanography, 95*: 93- 102.

O'Dor, R. K. and Coelho, M. L. (1993). Big squid, big currents, and big fisheries. In *Recent advances in cephalopod fisheries biology*, Okutani, T., O'Dor, R. K., and Kubodera, T. [eds]. Tokyo:Tokyo University Press, pp 385- 396.

Okutani, T. (1977). Stock assessment of cephalopod resources fished by Japan. *Food and Agriculture Organization of the United Nation, pp 31.*

Oschlies, A., and Garcon, V. (1998). Eddy-induced enhancement of primary production in a model of the North Atlantic Ocean. *Nature, 394*: 266- 269.

Otake, T., Nogami, K., and Maruyaka, K. (1990). Possible food sources of eel leptocephali. *La Mer. 2 8:* 218- 224.

Palko, B. J., Beardsley, G. L., and Richards, W. J. (1981). Synopsis of the biology of the Swordfish, *Xiphias gladius* Linnaeus*,* no. (127): National Oceanic and Atmospheric Administration, USA.

Parry, M. (2008). Trophic variation with length in two ommastrephid squids, *Ommastrephes bartramii* and *Sthenoteuthis oualaniensis*. *Marine Biology, 153*(3): 249- 256.

Parsons, T. R., and Lalli, C. M. (2002). Jellyfish Population Explosions: Revisiting a Hypothesis of Possible Causes. *La Mer, 40*(3): 111- 121.

Polunin, N. V. C., Morales-Nin, B., Pawsey, W. E., Cartes, J. E., Pinnegar, J. K., and Moranta, J. (2001). Feeding relationships in Mediterranean bathyal assemblages elucidated by stable nitrogen and carbon isotope data. *Marine Ecology Progress Series, 220*: 13- 23.

Post, D. M. (2002). Using stable isotopes to estimate trophic positions: Models, Methods, and Assumptions. *Ecology*, *83*(3): 703- 718.

Potier, M., Marsac, F., Cherel, Y., Lucas, V., Sabatie, R., Maury, O., and Menard, F. (2007). Forage fauna in the diet of three large pelagic fishes (lancetfish, swordfish and yellowfin tuna) in the western equatorial Indian Ocean. *Fisheries Research, 83*(1): 60- 72.

Potier, M., Bach, P., Ménard, F. and Marsac, F. (2014). Influence of mesoscale features on micronekton and large pelagic fish communities in the Mozambique Channel. *Deep Sea Research Part II: Topical Studies in Oceanography, 100*: 184- 199.

Pous, S., Lazure, P., André, G., Dumas, F., Halo, I., and Penven, P. (2014). Circulation around La Réunion and Mauritius islands in the south-western Indian Ocean: A modeling perspective. *Journal of Geophysical Research: Oceans, 119*(3): 1957- 1976.

Quartly, G. D., and Srokosz, M. A. (2004). Eddies in the southern Mozambique Channel. *Deep Sea Research Part II: Topical Studies in Oceanography, 51*: 69– 83.

Quinn, G. P., and Keough, M. J. (2002). *Experimental design and data analysis for biologists.* Cambridge: Cambridge University Press.

Rao, T. S. S. (1973). Zooplankton studies in the Indian Ocean. In *The Biology of the Indian Ocean.* B. Zeitschel, Ed. Berlin: Springer, 243- 255.

Reygondeau, G., Maury, O., Beaugrand, G., Fromentin, J. M., Fonteneau, A., and Curry, P. (2012). Biogeography of tuna and billfish communities. *Journal of Biogeography,* 39: 114- 129.

Rissik, D., and Suthers, I. M. (2000). Enhanced feeding by pelagic juvenile myctophid fishes within a region of island-induced flow disturbance in the Coral Sea. *Marine Ecology Progress Series, 203*: 263- 273.

Roberts, M. J., Ternon, J. F., and Morris, T. (2014). Interaction of dipole eddies with the western continental slope of the Mozambique Channel. *Deep Sea Research Part II: Topical Studies in Oceanography, 100*: 54- 67.

Rodhouse, P. G., and Nigmatullin, C. M. (1996). Role as consumers. *Philosophical Transactions of the Royal Society of London, 351*: 1003- 1022.

Rubenstein, D. R., and Hobson, K. A. (2004). From birds to butterflies: animal movement patterns and stable isotopes. *Trends in Ecology and Evolution,* 19(5): 256– 263.

Sabarros, P. S., Menard, F., Tew-Kai, E., Levenez, J. J., and Ternon, J. F. (2009). Mesoscale eddies influence distribution and aggregation patterns of micronekton in the Mozambique Channel. *Marine Ecology Progress Series,* 395: 101- 107.

Sarthou, G., Timmermans, K. R., Blain, S., and Tréguer, P. (2005). Growth physiology and fate of diatoms in the ocean: a review. *Journal of Sea Research, 53*(1-2): 25- 42.

Schindler, D. E., Essington, T. E., Kitchell, J. F., Boggs, C., and Hilborn, R. (2002). Sharks and tunas: Fisheries impacts on predators with contrasting life histories. *Ecological Applications: A Publication of the Ecological Society of America, 12*(3): 735- 748.

Schlitzer, R. (2013). Ocean Data View 4, (http://odv.awi.de).

Schott, F. A. and McCreary Jr., J. P. (2001). The monsoon circulation of the Indian Ocean. *Progress in Oceanography, 51*(1): 1- 123.

Schouten, M.W., de Ruijter, W. P. M., van Leeuwen, P. J., and Ridderinkhof, H. (2003). Eddies and variability in the Mozambique Channel. *Deep Sea Research Part II: Topical Studies in Oceanography, 50*(12–13): 1987- 2003.

Schmidt, K., Atkinson, A., Stubing, D., Mc Clelland, J. W., Montoya, J. P., and Voss, M. (2003). Trophic relationships among Southern Ocean copepods and krill: Some uses and limitations of a stable isotope approach. *Limnology and Oceanography, 48*(1): 277- 289.

Schram, F., von Vaupel Klein, J. C., Charmantier-Daures, M., and Forest, J. (2010). Treatise on Zoology - Anatomy, Taxonomy, Biology. The Crustacea, complementary to the volumes of the Traité de Zoologie, *vol. 9 Part A*: Koninklijke Brill,Leiden, The Netherlands.

Simenstad, C. A., and Wissmar, R. C. (1985). $\delta^{13}C$ evidence of the origins and fates of organic carbon in estuarine and nearshore food webs. *Marine Ecology Progress Series, 22*: 141- 152.

Steele, J. H. (2009). Mesopelagic fishes. In *Elements of Physical Oceanography: A derivative of the Encyclopedia of Ocean Sciences Marine Biology.* Thorpe, S. A., and Turekian, K. K. (Eds.), (2nd ed.), Elsevier Ltd, UK, pp 240- 242.

Stillwell, C. E., and Kohler, N. E. (1985). Food and feeding ecology of the swordfish *Xiphias gladius* in the western North Atlantic Ocean with estimates of daily ration. *Marine Ecology Progress Series, 22*: 239- 247.

Stramma, L., and Lutjeharms, J. R. E. (1997). The flow field of the subtropical gyre of the South Indian Ocean. *Journal of Geophysical Research, 102*(C3): 5513- 5530.

Tait, R. V. (1980). Some parameters of the environment. In *Elements of Marine Ecology: An Introductory Course*. 3rd ed. UK: Butterworths, pp 126.

Tanaka, H., Ohshimo, S., Sassa, C., and Aoki, I. (2007). Feeding habits of Mesopelagic fishes off the coast of western Kyushu, Japan. *PICES 16th: Bio_p-4200.* 1st November.

Ternon, J. F., Bach, P., Barlow, R., Huggett, J., Jaquemet, S., Marsac, F., Ménard, F., Penven, P., and Roberts, M. J. (2014). The Mozambique Channel: From physics to upper trophic levels. *Deep Sea Research Part II: Topical Studies in Oceanography, 100*: 1- 9.

Tew-Kai, E., and Marsac, F. (2009). Patterns of variability of sea surface chlorophyll in the Mozambique Channel: A quantitative approach. *Journal of Marine Systems, 77*(1-2): 77- 88.

Tyler, P. A. (2003). The Pelagic Environment of the Open Ocean. In *Ecosytems of the Deep Oceans***.** 1st ed. The Netherlands: Elsevier, pp57.

Vanderklift, M. A., and Ponsard, S. (2003). Sources of variation in consumer-diet $\delta^{15}N$ enrichment: a meta-analysis. *Oecologia,* 136(2): 169- 182.

Van Soest, R. W. M. (1974b). A revision of the genera *Salpa* Forskal, 1775, *Pegea* Savigny, 1816, and *Ritteriella* Metcalf, 1919 (Tunicata, Thaliacea). *Beaufortia, 22(293)*: 153- 191.

Vaulot, D., Marie, D., Olson, R. J. and Chrisholm, S. W. (1995). Growth of *Prochlorococcus*, a photosynthetic prokaryote, in the equatorial Pacific Ocean. *Science, 268*: 1480- 1482.

Veldhuis, M. J. W., and Kraay, G. W. (1993). Cell abundance and fluorescence of picoplankton in relation to growth irradiance and nitrogen availability in the Red Sea. *Netherlands Journal of Sea Research, 31(2)*: 135- 145.

Voituriez, B. (2003). The changing ocean: Its effect on climate and living resources. France: UNESCO Publishing, IOC Ocean Forum IV.

von Harbou, L. (2009). Trophodynamics of salps in the Atlantic Southern Ocean. Thesis. University of Bremen.

Ward, B. A., Dutkiewicz, S., Jahn, O., and Follows, M. J. (2012). A size-structured food-web model for the global ocean. *LNO Limnology and Oceanography,* 57(6): 1877- 1891.

Watanabe, H., Moku, M., Kawaguchi, K., Ishimaru, K., and Ohno, A. (1999). Diel vertical migration of myctophid fishes (Family Myctophidae) in the transitional waters of the western North Pacific. *Fisheries Oceanography, 8*(2): 115- 127.

Watanabe, H., Kubodera, T., Moku, M., and Kawaguchi, K. (2006). Diel vertical migration of squid in the warm core ring and cold water masses in the transition region of the western North Pacific. *Marine Ecology Progress Series, 315*: 187- 197.

Weimerskirch, H., Le Corre, M., Jaquemet, S., Potier, M., and Marsac, F. (2004). Foraging strategy of a top predator in tropical waters: great Frigatebirds in the Mozambique Channel. *Marine Ecology Progress Series, 275:* 297– 308.

Weimerskirch, H., Gault, A., and Cherel, Y. (2005). Prey distribution and patchiness: factors in foraging success and efficiency of wandering albatrosses. *Ecology, 86(10)*: 2611- 2622.

Woo, K. J., Elliott, K. H., Davidson, M., Gaston, A. J., and Davoren, G. K. (2008). Individual specialization in diet by a generalist marine predator reflects specialization in foraging behaviour. *Journal of Animal Ecology, 77*: 1083- 1091.

Yang, H., and Wang, F. (2009). Revisiting the thermocline depth in the equatorial Pacific. *Journal of Climate, 18(22)*: 3856- 3863.

Young, J. W., Hunt, B. P. V., Cook, T. R., Llopiz, J. K., Hazen, E. L., Pethybridge, H. R., Ceccarelli, D., Lorrain, A., Olson, R. J., Allain, V., Menkes, C., Patterson, T., Nicol, S., Lehodey, P., Kloser, R. J., Arrizabalaga, H., and Choy, C. A. (2015). The trophodynamics of marine top predators: Current knowledge, recent advances and challenges. *Deep Sea Research Part II: Topical Studies in Oceanography, 113*: 170- 187.

Young, J., Lansdell, M., Riddoch, S., and Revill, A. (2006). Feeding ecology of broadbill swordfish, *Xiphias gladius*, off eastern Australia in relation to physical and environmental variables. *Bulletin of Marine Science,* 79(3): 793- 809.

Zubkov, M. V., and Quartly, G. D. (2003). Ultraplankton distribution in surface waters of the Mozambique Channel-flow cytometry and satellite imagery. *Aquatic Microbial Ecology, 33*: 155- 161.

APPENDIX A.

Parameters	Collection Method	Pre-processing procedures
Environmental		
Temperature, salinity, dissolved oxygen, fluorescence	CTD rosette system (Sea Bird 911 +) equipped with: Wetlabs ECO-FL fluorometer SBE 43 oxygen sensor	❖ CTD salinity profiles were calibrated on board • Samples analysed on a Portasal salinometer). ❖ CTD fluorometry profiles used to assess the exact depth of the DCM. ❖ Qualitative concentrations of chlorophyll obtained on discrete samples by fluorometry and by HPLC. ❖ Oxygen profiles calibrated on board against oxygen determined by classical Winkler method on discrete water samples.
Current profiles	L-ADCP- current profiler attached to the CTD frame	L-ADCP was operated at the 300 kHz frequency, with an 8 m vertical resolution, to a maximum depth of 1000 m
Nutrients	CTD rosette system (Sea Bird 911 +)	❖ Pasteurisation of nutrients samples (at 80°C for 3 hours) ❖ Nutrients determined by standard auto-analyser techniques
Chlorophyll pigments	Water samples collected at 5 m and at the DCM and filtered	❖ Filters stored in liquid nitrogen ❖ Chlorophyll-a analysed by fluorometric technique of Welschmeyer (1994) ❖ High pressure liquid chromatography (Thermo Separations HPLC) on specific filters/ samples used to analyse phytoplankton pigments
Particulate organic matter	25 or 47 mm glass-fiber filters that filtered 4 to 8 L (depending on the load of each sample) of seawater at 5 m and the depth of the DCM	Filters stored frozen at -20°C

Biological parameter		
Zooplankton	Bongo zooplankton sampler with a 200 µm mesh size used for oblique profile (0-600 m depth)	
Methods of investigating micronekton		
Acoustic	❖ Simrad EK60 split-beam echosounder ❖ ER60 software: • To record the signal reflected by the target • To operate and control the echosounder	Data converted into the '*.hac' format before post-processing (removing background noises) with the IFREMER "Movies +" software
Pelagic trawls	❖ Micronekton samples collected with a 40-m long International Young Gadoid Pelagic Trawl having a cod-end lined with 5 mm knotless nylon delta mesh netting ❖ Trawl towed at a speed of 3-4 knots for 30 minutes ❖ 7 trawls conducted during the day; 5 deep (400- 600 m) trawls and 2 shallow (10- 200 m) trawls ❖ 12 trawls conducted during the night (10 shallow trawls and 2 deep trawls)	Each broad category was weighed, stored in plastic bags and frozen (if abundant) or preserved in 70% alcohol (if less abundant) Body length measurements taken: • Standard Length for fishes • Dorsal Mantle Length for squids • Cephalothorax lenght for crustaceans • Total Length for other taxen
Gut contents data	Swordfish caught by longline fishing	❖ Stomach contents separated and sorted into 4 broad categories • Species and individual prey items were identified to the lowest possible taxon Measurements: • Standard Length and Length of otoliths for fishes • Gladius length and lower rostral length of lower beaks for squids • Total and telson length for crustaceans

APPENDIX B. The pigment symbols, names, formulae and taxonomic designations for chloroplyll pigments, carotenoids, pigment sums and indices (Barlow *et al*., 2007).

Symbol	Pigment	Designation
Chla	Chlorophyll *a* (plus allomers and epimers)	
Chlb	Chlorophyll *b*	Chlorophytes
$Chlc_1$	Chlorophyll c_1	
$Chlc_2$	Chlorophyll c_2	
$Chlc_3$	Chlorophyll c_3	
Chlidea	Chlorophyllide *a*	
DVChla	Divinyl chlorophyll *a*	Prochlorophytes
DVChlb	Divinyl chlorophyll *b*	Prochlorophytes
All	Alloxanthin	Cryptophytes
But	19′-Butanoyloxyfucoxanthin	Chrysophytes
Caro	ββ-Carotene + βε-carotene	
Diad	Diadinoxanthin	
Diato	Diatoxanthin	
Fuc	Fucoxanthin	Diatoms
Lut	Lutein	
Hex	19′-Hexanoyloxyfucoxanthin	Prymnesiophytes
Per	Peridinin	Dinoflagellates
Viol	Violaxanthin	
Zea	Zeaxanthin	Cyanobacteria
	Pigment sum	*Formula*
TChla	Total chlorophyll *a*	Chla + DVChla + Chlidea
Chlbc	Sum of chlorophyll *b* and *c*	Chlb + $Chlc_1$ + $Chlc_2$ + $Chlc_3$
PPC	Photoprotective carotenoids	All + Caro + Diad + Diato + Lut + Viol + Zea
PSC	Photosynthetic carotenoids	But + Fuc + Hex + Per
TPig	Total pigments	TChla + Chlbc + PPC + PSC
DP	Diagnostic pigments	All + But + Chlb + Fuc + Hex + Per + Zea
	Pigment index	*Formula*
DVChla/TChla	Divinyl chlorophyll *a* to total chlorophyll *a*	DVChla/Tchla
$TChla_{TP}$	Total chlorophyll *a* to total pigments	TChla/Tpig
PPC_{TP}	Photoprotective carotenoids to total pigments	PPC/Tpig
PSC_{TP}	Photosynthetic carotenoids to total pigments	PSC/Tpig
$Diat_{DP}$	Diatom proportion of DP	Fuc/DP
$Flag_{DP}$	Flagellate proportion of DP	(All + But + Chlb + Hex)/DP
$Prok_{DP}$	Prokaryote proportion of DP	Zea/DP

APPENDIX C. Stable Isotope Analyses

Freeze-drying

Samples were freeze-dried with the Christ Alpha 1-4 LSC Freeze Dryer. A sublimation technique was employed whereby each sample was previously frozen and introduced in a vacuum container. The freeze-drying step (or lyophilisation) lasted for 48 hours. Upon completion, the cryotubes containing the samples were stored in a dry room where the humidity level was kept at 30% and the room temperature at 26°C.

Grinding

The samples were then ground to a fine homogeneous powder (Ménard *et al*., 2014; Fanelli *et al*., 2011) using the automatic ball mill RETSCH MM200. In the cryotubes containing the sample, 2mm steel balls were introduced. Due to their inertia, the balls impacted on the sample at high frequency for approximately 2 minutes, hence crushing the sample material to a fine powder.

Lipid extraction

The tissues of organisms used for isotope analysis contain various types of lipids- structural lipids in membranes and lipids used for storage. Dichloromethane was used on an accelerated solvent extraction system (ASE®, Dionex; Bodin *et al*., 2009) to remove those lipids. This process did not affect $\delta^{15}N$ isotopic signatures. The C/N mass ratio of the samples was used to confirm the extent of the lipid extraction.

All samples were sent to La Rochelle (LIENSS, UMR 7266 CNRS, La Rochelle) for stable isotope analysis by mass spectrometry whereby the samples were subjected to combustion in an elemental analyser. Gas chromatography and a mass spectrometer were employed to separate CO_2 and N_2 gas and to determine isotopic ratios. A reference gas set was used to determine isotopic ratios by comparison.